MEMBRANE AND NUCLEAR PROGESTERONE RECEPTORS ACTIVATE TUMOR SUPPRESSIVE SIGNALING MECHANISMS IN CELL LINE MODELS OF HUMAN OVARIAN CANCER

A DISSERTATION

SUBMITTED TO THE FACULTY OF THE GRADUATE SCHOOL

OF THE UNIVERSITY OF MINNESOTA

BY

NATHAN JON CHARLES

IN PARTIAL FULFILLMENT OF THE REQUIREMENTS

FOR THE DEGREE OF

DOCTOR OF PHILOSOPHY

Carol A. Lange, Ph.D.

July, 2010

ACKNOWLEDGEMENTS

I would like to thank the following for their encouragement, guidance, and support over the years for which I am forever indebted:

Research and Clinical Advisors: Peter A. Argenta, M.D., Peter B. Bitterman, M.D., Jennifer L. Hall, Ph.D., Carol A. Lange, Ph.D., Daniel L. Mueller, M.D., Harry T. Orr, Ph.D., and Douglas Yee, M.D.

University of Minnesota Training Programs: The Combined M.D./Ph.D. Medical Scientist Training Progam (MSTP) and The Microbiology, Immunology, and Cancer Biology (MICaB) Graduate Program.

Funding Support: The Minnesota Ovarian Cancer Alliance (MOCA)…and their passionate and inspiring members.

Classmates and Colleagues: Karen R. Armbrust, Ph.D., Yong Y. Kim, Ph.D., Serena K. Thompson, Ph.D. and past and present members of the Hall and Lange labs.

I would like to especially thank my Ph.D. thesis advisor,

Dr. Carol A. Lange, for her generosity, kindness,

and faith…thanks Carol.

DEDICATION

To my parents, Ronald and Barbara, who made all this possible.

ABSTRACT

Ovarian cancer is the leading cause of death from gynecologic malignancy in the United States. Mortality rates for ovarian cancer have been unchanged for more than 70 years even though surgical and chemotherapeutic strategies have become considerably more sophisticated. While a lack of clinical success is largely due to a poor etiologic understanding, recent observations suggest that the ovarian steroid hormone progesterone may be an endogenous ovarian cancer tumor suppressor. Therefore, the goal of our studies was to define progesterone receptor action in ovarian cancer and identify the signaling mechanisms responsible for its tumor suppressive function.

Membrane progesterone receptors (mPRs) represent a newly defined class of ~40 kDa GPCR-like progesterone receptors belonging to the adipoQ receptor (*PAQR*) gene family. Never studied in cancerous cells of ovarian surface epithelial origin, we identified positive expression of each isoform (mPRα/PAQR7, mPRβ/PAQR8, and mPRγ/PAQR5) in a panel of ovarian cancer cell lines. Contrary to breast cancer cells, progesterone stimulation of these receptors in ovarian cancer cells increased intracellular cAMP levels and cAMP response element (CRE) transcriptional activity, but required high, pregnancy equivalent levels of progesterone as well as $\beta_{1,2}$-adrenergic receptor co-stimulation. High-dose progesterone exposure also increased phosphorylation of the stress-activated JNK1/2 and p38 mitogen activated protein kinases (MAPKs). In particular, mPR-mediated p38 activation was responsible for increasing *BAX*

mRNA expression; a pro-apoptotic Bcl family member. These results demonstrate that functionally active mPRs are capable of activating signaling pathways associated with tumor suppression in ovarian cancer cells.

Clinical observations have shown that nuclear progesterone receptor (PR) expression is downregulated as ovarian tumors become progressively more malignant. Overexpression of PR in the ES-2 ovarian cancer cell line inhibited cellular proliferation and increased cell survival. As a result, prolonged ligand stimulation caused PR-expressing cells to undergo cellular senescence and exit the cell-cycle into G_0. Senescent cells expressed significantly higher mRNA levels of the cell-cycle inhibitor p21. When the inhibition of PR-induced p21 expression was removed by stably downregulating STAT3 expression, PR-mediated senescence occurred more quickly and p21 induction was enhanced as cells arrested in the G_1 phase of the cell-cycle. However, when increased p21 expression was prevented, ligand-stimulated PR-expressing cells also exhibited a heightened senescence response. These findings, along with the observation that ligand-stimulated PR-positive primary human ovarian cancer cells also become senescent, support our conclusion that PR-mediated cellular senescence is an endogenous ovarian cancer tumor suppressive mechanism.

Taken together, these results demonstrate that progesterone receptors possess tumor suppressing characteristics in ovarian cancer cells, and warrant further investigation into the use of progesterone as an ovarian cancer chemopreventive and chemotherapeutic agent.

TABLE OF CONTENTS

LIST OF FIGURES

CHAPTER 2

CHAPTER 3

CHAPTER 4

CHAPTER 1

INTRODUCTION

1.1 Progesterone Signaling in the Ovary

The adult female ovary is covered by a single layer of flat-to-cuboidal epithelial cells during embryologic development [1]. During each reproductive cycle, ovarian surface epithelial (OSE) cells are responsible for the controlled rupture and repair processes prior to and following ovulation, respectively [2]. OSE cells promote ovulation by producing proteolytic enzymes and undergoing apoptosis in the region adjacent to the pre-ovulatory follicle [3-5]. Following ovulation, OSE cells rapidly proliferate during the wound healing process to reconstitute a continuous epithelial layer surrounding the ovary [6]. This reparative process is regulated by a variety of hormones, growth factors, and cytokines commonly found at very high levels in the ovary [7-8].

OSE cells harbor receptors for stimuli that both promote and inhibit cellular growth, proliferation, and differentiation. Receptors for gonadotropin peptide hormones, including gonadotropin-releasing hormone (GnRH), human chorionic gonadotropin (hCG), leutinizing hormone (LH), and follicle-stimulating hormone (FSH), have been shown to both stimulate and inhibit OSE cell proliferation [9-16]. These differences might be explained by variations in hormone concentrations or receptor expression levels corresponding to different phases of the reproductive cycle [2]. The sex steroids estrogen, progesterone, and androgen also have receptors in OSE cells (i.e. ER, PR, and AR) [2]. These receptors serve as hormone binding nuclear transcription factors and, with the exception of AR, are often downregulated in ovarian cancer cells [2]. In contrast, the expression of epidermal growth factor (EGF) family members and their

receptors is often progressively increased during the malignant transformation of OSE cells [2]. EGF harbors potent mitogenic properties and stimulation of its receptors activates a complex network of signaling pathways regulating various cellular responses [17-18]. Other stimulatory growth factors in OSE cells include basic fibroblast growth factor (bFGF), keratinocyte growth factor (KGF), insulin-like growth factor I (IGF-I), platelet-derived growth factor (PDGF), and hepatocyte growth factor (HGF) [19-23]. This latter growth factor, HGF, is secreted by OSE cells themselves and binds its receptor (Met) in a paracrine fashion to regulate normal ovarian physiology [2]. However, autocrine HGF-Met signaling may contribute to ovarian tumorigenesis by stimulating the proliferation and motility of ovarian cancer cells [24-25]. Key members of the TGF-β protein family, particularly TGF-β1-3, activin, and inhibin, may counteract malignant progression as they have been shown to prevent proliferation and induce apoptosis of OSE cells [2,26-27]. Finally, several cytokines (i.e. interleukins-1, -6, and -18, macrophage colony-stimulating factor (M-CSF), granulocyte colony-stimulating factor (GM-CSF), and tumor necrosis factor-α (TNF-α)) are also produced by OSE cells during the ovulatory process [2]. Cytokine expression can be regulated by gonadotropins and sex steroids, but their misregulation may cause neoplastic transformation [2].

Taken together, there are an extensive number of extracellular signaling molecules responsible for controlling OSE cell biology. Additionally, temporally-specific changes in hormone levels and influence throughout the reproductive cycle add another layer of complexity to normal ovarian physiology. Therefore,

determining which factors are most important for either promoting or inhibiting ovarian carcinogenesis is especially difficult. However, of all the aforementioned targets and their respective activities, we found the influence of progesterone on ovarian tumorigenesis to be the most striking. In contrast to the pro-proliferative, pro-tumorigenic actions of progesterone in the breast [28], several reports have suggested that progesterone has an opposite impact in the ovary [2] and that progesterone receptors may be ovarian cancer tumor suppressors.

1.2 Progesterone Receptors in the Ovary

Progesterone is a steroid hormone produced by ovarian granulosa, thecal, and luteal cells in response to gonadotropin (i.e. FSH and LH) stimulation [29]. Secreted progesterone regulates the hypothalamic-pituitary axis and causes breast and uterine cell proliferation [29]. In the ovary, where localized concentrations are highest, progesterone acts to 1.) inhibit continual follicular development, 2.) cause granulosa cells to differentiate into luteal cells, and 3.) promote further progesterone synthesis by inhibiting luteal cell apoptosis [29]. The intraovarian activities regulated by progesterone are controlled by four types of progesterone receptors: membrane progesterone receptors (mPRs), serpine mRNA-binding protein 1 (SERBP1), progesterone membrane component 1 (PGRMC1), and nuclear progesterone receptors (PR).

Membrane progesterone receptors

Membrane progesterone receptors (mPRs) were originally identified by Zhu et al. in sea trout ovaries [30-31]. These ~40 kDa proteins are seven-transmembrane spanning proteins belonging to the larger progesterone and adipoQ (*PAQR*) gene family [30-32]. While mPRs activate small G-proteins and resemble seven-transmembrane spanning G-protein coupled receptors (GPCR), they are not part of this larger GPCR superfamily [33]. mPRs are typically coupled to the inhibitory G-protein $G_{\alpha i}$, whereby progesterone stimulation decreases cAMP synthesis that is sensitive to pertussis toxin inhibition [31]. mPR stimulation also causes activating phosphorylations of the mitogen activated protein kinases ERK1/2 and JNK1/2 [31,34]. Most recently, however, mPR stimulation has been shown to increase cAMP levels in sperm cells of the Atlantic croaker by activating the G_{olf} stimulatory G-proetin [35].

Three mPR isoforms have been identified (mPRα/PAQR7, mPRβ/PAQR8, and mPRγ/PAQR5) and shown to bind progesterone with high affinity (K_d = 4.2-7.8 nM) while not interacting with either synthetic progestins (i.e. R5020) or anti-progestins (i.e. RU486) [32]. Although originally seen in breast cancer cell lines and biopsies, all three mPR isoforms are expressed in mammalian ovaries [30]. However, mPRα and mPRγ expression increases in the corpus luteum throughout pregnancy while mPRβ levels remain unchanged [36]. Interestingly, ovarian mPRα and mPRβ expression rapidly decreases just prior to partuition [37]. Most recently, however, mPRα, mPRβ, and mPRγ have all been identified in human ovarian cancer tissues of all major histologic sub-types [38].

Progesterone receptor membrane component 1

Progesterone receptor membrane component 1 (PGRMC1) is also a membrane bound progesterone receptor but only possesses a single membrane-spanning domain [39-40]. Originally cloned from porcine liver, PGRMC1 has both high-affinity (K_d = 11 nM) and low-affinity (K_d = 286 nM) progesterone binding sites [39-40]. Although not identified in OSE cells, PGRMC1 expression has been observed in human granulosa and luteal cells [41]. Interestingly, hCG treatment causes granulosa cells to increase PGRMC1 expression and leads to redistribution of PGRMC1 from the nucleus to the plasma membrane [29]. Limited functional studies have shown that PGRMC1 may be responsible for regulating progesterone's anti-apoptotic activity in ovarian granulsoa and luteal cells [29].

Serpine mRNA-Binding Protein 1

In addition to the effects of PGRMC1, a second membrane progesterone receptor, serpine mRNA-binding protein 1 (SERBP1), also antagonizes progesterone's anti-apoptotic activity in ovarian granulosa cells [42]. SERBP1 is expressed in OSE cells, thecal cells, luteal cells, and is increased in granulosa cells during follicular development [43]. SERBP1 does not possess a transmembrane domain, does not affect progesterone binding, and has not been seen to affect signal transduction [43]. However, SERBP1 does form a complex with PGRMC1 on the extracellular surface of the plasma membrane where it is thought to mediate progesterone's anti-apoptotic actions [29,43].

Nuclear Progesterone Receptors

Nuclear, non-membrane bound progesterone receptors (PRs) make up the final group of progesterone receptors found in the ovary. Although PR expression and function is well-characterized in the breast [28], little is known about PR in the ovary. Three PR isoforms (PR-A, PR-B, and PR-C), each encoded by a single PR gene on chromosome 11 at q22-23, are part of a larger steroid hormone receptor family that includes estrogen, androgen, glucocorticoid, and mineralocorticoid receptors [28]. PR-B is the full length isoform (116 kDa), while N-terminally truncated PR-A (94 kDa) and PR-C (60 kFa) are smaller isoforms created by distinct promoter regions [28,44]. PR-A and PR-B are characterized as ligand-activated transcription factors possessing distinct transcriptional activities that can be modulated by PR-C [45-49]. Stimulation of PRs with the ovarian steroid hormone progesterone or synthetic progestins (i.e. R5020) cause receptor homo-dimerization, heat shock protein dissociation, nuclear translocation, and nuclear retention [28]. Nuclear localized PR upregulates target gene transcription by directly binding DNA via progesterone response element (PRE) consensus sequences or tethering itself to other DNA-binding transcription factors is often regulated by additional transcriptional co-activators or co-repressors [28]. The targeted phosphorylation of specific amino-acid residues by CDK2, MAPK, and casein kinase II can also control PR transcriptional activity, while cross-talk with PKA, PKC, and protein phosphatases 1 and 2A serve to modulate hormone-dependent transactivation [50-53]. PR can

also directly interact with SH3-containing molecules such as Src to cause rapid non-genomic effects [54-55]. However, while PR's influence on signaling and transcription is well studied in breast cancer, very little is known regarding the action of PR in ovarian cancer cells.

1.3 Progesterone and Ovarian Cancer

Ovarian cancer is the most lethal form of gynecologic malignancy, where United States projections for 2009 alone estimated 14,600 ovarian cancer-related deaths compared to 21,550 newly diagnosed cases [56]. Thus, while ovarian cancer is only the 9th most commonly diagnosed cancer in women, it ranks 5th in terms of total cancer-related deaths [56]. Over the past 70 years, ovarian cancer mortality rates have been unchanged despite advancements in detection methods, surgical techniques, and treatment regimens, even though hormonally-responsive cancers of the breast and uterus have seen marked improvements in long-term patient survival [56]. Such high mortality is largely due to the fact that most ovarian cancers (approximately 70%) are diagnosed at an advanced stage where 5-year survival rates drop to 30% as compared to 90% for women with localized disease [57]. The ineffectiveness of current therapy for advanced disease is complicated by a poor understanding of the molecular mechanisms governing ovarian cancer progression, and belie the fact that too little is known about the origin and biology of ovarian cancer for current treatment strategies to

be more effective [58]. However, clinical observations made within the past 15 years suggest that the ovarian steroid hormone progesterone may protect against ovarian cancer occurrence and progression.

Clinical findings have shown that multiparity, twin pregnancy, and pregnancy occurring later in life dramatically increase circulating progesterone levels and reduce a woman's lifetime risk of developing ovarian cancer [59-62]. These observations are supported by *in vitro* work demonstrating that ovarian cancer cell proliferation is inhibited when cells are exposed to high concentrations of progesterone comparable to those achieved during pregnancy [11,63]. In contrast, the likelihood of developing ovarian cancer dramatically increases when circulating progesterone levels decrease, such as occurs in women with inherent progesterone deficiencies and after menopause when production and secretion are drastically reduced [11,64]. Furthermore, a genetic loss of heterozygosity at the progesterone receptor (PR) gene locus (ch. 11q23.3-24.3) has been observed in as many as 75% of ovarian cancers and is associated with an overall worse patient prognosis [65-68].

Perhaps of greatest interest, however, are observations made by multiple groups demonstrating that women taking estrogen-progestin containing oral contraceptives (OC), for even a brief period, have a significantly decreased lifetime risk of developing ovarian cancer compared to women not receiving OCs [69-72]. These findings were corroborated by data from 45 epidemiological studies of over 100,000 women concluding that: 1.) OC use for 10 years

decreased the incidence rate from 1.2 to 0.8 per 100 users, 2.) OC use for 10 years decreased the mortality rate from 0.7 to 0.5 per 100 users, and 3.) the authors estimate that OC use has already prevented 200,000 ovarian cancer cases and 100,000 ovarian cancer deaths since their inception [73]. Further investigation of this phenomenon by Rodriguez *et al*., has demonstrated that the protective effects of estrogen-progestin containing oral contraceptives is mainly due to the progestin component which causes an increase in the apoptosis of ovarian surface epithelial cells [26-27]. The pro-apoptotic effects of progesterone have also been documented in human ovarian cancer cell lines due to the activation of both intrinsic and extrinsic apoptotic signaling mechanisms [74-77].

However, to counteract the inhibitory actions of progesterone on ovarian cancer cell survival and proliferation, a growing body of evidence has revealed an inverse relationship between progesterone receptor (PR) expression and malignant transformation. Original studies in the ovary demonstrated that while expressed in normal ovarian surface epithelial (OSE) cells, PR mRNA and protein levels decrease as ovarian cancer cells become more malignant [78-80]. Several studies have since concluded that expression of PR is a favorable prognostic indicator, whereby patients with PR positive ovarian tumors exhibit increases in progression-free and overall survival compared to PR negative counterparts [81-86]. While it is widely believed that progesterone's protective effects are mediated by nuclear PR, the recent discovery of an unrelated class of membrane-bound progesterone receptors (mPRs) in advanced stage ovarian

cancer creates additional targets available to progesterone in the face of PR downregulation [38].

When taken together, these findings and observations create a strong case for defining progesterone-progesterone receptor signaling as an endogenous means of inhibiting the malignant transformation of ovarian surface epithelial cells and suppressing ovarian cancer progression. However, the inherent signaling pathways and mechanisms responsible for mediating progesterone's tumor suppressive properties at the cellular level are vastly understudied and thus poorly understood. Therefore, the goal of our studies was three-fold. We first sought to determine the expression profile and signaling pathways activated by the newly-defined class of mPRs in advanced-stage ovarian cancer cell lines of different origins. We then aimed to define the impact PR re-expression and activity would have on ovarian cancer cell biology. Lastly, we intended to identify the signaling intermediates responsible for mediating PR-induced phenotypic changes and characterize them as potential therapeutic targets for treating ovarian cancer in humans.

CHAPTER 2

SIGNALING EVENTS MEDIATED BY MEMBRANE-PROGESTERONE RECEPTORS (mPRs) IN OVARIAN CANCER CELLS

2.1 Introduction

Originally cloned from sea trout ovaries, membrane progesterone receptor alpha (mPRα/PAQR7) and two other membrane-bound progestin receptors (mPRβ/PAQR8 and mPRγ/PAQR5) are defined as novel ~40 kDA seven-transmembrane spanning proteins belonging to the larger progesterone and adipoQ receptor (*PAQR*) gene family [30-32]. The mPRs activate G-proteins but are not members of the G protein-coupled receptor (GPCR) superfamily [23]. Typically, mPRs couple to the inhibitory G-protein, $G_{\alpha i}$ [32]. Stimulation of mPRs with progesterone has shown an ability of mPRs to decrease cAMP synthesis which is sensitive to pertussis toxin inhibition and increase the activity of mitogen activated protein kinases (MAPKs) [31,34]. However, more recent studies have also linked mPRα to a stimulatory G-protein, G_{olf}, responsible for increasing cAMP levels in sperm cells of the Atlantic croaker [35]. These receptors bind progesterone with high affinity (K_d = 4.2-7.8 nM) and do not interact with the synthetic progestin R5020 or the n-PR antagonist RU486 [32]. The mPRs (α, β, and γ) are expressed in mammalian ovaries and their abundance changes during pregnancy, suggesting they have important roles in ovarian physiology [30,36,87-88]. Originally seen in breast cancer biopsies and cell lines, mPR expression has also recently been observed in human ovarian cancer specimens originating from each histologic subtype [38]. Therefore, we focused our studies on this newly defined class of membrane-bound progesterone receptors (mPRs) to begin defining the impact progesterone-mediated mPR signaling has on ovarian cancer cell lines representing advanced stage disease [89].

2.2 Materials and Methods

Cell culture

All cell lines were grown at 37ºC under 5% CO_2 in water-jacketed incubators (Forma Scientific, Marietta, OH). MCF-7 cells were kindly provided by Dr. Douglas Yee (University of Minnesota). 1816-575 cells were kindly provided by Dr. Patricia Kruk (University of South Florida). HEY, CAOV-3, and ES-2 cells were kindly provided by Dr. Amy Skubitz (University of Minnesota). OVCAR-3, OVCAR-5, and SKOV-3 cells were kindly provided by Dr. Sundaram Ramakrishnan (University of Minnesota). TOV-21G cells (Cat. No. CRL-11730™) and TOV-112D cells (Cat. No. CRL-11731™) were purchased from American Type Culture Collection (ATCC®, Manassas, VA). The MCF-7 breast cancer cell line was maintained in DMEM cell culture media (cellgro®, Manassas, VA; 10-013-CV) supplemented with 5% FBS and 1% penicillin/streptomycin (GIBCO®, Carlsbad, CA; 15140122). The SKOV-3 ovarian cancer cell line was maintained in DMEM cell culture media (cellgro®, Manassas, VA; 10-013-CV) supplemented with 10% FBS and 1% penicillin/streptomycin. The ES-2 ovarian cancer cell line was maintained in McCoy's 5A cell culture media (cellgro®, Manassas, VA; 10-050-CV) supplemented with 15% FBS and 1% penicillin/streptomycin. The OVCAR-3 ovarian cancer cell line was maintained in RPMI 1640 cell culture media (GIBCO®, Carlsbad, CA; 11875-093) supplemented with 15% FBS and

1% penicillin/streptomycin. With the exception of the experiments performed on growing cells in Fig. 1A and 1B, 24 hours prior to all experiments, cells were washed with 1X PBS and placed in Modified IMEM (GIBCO®, Carlsbad, CA; A10488) supplemented with 1% charcoal-stripped serum (i.e. DCC) (Hyclone, Fremont, CA; SH30068.03) in which the remainder of the experiment was carried out.

Immunoblotting

Total protein was extracted from whole cell lysates with a modified RIPA extraction buffer containing PMSF (1 mM), NaF (5 mM), Na_3VO_4 (10 mg/mL), β-glycerophosphate (25 mM), β-ME (14.3 mM), aprotonin (11,140 KIU/mL), and 1 Complete Mini-Protease Inhibitor Cocktail tablet (Roche, Indianapolis, IN; 1 836 153 001). Protein concentration was quantified with Bio-Rad Protein Assay (Bio-Rad, Hercules, CA; 500-0001), and protein was transferred to Immobilon-P™ PVDF membranes (Millipore, Billerica, MA; IPVH00010) after fractionation by 10% SDS-PAGE (20 µg of total protein for Fig. 1B and 30 µg of total protein for Fig. 3). All Western blots were blocked for 1 hour at RT in phosphate-buffered saline/0.1% Tween-20 (PBS-T) containing 5% dried milk (Sanalac, Middleton, WI). mPR Western blots were probed overnight at 4°C in PBS containing 5% milk using anti-human mPR-α, -β, and -γ primary antibodies [32,34]. All other Western blots were probed overnight at 4°C in PBS-T containing 1% milk using the following primary antibodies: n-PR-A/B Ab-8 (NeoMarkers, Fremont, CA; MS-298-P), phospho-SAPK/JNK (Thr183/Tyr185) (Cell Signaling Technology,

Danvers, MA; 9255), SAPK/JNK (Cell Signaling Technology, Danvers, MA; 9258), phospho-p38 MAPK (Thr180/Tyr182) (Cell Signaling Technology, Danvers, MA; 9211), p38 MAPK (Cell Signaling Technology, Danvers, MA; 9212), and Actin (Sigma-Aldrich, St. Louis, MO; A 4700). HRP-conjugated goat anti-rabbit (Bio-Rad, Hercules, CA; 170-6515) and rabbit anti-mouse (Bio-Rad, Hercules, CA; 170-6516) secondary antibodies were used to detect their respective primary antibodies, and immunoreactive proteins were visualized on radiographic film (Kodak, Rochester, NY) following ECL detection with Super Signal® West Pico Maximum Sensitivity Substrate (Pierce, Rockford, IL; 34080).

Quantitative PCR (qPCR)

Total RNA was extracted from whole cells using TRIzol® (Invitrogen, Carlsbad, CA; 15596-018) separation and isopropanol precipitation. 1.0 μg of RNA was reverse transcribed to cDNA using random hexameric primers, dNTP nucleotides, RNaseOUT™ and SuperScript™ II reverse transcriptase (Invitrogen, Carlsbad, CA; 11904-018) as described by Invitrogen. qPCR was performed using Light Cycler® FastStart DNA Master SYBR Green I (Roche, Indianapolis, IN; 03 515 885 001) on a Mastercycler ep realplex^4 S qPCR platform (eppendorf, Hauppage, NY; 63002 000.601). Primers (from Integrated DNA Technologies, Coralville, IA) were specific for h-mPR-α (5'-cgctcttctggaagccgtacatctatg-3' and 5'-cagcaggtgggtccagacattcac-3'), h-mPR-β (5'-agcctcctacatagatgctgccc-3' and 5'-ggtgcctggttcacatgttcttca-3'), and h-mPR-γ (5'-cagctgtttcacgtgtgtgtgatcctg-3' and 5'-gcacagaagtatggctccagctatctgag-3'). qPCR cycling conditions used for the

mPR isoforms were as follows: initial denature @ 95^{o}C for 10 min; 40 X's: denature @ 95^{o}C for 10 s, anneal @ 55^{o}C for 10 s, and extension @ 72^{o}C for: 5 s (mPR-α), 10 s (mPR-β), and 8 s (mPR-γ). Primers were specific for h-n-PR-A/B (5'-aaatcattgccaggttttcg-3' and 5'-tgccacatggtaaggcataa-3'), whose qPCR cycling conditions were as follows: initial denature @ 95^{o}C for 10 min; 40 X's: denature @ 95^{o}C for 10 s, anneal @ 54^{o}C for 10 s, and extension @ 72^{o}C for 11 s. Primers were specific for h-BAX (5'-tctgacggcaacttcaactg-3' and 5'-ttgaggagtctcacccaacc-3'), whose qPCR cycling conditions were as follows: initial denature @ 95^{o}C for 10 min; 35 X's: denature @ 95^{o}C for 10 s, anneal @ 58^{o}C for 10 s, and extension @ 72^{o}C for 11 s. All qPCR results were normalized to expression of the housekeeping genes h-GAPDH (5'-ttgttgccatcaatgaccc-3' and 5'-catcgccccacttgattt-3') or h-β-actin (5'-tcagaaggattcctatgtgggc-3' and 5'-atcttctcgcggttggcctt-3'). Conditions for h-GAPDH qPCR were as follows: initial denature @ 95^{o}C for 10 min; 35 X's: denature @ 95^{o}C for 10 s, anneal @ 52^{o}C for 10 s, and extension at 72^{o}C for 11 s. Conditions for h-β-actin qPCR were as follows: initial denature @ 95^{o}C for 10 min; 35 X's: denature @ 95^{o}C for 10 s, anneal @ 60^{o}C for 10 s, and extension at 72^{o}C for 11 s.

cAMP EIA

SKOV-3 cells were plated at a density of 100,000 cells/100 mm plate and the following day they were starved for 24 hours in 1% DCC (as described earlier). Two days after plating, cells were treated for 10 min. as described in the results section with vehicle control, progesterone (Calbiochem, Los Angeles, CA; 5341),

and/or (-)-isoproterenol hydrochloride (Sigma-Aldrich, Indianapolis, IN; I 6504). All samples were co-treated at the same time with the phosphodiesterase inhibitor 3-isobutyl-1-methylxanthine (IBMX) (1 mM) (Sigma-Aldrich, St. Louis, MO; I 5879). Cells were immediately washed with ice-cold PBS and harvested with 1 mL of 0.1 N HCl. Cellular debris was removed by centrifugation and the remainder of the cAMP enzyme immunoassay (EIA) was performed according to the manufacturer's recommendations (Cayman Chemical, Ann Arbor, MI; 581001). Individual absorbance readings taken at 405 nm were read in duplicate and converted to cAMP concentrations via an on-line Xcel worksheet provided by Cayman Chemical (http://www.caymanchem.com).

Luciferase Assays

ES-2 cells were plated at a density of 100,000 cells/well of a 6-well plate. The following day, cells were co-transfected overnight with 0.9 µg of a CRE-firefly luciferase reporter construct (kindly provided by Dr. Paul Mermelstein as previously described [90]) and 0.1 µg of a constitutively active pRL-TK-*Renilla* luciferase construct (Promega; E2241) using FuGene HD® transfection reagent (Roche, Indianapolis, IN; 04 709 713 001) according to the manufacturer's recommendations. The next day, cells were washed with PBS and starved for 24 hours in 1% DCC as previously described. After starvation, cells were treated for 24 hours with vehicle control, progesterone, and/or isoproterenol at which point they were washed with ice-cold PBS and harvested in 200 µL of 1X passive lysis buffer (Promega, Madison, WI; E1941). All samples were co-treated at the same

time with IBMX (1 mM). Cellular debris was removed by centrifugation and samples were analyzed for 10.0 s each by a Monolight™ 3010 luminometer (PharMingen, San Diego, CA) that injected 80 µL of firefly-luciferase substrate followed by 100 µL of Stop-N-Glo® *Renilla*-luciferase substrate (Promega, Madison, WI; E1960). PRE-luciferase assays were carried out as described for the CRE-luciferase assays using a previously described wild-type n-PR-B overexpression construct and PRE-luciferase reporter construct [91].

qPCR Superarray

SKOV-3 cells were plated at a density of 1,000,000 cells/150 mm plate and allowed to grow to approximately 75% confluency at which point they were washed with PBS and starved for 24 hours with un-supplemented Modified IMEM. Cells were treated for 24 hours with vehicle control or progesterone, washed with ice-cold PBS, and RNA was isolated using TRIzol® (Invitrogen, Carlsbad, CA; 15596-018) and isopropanol extraction. After isolation, 12.0 µg of RNA was converted to cDNA as previously described (see qPCR section). Samples were aliquoted onto the Human Cancer PathwayFinder™, RT^2 Profiler™ PCR Array (SABiosciences™, Frederick, MD; PAHS-033A). qPCR was performed using Light Cycler® FastStart DNA Master SYBR Green I (Roche, Indianapolis, IN; 03 515 885 001) on a Mastercycler ep realplex^4 S qPCR platform (eppendorf, Hauppage, NY; 63002 000.601). Gene expression changes were determined by normalizing the value of each target gene in the progesterone-treated group to its corresponding value from the vehicle control-treated group using on-line analysis

software provided by SABiosciences™ (http://www.sabiosciences.com/pcr/arrayanalysis.php).

Statistical Analysis

All reported values represent the mean ± the standard deviation (SD). Statistical analyses were performed using a Student's *t*-test where significance was determined with 95% confidence (*$p \leq 0.05$).

2.3 Results

mPRs Expressed in Ovarian Cancer Cells Modulate cAMP Levels.

Initial characterization of mPRs demonstrated that expression of mPRα in humans was limited to the kidney, placenta, testis, and ovary [30]. Since then, mPRα expression has also been observed in human breast and ovarian cancer specimens and human breast cancer cell lines [38,92]. Therefore, we began our studies by measuring the basal mRNA expression levels of each mPR isoform (α, β, and γ) in a panel of eight distinct ovarian cancer cell line models and one non-tumorigenic immortalized ovarian surface epithelial cell line (1816-575) using quantitative-PCR (Fig. 1a). We also confirmed the absence of protein or mRNA encoding nuclear-PR-A and -B isoforms from all eight ovarian cancer cell lines using n-PR positive MCF-7 breast cancer cells as a positive control (data not shown). Based on these observations, we focused our attention on two ovarian cancer cell lines demonstrating differences in mPR isoform transcript levels that

were derived from aggressive human tumors of different histologic sub-types. SKOV-3 ovarian cancer cells were originally isolated from a metastatic adenocarcinoma of the ovary and ES-2 ovarian cancer cells were established from a poorly differentiated ovarian clear cell carcinoma. Using MCF-7 breast cancer cells as a reference for mPR expression, we positively identified mPRα, β, and γ protein expression by immunoblot analysis in SKOV-3 and ES-2 cells (Fig. 1b). Interestingly, SKOV-3 cells express lower levels of mPRγ protein compared to MCF-7 and ES-2 cells while expressing higher levels of mPRγ mRNA (Fig. 1a-b). Although n-PR-A/B expression appears to be limited to the MCF-7 breast cancer cell line relative to the ovarian cancer cell lines in our panel, the possibility of endogenous n-PR activity was further excluded, as OVCAR-3 (Fig. 1c) and ES-2 (unpublished data) ovarian cancer cells failed to elicit a transcriptional response from a progesterone response element (PRE)-driven luciferase reporter gene unless cells were also co-transfected with a human PR-B expression vector. Importantly, these cells also failed to respond to synthetic progestins in soft-agar and MTT growth assays (not shown). Finally, mPR mRNA expression levels did not change in response to treatment (24 hrs) of cells with either progesterone or estrogen (data not shown).

After confirming abundant mPR isoform expression in the absence of n-PR, we next sought to examine progesterone-mediated signaling events in ovarian cancer cells. Prior characterization of mPRα activity in a variety of cell types, including MDA-MB-231 breast cancer cells transfected with mPRα and pregnant human myometrial cells, revealed the coupling of mPRα to an inhibitory

G protein ($G_{\alpha i}$) [32,34,89]. However, in contrast to a progesterone-induced reduction in cAMP levels, we observed no significant alterations of intracellular cAMP concentration in SKOV-3 ovarian cancer cells stimulated with progesterone alone or upon the inclusion of IBMX to block phosphodiesterase activity (Fig. 2a). One interpretation of this surprising observation is that in these cells, mPRs are not functionally linked (i.e. at least directly) to inhibitory or stimulatory G-proteins. Signal transduction from the cell surface through the G-protein alpha subunit may be functionally impaired, as observed in MDA-MB-231 breast cancer cells not overexpressing mPRs [32]. Notably, however, treatment of SKOV-3 cells with isoproterenol, a well-characterized $\beta_{1,2}$-adrenergic receptor agonist resulted in robust production of cAMP (Fig. 2a).

Stimulation of mPRs in human myometrial cells has been reported to inhibit isoproterenol-induced cAMP synthesis [34]. We therefore examined the impact of mPR activation on isoproterenol-induced $\beta_{1,2}$-adrenergic signaling in ovarian cancer cells. SKOV-3 cells were co-treated with either isoproterenol and vehicle or isoproterenol and progesterone (Fig. 2b). Progesterone significantly enhanced isoproterenol-induced cAMP levels. Similar augmentation of isoproterenol-induced cAMP levels by progesterone was also observed in ES-2 ovarian cancer cells (data not shown). These results are in contrast to decreases observed in human myometrial cells acting through an inhibitory G-protein ($G_{\alpha i}$) under similar experimental conditions [24]. These findings suggest that mPR activity alters $\beta_{1,2}$-adrenergic signaling differently in different cell types, thus providing context-specific responses to progesterone action. To test whether

mPR-mediated increases in isoproterenol-induced cAMP synthesis also translate to changes in gene expression, we transfected ES-2 cells with a cAMP response element (CRE)-driven luciferase reporter construct. Cells were treated for 24 hrs with either vehicle, progesterone alone, isoproterenol alone, or both agents. In accordance with previous results demonstrating that progesterone alone does not alter cAMP levels (Fig. 2a), stimulation of reporter gene-transfected ES-2 cells with progesterone for 24 hours did not elicit an appreciable transcriptional response as measured by CRE-luciferase expression (Fig. 2c). However, co-treatment of cells with progesterone and the $\beta_{1,2}$-adrenergic agonist, isoproterenol, led to a significant increase in CRE-luciferase activity relative to isoproterenol alone (Fig. 2c). This result was specific to the hormone progesterone, as stimulation of either follicle stimulating hormone (FSH) or luteinizing hormone (LH) receptors with their respective ligands failed to augment isoproterenol-induced cAMP levels (not shown).

mPRs Expressed in Ovarian Cancer Cells Activate JNK and p38 MAPKs.

In addition to its effects on intracellular cAMP concentrations, progesterone-mediated mPR activity has also been shown to alter other key intracellular signaling pathways [89]. In particular, progesterone stimulation of mPRs in breast and human myometrial cells causes an increase in the activity of ERK1/2 and p38, both members of the mitogen activated protein kinase (MAPK) family of signaling intermediates [31,34]. Therefore, we sought to determine whether signaling from mPRs affected the activity of these kinases similarly in

SKOV-3 ovarian cancer cells. When stimulated with progesterone, SKOV-3 ovarian cancer cells demonstrated a significant increase in phosphorylation of JNK1/2 and p38 MAPKs, as measured by Western blotting using phospho-specific antibodies (Fig. 3). JNK1/2 activation occurred in a time- and dose-dependent manner, where treatment with progesterone concentrations of 100 and 1000 nM lead to increased JNK1/2 phosphorylation at both 5 and 15 minutes. JNK1/2 activity was sustained for 30 minutes with the higher dose of progesterone (Fig. 3). Similar to JNK1/2, p38 MAPK was transiently activated by both low and high concentrations of progesterone. However, p38 phosphorylation increased at 5 and 15 minutes, but returned to baseline by 30 minutes (Fig. 3). Lower concentrations of progesterone (1, 10, and 50 nM) failed to reproducibly activate these kinases under similar conditions (data not shown). When cells were co-treated with both progesterone (1 μM) and isoproterenol (100 nM), there was no further increase in either JNK1/2 or p38 MAPK activity as measured by phosphorylation (data not shown). These results are consistent with the activation of an alternate mPR signaling pathway (possibly mediated by the βγ subunits of hetero-trimeric G-proteins); mPR-mediated increases in MAPK activity appear to be independent of changes in cAMP signaling.

It is now well documented that JNK1/2 and p38 have the ability to significantly impact gene expression, often by altering the activation of transcription factor targets or their co-regulators that act as nuclear substrates for these kinases. To identify gene targets downstream of mPR signaling, we

analyzed progesterone-dependent changes in the expression level of selected genes commonly associated with cellular transformation and tumorigenesis (qPCR Superarray; SABiosciences™). cDNA was made using mRNA isolated from vehicle or progesterone-treated (24 hrs) SKOV-3 ovarian cancer cells. Following qPCR reactions, we identified a significant increase in *BAX* gene expression (data not shown). Bax is a prominent member of the pro-apoptotic Bcl-protein family. In studies to independently validate *BAX* as a mPR gene target, we again observed a significant dose-dependent up-regulation of *BAX* mRNA in SKOV-3 ovarian cancer cells treated with 10-100 nM progesterone (Fig. 4a). To further link *BAX* regulation to mPR signaling, we tested the requirement of JNK1/2 and p38 MAPK activities for progesterone induced upregulation of *BAX* mRNA. Cells were again treated with progesterone, but in this set of experiments, we included small molecule inhibitors for either JNK1/2 or p38 MAPKs. Notably, *BAX* mRNA expression was significantly decreased in SKOV-3 ovarian cancer cells exposed to both progesterone (100 nM) and the JNK1/2 small-molecule inhibitor SP 600125 (10 μM), but not the p38 small-molecule inhibitor SB 203580 (2.6 μM) (Fig. 4b). Taken together, these observations identify a known pro-apoptotic mediator (Bax) regulated downstream of mPR signaling to JNK1/2 and distinct from cAMP signaling.

2.4 Discussion

Mounting evidence suggests that the ovarian steroid hormone progesterone plays both a protective role in preventing ovarian cancer

development and a therapeutic role acting against further tumor progression. Unfortunately, advanced ovarian tumors lose expression of the well-characterized classical nuclear progesterone receptors (n-PR-A/B), and are thus assumed to be entirely resistant to the potential benefits of progesterone's anti-tumorigenic effects. However, recent work demonstrating the presence of a newly-defined family of membrane progesterone receptors (mPRs) in human ovarian tumor specimens raises the possibility that progesterone, acting through this class of novel receptors that are unrelated to n-PRs, may continue to limit ovarian cancer progression in tumors of all stages and independently of n-PR expression.

Notably, mPRs were recently discovered in ovarian cancer tissue samples [38]. Our goal was to begin defining how these novel GPCR-like steroid hormone receptors might alter intracellular signaling networks in ovarian cancer cells. We first confirmed robust expression of each mPR isoform in normal (non-tumorigenic, immortalized) ovarian surface epithelial cells and ovarian cancer cell lines that model advanced stage disease. Importantly, these cell lines lack n-PR, making them excellent model systems in which to study mPRs. Based on current literature [32,34], we assumed mPRs would primarily negatively regulate intracellular cAMP levels. Surprisingly, our results demonstrated that mPRs, when stimulated with progesterone alone, do not appreciably alter cAMP concentrations either positively or negatively in SKOV-3 and ES-2 cells as they do in other cell types [32]. Instead, however, we found that progesterone-induced mPR activity enhanced $\beta_{1,2}$-adrenergic receptor-mediated increases in cAMP

levels and CRE-mediated transcription (Fig. 5a). This may occur by receptor crosstalk, including GPCR hetero-dimerization [93] of adrenergic receptors with mPRs (Fig. 5a), although there are currently no reports of mPRs forming hetero-dimers with other receptors. Nonetheless, the observation that mPR activity increases isoproterenol-induced cAMP levels in ovarian cancer cells suggests a means for limiting their proliferative potential; increased cAMP levels cause up to a 62% decrease of cellular proliferation in HEY ovarian cancer cells [94]. Thus, mPR-dependent augmentation of cAMP levels in ovarian cancer cells could function to limit proliferation in response to other signals, possibly by increasing the expression of pro-apoptotic markers. For example, activating transcription factor-3 (*ATF-3*), a known gene target of the cAMP-CREB signaling pathway has been shown to be significantly upregulated in progesterone-treated ovarian cancer cells, and when overexpressed *in vitro*, causes ovarian cancer cell apoptosis [95-96]. These studies were performed prior to the discovery of mPRs in human ovarian cancer cells [38]. However, the ability of mPRs to augment the natural induction of cAMP by other hormones provides a rationale to consider adding progesterone to current therapies for the treatment of advanced stage ovarian cancer.

Based on our work herein, and previous observations, progesterone-mediated mPR activity clearly leads to the activation of downstream MAPK family members [34]. In response to mPR stimulation, we observed activation of JNK1/2 and p38 MAPKs and genomic changes (i.e. in *BAX* expression) associated with JNK1/2 signaling (Fig. 5b). While the mechanism(s) behind progesterone-

dependent JNK1/2 and p38 phosphorylation remain unknown in ovarian cancer cells, we hypothesize that mPRs may be linked to these downstream kinases by increasing the activity of apoptosis signal-regulating kinase 1 (ASK1) (Fig. 5b). Previous work has shown that GPCR signaling can directly activate ASK1, which in turn leads to the phosphorylation of both JNK1/2 and p38 via their upstream kinases, MKK4/7 and MKK3/6, respectively [97]. Furthermore, each of these kinases may be physically linked to GPCRs by the β-arrestin family of scaffolding proteins, which have also been shown to uncouple heterotrimeric G-proteins from their cognate GPCRs (Fig. 5b). This mode of signal transduction (i.e. uncoupling from G-protein effectors) may explain our modest cAMP results (Fig. 2 and discussed above) [98]. However, it is not yet known whether similar interactions occur between mPRs and these macromolecules.

Of great interest is the linkage of progesterone/mPR-mediated JNK1/2 activity with *BAX* gene expression. BAX is a known pro-apoptotic effector of ovarian cancer cells both *in vitro* and *in vivo* [99]. Prior work has demonstrated that 1) human ovarian cancer tissue samples possess higher expression levels of *BAX* mRNA compared to normal tissues, 2) the p53 tumor suppressor protein is a substrate that is phosphorylated and activated by JNK1/2 signaling, and 3) activated p53 directly increases *BAX* expression, a transcriptional response often disrupted in cisplatin-resistant ovarian cancer cells [33,100-101]. Additionally, increased JNK1/2 and p38 MAPK activities have been shown to induce ovarian cancer cell apoptosis; these kinases posses the ability to stimulate the activation and translocation of Bax to the outer mitochondrial membrane leading to cell

death via the intrinsic pathway [102-103]. Furthermore, in ovarian cancer, JNK1/2 and p38 have been shown to mediate both cisplatin- and paclitaxel-induced cytotoxicity, which may explain the improved prognosis of ovarian cancer patients whose tumors demonstrate increased MAPK activity [104-106]. Taken together, these exciting observations implicate a complete signaling pathway leading to ovarian cancer cell death that can be induced in part by the input of activated mPRs to pro-apoptotic MAPK signaling modules; we are currently pursuing this idea.

Over the past decade, numerous *in vitro* studies have documented the ability of progesterone to inhibit ovarian cancer cell proliferation and promote ovarian cancer cell death by a variety of different mechanisms including: p53 upregulation [74], differential regulation of TGF-β [26], increased FasL expression [76], and enhancing TRAIL-induced cell death [77]. It has also been shown that exposing ovarian cancer cells to the high levels of progesterone achieved during pregnancy decreases ovarian cancer cell proliferation, while treating n-PR negative ovarian cancer cells with progesterone decreases cell survival [107]. Additionally, patient clinical trials using medroxyprogesterone acetate (MPA) to treat ovarian cancer demonstrated up to 16 months of disease stabilization and improved the prognosis for advanced stage ovarian cancer patients also receiving platinum-based chemotherapy [108-109]. The relative contributions of mPRs and classical nuclear-PRs to these effects remain to be determined. However, the success of these clinical trials, and prior *in vitro* studies using progesterone and progesterone analogues combined with the

potentially anti-tumorigenic mPR-mediated signaling events discussed herein, suggest that high-dose progesterone therapy (or newly defined mPR agonists) may improve upon current chemotherapeutic approaches. In sum, the presence of abundant mPR and progesterone-dependent signaling events in ovarian cancer cells described herein suggest that progesterone-based hormone therapy, alone or in conjunction with other standard regimens, may provide an effective strategy for treating advanced stage ovarian cancer.

2.5 Acknowledgements

This work was supported by a grant from the Minnesota Ovarian Cancer Alliance (MOCA). From the University of Minnesota Masonic Cancer Center, we would like to thank Dr. Douglas Yee, Dr. Amy Skubitz, Dr. Patricia Kruk, and Dr. Sundaram Ramakrishnan for providing us with ovarian cancer cell line models and Dr. Paul Mermelstein for the CRE-luciferase reporter construct. We would also like to thank Dr. Patricia Kruk (University of South Florida) for providing us with the 1816-575 cell line.

2.6 Conflict of Interest

The authors declare that they have no conflict of interest.

2.7 Figure Legends

Figure 1 Ovarian cancer cell lines express membrane-progesterone receptor (mPR) mRNA and protein. A.) Quantitative PCR (qPCR) identified and compared gene expression levels of each mPR isoform (α, β, and γ) in a panel of ovarian cancer cell lines relative to control MCF-7 breast cancer cells (mean ± SD, n = 3). **B.)** Immunoblot analysis defined protein expression of each mPR isoform (α, β, and γ) in the SKOV-3 and ES-2 ovarian cancer cell lines relative to control MCF-7 breast cancer cells. SKOV-3 and ES-2 cells do not express nuclear-progesterone receptor (n-PR-A or -B) protein. **C.)** OVCAR-3 ovarian cancer cells transiently transfected with a n-PR-specific progesterone response element (PRE)-luciferase reporter construct only respond to stimulation with the n-PR specific ligand R5020 (10 nM) for 18 hours when co-transfected with a n-PR-B overexpression construct (mean ± SD, n = 3, *p ≤ 0.05). (note: all firefly luciferase values are individually normalized to the expression of a *Renilla*-based luciferase reporter construct serving as an internal control.)

Figure 2 Membrane-progesterone receptor (mPR) activity enhances $\beta_{1,2}$–adrenergic receptor stimulated cAMP levels and cAMP-mediated transcription. A.) Stimulating SKOV-3 cells with progesterone (1 μM) for 10 minutes did not alter cAMP levels relative to vehicle control. Treatment with the $\beta_{1,2}$-adrenergic agonist isoproterenol (100 nM) served as a positive control for the cAMP EIA (mean ± SD, n = 4, *p ≤ 0.05). **B.)** Co-treating SKOV-3 cells with progesterone (1 μM) for 10 minutes significantly increased cAMP induction by

isoproterenol (100 nM) (mean ± SD, n = 3, *p ≤ 0.05). **C.)** ES-2 cells transiently transfected with a CRE-luciferase reporter demonstrated a significant increase in transcription when treated with progesterone (1 µM) and isoproterenol (100 nM) for 24 hours compared to cells exposed to isoproterenol alone (mean ± SD, n = 6, *p ≤ 0.05). (note: all firefly luciferase values are individually normalized to the expression of a *Renilla*-based luciferase reporter construct serving as an internal control.)

Figure 3 Stimulation of the membrane-progesterone receptor (mPR) with progesterone increases JNK1/2 and p38 MAPK activity. Immunoblot analysis of SKOV-3 cells stimulated with progesterone (100 or 1000 nM) demonstrated a time- and dose-dependent increase in phosphorylation of both JNK isoforms (p-JNK1 and p-JNK2) as well as p38 (p-p38). Total JNK1/2 (t-JNK-1 and t-JNK-2) and total p38 (t-p38) expression was unchanged with progesterone treatment.

Figure 4 Membrane-progesterone receptor (mPR) activity in ovarian cancer cells increases BAX gene expression in a JNK1/2-dependent manner. A.) SKOV-3 ovarian cancer cells treated for 24 hours with varying concentrations of progesterone demonstrated a significant increase in *BAX* gene expression as determined by quantitative PCR (qPCR) relative to the *GAPDH* house-keeping gene (mean ± SD, n = 4, * p ≤ 0.05). **B.)** The JNK1/2 inhibitor SP 600125 (10 µM), but not the p38 inhibitor SB 203580 (2.6 µM), significantly decreased *BAX* gene expression in SKOV-3 ovarian cancer cells stimulated with progesterone

(100 nM) for 24 hours as determined by qPCR relative to the *β-ACTIN* house-keeping gene (mean ± SD, n = 3, * $p \leq 0.05$).

Figure 5 The membrane-progesterone receptor (mPR) independently activates two distinct signaling pathways in the SKOV-3 and ES-2 ovarian cancer cell lines. A.) Progesterone (P4)-activated mPR's enhance increased cyclic AMP (cAMP) concentrations caused by isoproterenol (Iso)-mediated activation of $\beta_{1,2}$-adrenergic receptors ($\beta_{1,2}$-AR). Progesterone augmented cAMP levels, potentially occurring via mPR/$\beta_{1,2}$-AR heterodimerization, ultimately lead to an increase in transcription from a genetic cyclic AMP response element (CRE). **B.)** Progesterone-stimulated mPR's activate the JNK1/2 and p38 MAPK's and increase *BAX* gene expression. The mPR may activate JNK1/2 and p38 by directly stimulating ASK1 via the MAPK-GPCR scaffolding protein β-arrestin. Additionally, activated JNK1/2 (inhibited by the small molecule inhibitor SP 600125 (SP)) may stimulate *BAX* gene expression via the p53 tumor suppressor protein.

2.8 Figures

Ch. 2 – Figure 1

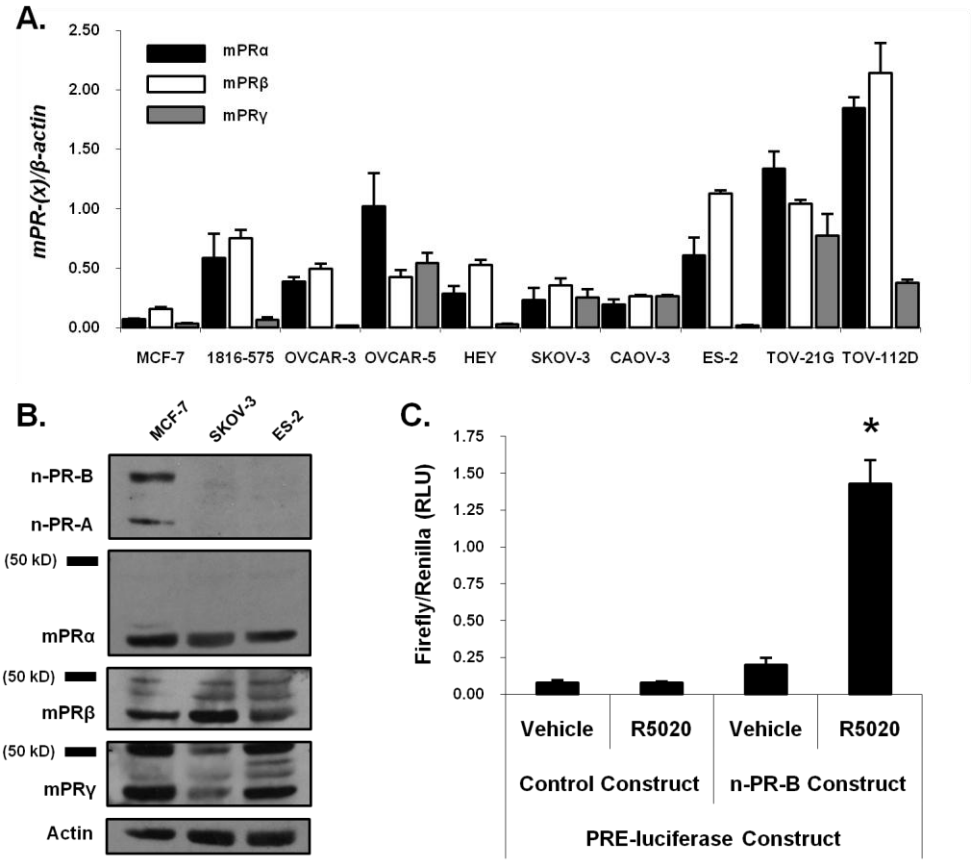
A.
mPR-(x)/β-actin
2.50
2.00
1.50
1.00
0.50
0.00
mPRα
mPRβ
mPRγ
MCF-7
1816-575
OVCAR-3
OVCAR-5
HEY
SKOV-3
CAOV-3
ES-2
TOV-21G
TOV-112D
B.
MCF-7
SKOV-3
ES-2
n-PR-B
n-PR-A
(50 kD)
mPRα
(50 kD)
mPRβ
(50 kD)
mPRγ
Actin
C.
Firefly/Renilla (RLU)
1.75
1.50
1.25
1.00
0.75
0.50
0.25
0.00
*
Vehicle
R5020
Vehicle
R5020
Control Construct
n-PR-B Construct
PRE-luciferase Construct

Ch. 2 – Figure 2

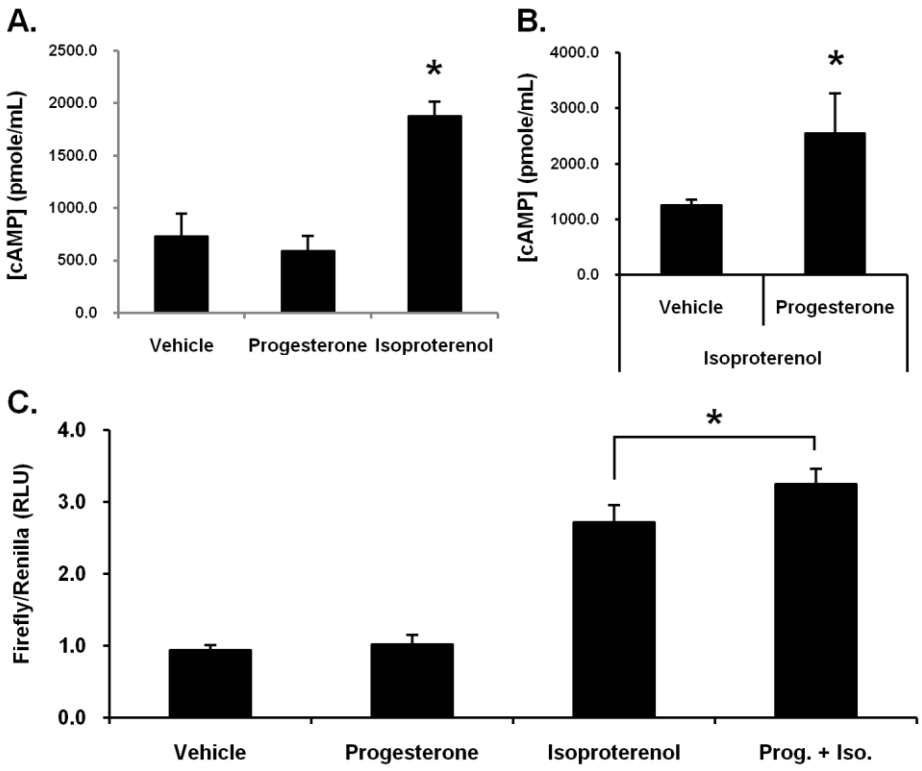
A.
[cAMP] (pmole/mL)
2500.0
2000.0
1500.0
1000.0
500.0
0.0
*
Vehicle
Progesterone
Isoproterenol
B.
[cAMP] (pmole/mL)
4000.0
3000.0
2000.0
1000.0
0.0
*
Vehicle
Progesterone
Isoproterenol
C.
Firefly/Renilla (RLU)
4.0
3.0
2.0
1.0
0.0
*
Vehicle
Progesterone
Isoproterenol
Prog. + Iso.

Ch. 2 – Figure 3

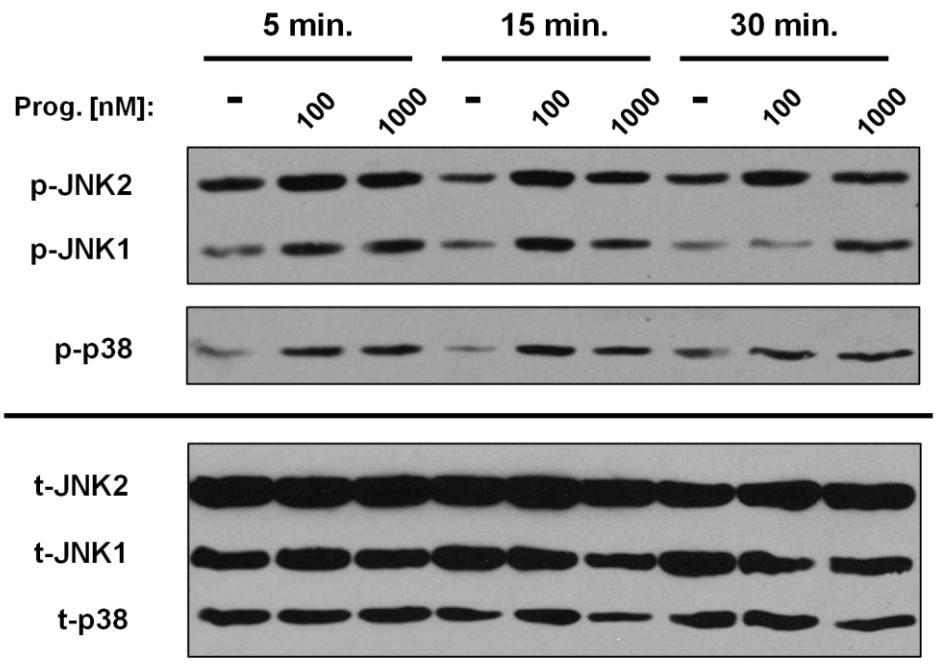
5 min.
15 min.
30 min.
Prog. [nM]:
-
100
1000
-
100
1000
-
100
1000
p-JNK2
p-JNK1
p-p38
t-JNK2
t-JNK1
t-p38

Ch. 2 – Figure 4

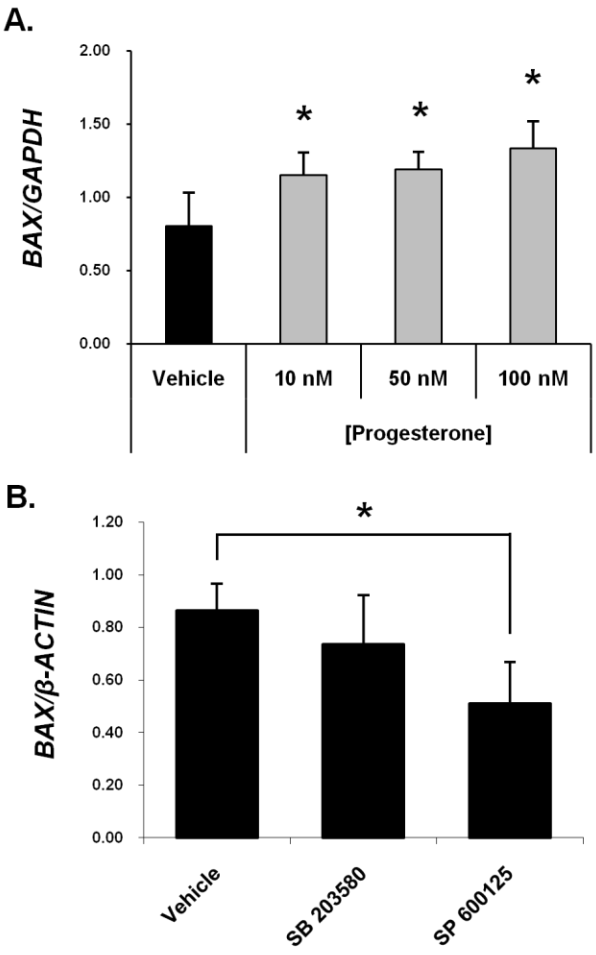
A.
BAX/GAPDH
2.00
1.50
1.00
0.50
0.00
*
*
*
Vehicle
10 nM
50 nM
100 nM
[Progesterone]
B.
BAX/β-ACTIN
1.20
1.00
0.80
0.60
0.40
0.20
0.00
*
Vehicle
SB 203580
SP 600125

Ch. 2 – Figure 5

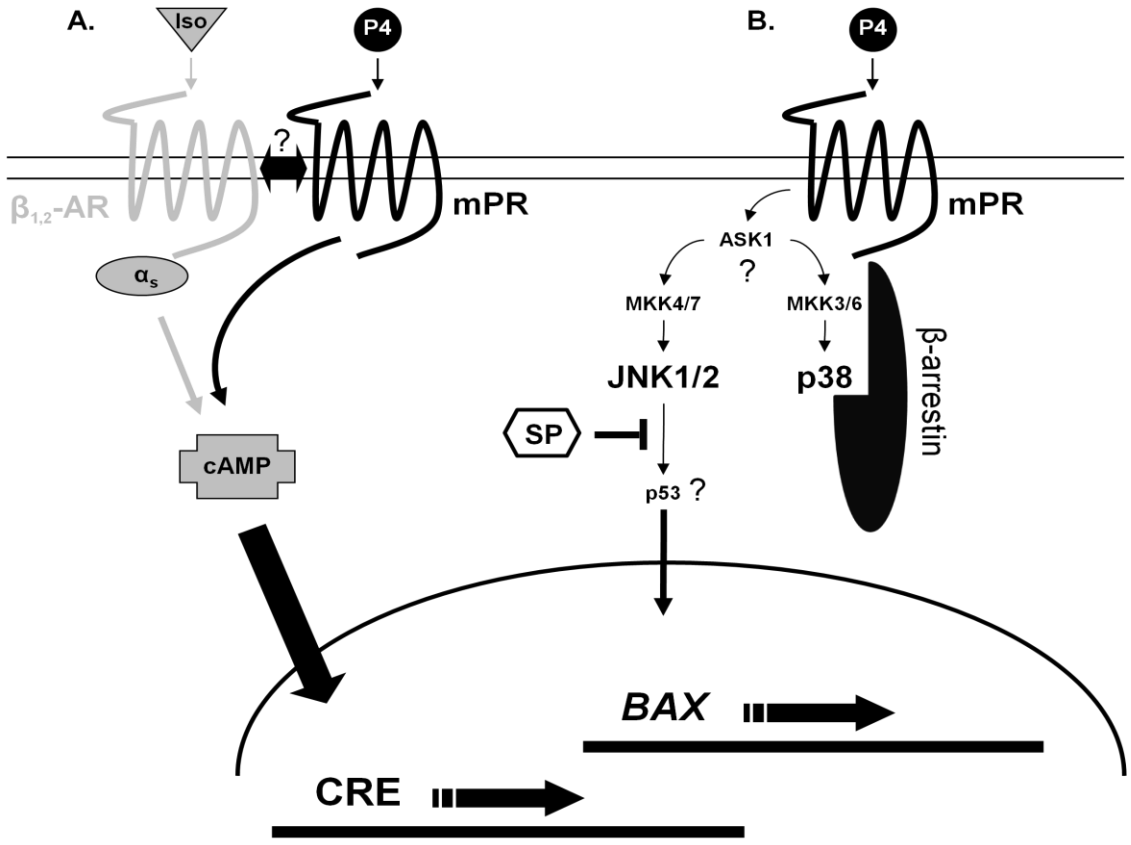
A.
Iso
P4
?
$\beta_{1,2}$-AR
mPR
α_s
cAMP
B.
P4
mPR
ASK1
?
MKK4/7
MKK3/6
JNK1/2
p38
β-arrestin
SP
p53 ?
BAX
CRE

CHAPTER 3

PROGESTERONE RECEPTOR STIMULATION INDUCES CELLULAR SENESCENCE OF OVARIAN CANCER CELLS IN A p21-ASSOCIATED MANNER

3.1 Introduction

Nuclear, non-membrane bound progesterone receptors (PRs) belong to a larger family of related steroid hormone receptors that includes estrogen, androgen, glucocorticoid, and mineralocorticoid receptors [28]. Two PR isoforms (full-length PR-B and N-terminally truncated PR-A) have been identified and characterized as ligand-activated transcription factors with different transcriptional activities on different promoters, while a third (PR-C) modulates the other two [45-48,110]. When bound to the ovarian steroid hormone progesterone or synthetic versions (i.e. progestins), PRs dimerize, disassociate from heat shock proteins (HSPs), and are withheld in the nucleus following their translocation [28]. Once inside, PRs upregulate gene transcription by either directly binding to specific progesterone response elements (PREs) or tethering to other DNA-binding transcription factors [28]. PR transcriptional activity is commonly linked to the expression of many cell-cycle regulators including members of the cyclin, cyclin-dependent kinase (CDK), and p21/p27 families [49]. PR is often associated with survival, cell-cycle progression, and proliferation of breast and prostate cancer cells [111-113]. Interestingly, however, a handful of reports have suggested that progesterone may inhibit these effects in ovarian cancer cells [11,26-27,63,76,114] coinciding with clinical findings defining PR expression as a favorable prognostic marker in ovarian cancer [81-86,115]. Of particular interest, is the association of PR-B expression with the induction of cell-cycle arrest first observed in Ras-transformed NIH3T3 cells [116] and later extended to include ovarian cancer cells [117]. Therefore, the goal of our studies

was to further investigate the impact of PR expression and action on ovarian cancer cell proliferation and to determine the signaling mechanisms responsible for PR-mediated cell-cycle control.

3.2 Materials and Methods

Cell culture

All cell lines were grown at 37º C under 5% CO_2 in water-jacketed incubators (Forma Scientific, Marietta, OH). HEY, CAOV-3, and ES-2 cells were kindly provided by Dr. Amy Skubitz (University of Minnesota). OVCAR-3, OVCAR-5, and SKOV-3 cells were kindly provided by Dr. Sundaram Ramakrishnan (University of Minnesota). TOV-21G cells (Cat. No. CRL-11730™) and TOV-112D cells (Cat. No. CRL-11731™) were purchased from American Type Culture Collection (ATCC®, Manassas, VA). The T47D and T47D-YB breast cancer cell lines were maintained in MEM cell culture media (cellgro®, Manassas, VA; 10-010-CV) supplemented with 5% fetal bovine serum (FBS), 1% penicillin/streptomycin (GIBCO®, Carlsbad, CA; 15140122), 1% MEM non-essential amino acids (cellgro®, Manassas, VA; 25-025-Cl), and 6 ng/mL of insulin. Media for T47D-YB cells also contained 200 µg/mL of G418 sulfate (Fisher Scientific, Pittsburgh, PA; MT-61-234-RG). The parental ES-2 ovarian cancer cell line was maintained in McCoy's 5A cell culture media (cellgro®, Manassas, VA; 10-050-CV) supplemented with 15% FBS and 1%

penicillin/streptomycin (GIBCO®, Carlsbad, CA; 15140122). With the exception of the experiments performed on unstarved and untreated growing cell lines in Fig. 1, 24 hours prior to all experiments, cells were washed with PBS and placed in Modified IMEM (GIBCO®, Carlsbad, CA; A10488) supplemented with either 1% or 5% charcoal-stripped FBS (i.e. DCC) (Hyclone, Fremont, CA; SH30068.03).

Immunoblotting

Total protein was extracted from whole cell lysates with a modified RIPA extraction buffer containing PMSF (1 mM), NaF (5 mM), Na_3VO_4 (10 mg/mL), β-glycerophosphate (25 mM), β-ME (14.3 mM), aprotonin (11,140 KIU/mL), and 1 Complete Mini-Protease Inhibitor Cocktail tablet (Roche, Indianapolis, IN; 1 836 153 001). Lysates were sonicated with a Microson™ ultrasonic homogenizor for 10 s (setting 10) (Misonix, Farmingdale, NY; XL2000) and clarified by 10 min of centrifugation at 14,000 rpm at 4º C. Protein concentration was quantified by the Bradford method (Bio-Rad Protein Assay, Bio-Rad, Hercules, CA; 500-0001) and equal protein amounts were transferred to Immobilon-P™ PVDF membranes (Millipore, Billerica, MA; IPVH00010) after fractionation by 10% SDS-PAGE. All Western blots were blocked for 1 hour at RT in phosphate-buffered saline/0.1% Tween-20 (PBS-T) containing 5% dried milk (Sanalac, Middleton, WI). All Western blots were probed overnight at 4º C in PBS-T containing 1% dried milk using the following primary antibodies: PR-A/B (Ab-8, NeoMarkers, Fremont, CA; MS-298-P), full-length and cleaved-PARP (Asp214) (19F4, Cell Signaling Technology, Danvers, MA; 9546), p21 (DCS60, Cell Signaling Technology,

Danvers, MA; 2946), phospho-STAT3 (Tyr705) (Cell Signaling Technology, Danvers, MA; 9131), STAT3 (Cell Signaling Technology, Danvers, MA; 9132), and Actin (Sigma-Aldrich®, St. Louis, MO; A4700). HRP-conjugated goat anti-rabbit (Bio-Rad, Hercules, CA; 170-6515) and rabbit anti-mouse (Bio-Rad, Hercules, CA; 170-6516) secondary antibodies were used to detect their respective primary antibodies, and immunoreactive proteins were visualized on radiographic film (Kodak, Rochester, NY) following ECL detection with Super Signal® West Pico Maximum Sensitivity Substrate (Pierce, Rockford, IL; 34080).

Quantitative-PCR (qPCR)

Total RNA was extracted from cell samples using TRIzol® (Invitrogen, Carlsbad, CA; 15596-018) separation and isopropanol precipitation. RNA (1.0 μg) was reverse transcribed to cDNA according to manufacturer's instructions using the Transcriptor First Strand cDNA Synthesis Kit (Roche, Indianapolis, IN; 04 897 030 001). qPCR was performed using Light Cycler® FastStart DNA Master SYBR Green I (Roche, Indianapolis, IN; 03 515 885 001) on a Light Cycler® 480 II Real-Time PCR System (Roche, Indianapolis, IN; 05 015 278 001). Human primers (Integrated DNA Technologies, Coralville, IA) were specific for: PR-A/B (5'-aaatcattgccaggttttcg-3' and 5'-tgccacatggtaaggcataa-3'), p14 (5'-tgctcacctctggtgccaaag-3' and 5'-tggtcttctaggaagcggctg-3'), p53 (5'-gcgcacagaggaagagaatc-3' and 5'-cctcattcagctctcggaac-3'), p21 (5'-gactctcagggtcgaaaacg-3' and 5'-ggattagggcttcctcttgg-3'), p27 (5'-tgcaaccgacgattcttctactcaa-3' and 5'-caagcagtgatgtatctgataaacaagga-3'), p16 (5'-

gctgcccaacgcaccgaata-3' and 5'-accaccagcgtgtccaggaa-3'), pRb (5'-tgcatggctctcagattcac-3' and 5'-aaggctgaggttgcttgtgt-3'), HDM2 (5'-atctacagggacgccatcga-3' and 5'-tgcctgatacacagtaacttgatatacct-3'), E2F1 (5'-gccctcaaggacgttggtg-3' and 5'-ccgccatccaggaaaaggt-3'), STAT1 (5'-tggtgaaattgcaagagctg-3' and 5'-gttctggtgccagcattttt-3'), STAT3 (5'-tttcacttgggtggagaagg-3' and 5'-tctggccgacaatactttcc-3'), STAT5A (5'-ctgaacaactgctgcgtgat-3' and gtggacgatgacaaccacag-3'), and STAT5B (5'-gtgaagccacagatcaagca-3' and 5'-tacgtccattgtgtcctcca-3'). Target gene qPCR values were normalized to expression of the housekeeping genes β-actin (5'-tcagaaggattcctatgtgggc-3' and 5'-atcttctcgcggttggcctt-3') or GAPDH (5'-ttgttgccatcaatgaccc-3' and 5'-catcgccccacttgattt-3').

Stable Cell Line Generation

All cell lines created herein were generated by transfecting 1 X 10^5 cells growing in 100 mm plates overnight with 2.0 µg of their respective plasmids (see below) using FuGene HD® transfection reagent (Roche, Indianapolis, IN; 04 709 713 001) according to manufacturer's instructions. After transfection, all cell lines were washed with PBS and immediately placed into their respective selection media (see below). When distinct clonal cell colonies became present, they were removed with 3 mm cloning discs (Fisher Scientific, Pittsburgh, PA; 378470001) soaked in 0.25% trypsin-EDTA (GIBCO®, Carlsbad, CA; 25200-056) and re-plated into 6-well plates. Selected cell colonies were expanded and screened for stable changes in target gene expression (see Results). Control-GFP and PR-B-

GFP stable cell lines were generated using the parental ES-2 cell line as a model system. The human PR-B gene was previously cloned into the pEGFP-N3 vector (Clontech Laboratories, Inc., Mountain View, CA; 6080-1) which also served as the empty Control-GFP vector [118]. Stably expressing cell colonies were selected in and maintained with McCoy's 5A cell culture media (cellgro®, Manassas, VA; 10-050-CV) supplemented with 15% FBS, 1% penicillin/streptomycin (GIBCO®, Carlsbad, CA; 15140122), and 0.5 mg/mL of G418 sulfate (Fisher Scientific, Pittsburgh, PA; MT-61-234-RG). Fluorescence-activated cell sorting (FACS) with a FACSDiva™ cell sorter (BD Biosciences, San Jose, CA) was used to purify Control-GFP (1X) and PR-B-GFP (2X's) stable cell lines by removing any low and non-GFP-expressing cells. Stable shRNA cell lines were created by transfecting PR-B-GFP expressing ES-2 cells with lentiviral vectors containing target gene shRNA sequences from the Open Biosystems Expression Arrest™ TRC Library. shRNA cell colonies were selected in and maintained with McCoy's 5A cell culture media (cellgro®, Manassas, VA; 10-050-CV) supplemented with 15% FBS, 1% penicillin/streptomycin (GIBCO®, Carlsbad, CA; 15140122), 0.5 mg/mL of G418 sulfate (Fisher Scientific, Pittsburgh, PA; MT-61-234-RG), and 0.5 µg/mL of puromycin (Clontech Laboratories, Inc., Mountain View, CA; 631305). 1.) Stably expressing control shRNA PR-B-GFP cells were created using a pLKO.1 empty vector (Thermo Scientific Open Biosystems, Huntsville, AL; RHS4080) containing an 18 bp non-targeting, non-specific "stuffer sequence". 2.) Stably expressing STAT3 shRNA PR-B-GFP cells were created using a pLKO.1 lentiviral vector targeting STAT3

transcript variants 1-3 (Thermo Scientific Open Biosystems, Huntsville, AL; Clone I.D. TRCN0000020843). 3.) Stably expressing p21 shRNA PR-B-GFP cells were created using a pLKO.1 lentiviral vector targeting p21 transcript variants 1 and 2 (Thermo Scientific Open Biosystems, Huntsville, AL; Clone I.D. TRCN0000010401).

Luciferase Assays

All cell lines used herein were plated at a density of 1 X 10^5 cells/well in 6-well plates. The following day, cells were co-transfected overnight using FuGene HD® transfection reagent (Roche, Indianapolis, IN; 04 709 713 001) according to manufacturer's instructions with 0.9 µg of either a PRE-containing [91] or a p21 promoter-containing [119] firefly luciferase reporter construct and 0.1 µg of a constitutively active pRL-TK-*Renilla* luciferase construct (Promega, Madison, WI; E2241). The next day, cells were washed with PBS and starved for 24 hours in 1% DCC. After starvation, cells were treated as described (see Results) for the indicated times in 1% DCC. After treatment, samples were washed with ice-cold PBS and harvested in 200 µL of 1X passive lysis buffer (Promega, Madison, WI; E1941). Cellular debris was removed by 10 min of centrifugation at 14,000 rpm at 4º C. Samples were analyzed for 10.0 s each by a Monolight™ 3010 luminometer (BD Biosciences, San Jose, CA; 556861) that injected 80 µL of firefly-luciferase substrate followed by 100 µL of Stop-N-Glo® *Renilla*-luciferase substrate (Promega, Madison, WI; E1960).

Histology and Microscopy

All brightfield and fluorescent cell images described herein were acquired with an Axioplan 2 upright microscope (Zeiss, Thornwood, NY) and captured using a SPOT™ camera and SPOT™ imaging software (Diagnostic Instruments, Inc., Sterling Heights, MI). Cellular membranes were stained for 15 min at RT with Texas Red®-X-conjugated wheat germ agglutinin (1 µg/mL) (Invitrogen, Carlsbad, CA; W21405), and all cell nuclei were stained with DAPI containing ProLong® Gold antifade reagent (Invitrogen, Carlsbad, CA; P36935). Fixed and live cell soft-agar images were acquired with a Leica DM IL inverted microscope (Leica Microsystems, Inc., Bannockburn, IL) and captured using a MagnaFire® camera and MagnaFire® imaging software (Olympus®, Melville, NY).

MTT Assays

All cell lines used herein were plated at a density of 1 X 10^5 cells/well in 24-well plates. The following day, cells were washed with PBS and starved for 24 hours in 5% DCC. After starvation, cells were continuously treated as described (see Results) for the indicated times in 0.5 mL of 5% DCC. Cell samples did not receive treatment replenishment or media re-supplementation during the course of the experiment. At each respective timepoint, 60 µL of MTT dye (5 mg/mL) (Sigma-Aldrich®, St. Louis, MO; M2128) was added to each sample and allowed to incubate at 37º C for 3.0 hours. Media and dye were removed and cell samples were resuspended in 500 µL of solubilization solution (95% DMSO, 5%

IMEM). Absorbance measurements from each sample were read in duplicate using Ascent Software (Thermo Scientific, Waltham, MA; 50-950-541) on a Multiskan Plus Microplate Reader (Thermo Scientific, Waltham, MA; 14-386-27) at 570 nm with background subtraction at 650 nm. All timepoint values were normalized to absorbance measurements of untreated samples taken at the beginning of each experiment (i.e. Day 0).

Anchorage-independent Growth Assays (i.e. Soft-agar)

One mL of 0.8% SeaPlaque® GTG® LMP agarose (BioWhittaker, Rockland, ME; 50110) containing 5% DCC was solidified per well in 6-well plates as the lower agarose base. A total of 2 X 10^4 cells from each cell line were suspended in 0.48% agarose containing 5% DCC with their respective treatments (see Results) and overlaid on the lower agarose base. After 4 weeks of growth at 37º C, cell colonies were stained with 0.1% crystal violet for 1 hr at RT and washed with PBS. 1,000 randomly chosen cell colonies per well were separated according to size (total pixels/colony area) and quantified using Photoshop® version 7.0 (Adobe® Systems, Inc., San Jose, CA).

Senescence Associated-β-galactosidase (SA-β-gal) Activity Assays

All cell lines used herein were plated at a density of 1 X 10^4 cells/well on glass coverslips in 6-well plates. The following day, cells were washed with PBS and starved for 24 hours in 5% DCC. After starvation, cells were continuously treated as described (see Results) in 5% DCC for the indicated times. Cell samples did

not receive treatment replenishment or media re-supplementation during the course of the experiment. At the given timepoints, cells were washed, fixed, and stained for SA-β-gal activity according to manufacturer's instructions using the Senescence β-Galactosidase Staining Kit (Cell Signaling Technology, Danvers, MA; 9860). After staining, cell samples were washed two times with PBS and mounted onto glass slides for brightfield microscopy.

Flow Cytometry

All cell lines used herein were plated at a density of 1 X 10^4 cells/well in 6-well plates. The following day, cells were washed with PBS and starved for 24 hours in 5% DCC. After starvation, cells were continuously treated as described (see Results) in 5% DCC for the indicated times. Cell samples did not receive treatment replenishment or media re-supplementation during the course of the experiment. At the given timepoints, cell culture media was collected, PBS washings were collected, and cells were harvested by trypsinization and centrifugation at 1,000 x *g* for 4 min at RT. Cells were resuspended in 300 µL of PBS containing 10% FBS and fixed by adding 4 mL of ice-cold 80% ethanol dropwise while vortexing. Samples were stored overnight at -20º C. Samples were washed three times with 5 mL of ice-cold PBS, resuspended in 1 mL of PBS containing 1% FBS, and cleared through the cell-strainer cap of a BD Falcon™ round bottom tube (BD Biosciences, San Jose, CA; 352235). Cells were stained with 2 µg/mL of Hoechst 33342 DNA-specific dye (Invitrogen, Carlsbad, CA; H3570) and 0.5 µg/mL of Pyronin Y RNA-specific dye (Sigma-Aldrich®, St.

Louis, MO; P9172). FACS analysis performed on a BD™ LSR II Flow Cytometer System (BD Biosciences, San Jose, CA) was used for cell-cycle analysis and separation of the G_0 (Hoescht-low and Pyronin Y-low) and G_1 (Hoescht-low and Pyronin Y-high) phases of the cell-cycle as previously described [120].

Chromatin Immunoprecipitation (ChIP)

All cell lines used herein were plated at a density of 1 X 10^6 cells per 150 mm plate. The following day, cells were washed with PBS and starved for 24 hours in 1% DCC. After starvation, cells were treated as described (see Results) for 1.0 hr in 1% DCC and cell samples were harvested, fixed, and lysed according to manufacturer's instructions using the ChIP-IT™ Express Magnetic Chromatin Immunoprecipitation Kit (Active Motif®, Carlsbad, CA; 53008). Samples were homogenized using a Bioruptor® sonicator (Diagenode, Inc., Sparta, NJ; UCD-200 TM) operating at 30 s pulse intervals for 30 min at 4º C. ChIP reactions were incubated overnight on an end-to-end rotator using 60 µL of isolated chromatin and either 2 µg of PR-A/B antibody (Ab-8, NeoMarkers, Fremont, CA; MS-298-P) or 0.4 µg of normal mouse IgG (Santa Cruz Biotechnology, Inc., Santa Cruz, CA; SC-2025). Samples were washed, eluted, reverse cross-linked, and treated with Proteinase K according to manufacturer's instructions (Active Motif®, Carlsbad, CA; 53008). Standard PCR using a PTC-100® Thermal Cycler (MJ Research, Inc., Waltham, MA; PTC-1196) and qPCR using a Light Cycler® 480 II Real-Time PCR System (Roche, Indianapolis, IN; 05 015 278 001) were performed on isolated chromatin samples using primers spanning the proximal Sp1 sites of the

p21 gene promoter from bases -117 to -65 (5'-ggcactcttgttcccccaggc-3' and 5'-accatccccttcctcacctg-3') [121]. Touchdown PCR and touchdown qPCR cycling conditions were as follows: initial denaturation for 10 min @ 95° C; denature for 20 s @ 95° C, anneal for 20 s @ 66º → 56º C for cycles 1-10 and 56º for cycles 11-50, and extension at 72º C for 20 s.

Human Tissue Sampling and PR Immunohistochemistry

Tissue microarrays (TMA's) were constructed as previously described [122] from representative tumor areas using a tissue arrayer (Beecher Instruments, Silver Spring, MD and Pathology Devices, Westminster, MD). Two cores of 0.6 mm diameter were taken from each donor block and transferred to the recipient block. 4 µm thick sections were cut and stained within 2 weeks after sectioning. Arrays were stained for PR as outlined below:

Marker	Supplier	Cat#	Host	Clone	Antigen Retrieval	Primary incubation time	Dilution	Detection system
PR	Ventana	790-2223	Rabbit	1E2	Standard CC1	8min with heat	prediluted	DABMap

Immunohistochemistry was scored using a subjective assessment of percent positive cells in a TMA core where scores of '0' = no positive cells, '1' = > 0% but < 15%, '2' = ≥ 15% but < 50%, and '3' = ≥ 50%. Recursive partitioning was used to determine the binarisation cutpoint for optimal separation of the five major sub-types of ovarian carcinoma and resulted in raw scores of '0' being considered negative (coded as '0') and raw scores greater than '0' being considered positive

(coded as '1'). Contingency analysis was used to determine if there was differential expression of PR across the five major sub-types of ovarian carcinoma, and the significance of those differences was determined by the Pearson Chi Square (X^2) statistic.

Primary Human Ovarian Cancer Cell Isolation

Cancerous human tissue samples were harvested at the time of surgery and immediately placed in 37º C PBS. Tissue samples were dissected into small pieces and placed in 6-well plates containing 0.25% trypsin-EDTA (1mM) (GIBCO®, Carlsbad, CA; 25200-056) for 3 hours at 37º C. Trypsinization was neutralized 1:1 with serum supplemented cell culture media and cells were allowed to plate overnight. The following day, partially digested tissue was removed and adherent cells were extensively washed with PBS before cell culture media was replaced. All tissue samples were typed and graded by in-house surgical pathologists.

Statistical Analysis

All reported values represent the mean ± the standard deviation (SD). Where used, fold-change was determined by dividing each individual sample of the "treatment" group by the mean of the "control" group. Statistical analyses were performed using a Student's *t*-test where significance was determined with 95% confidence ($p \leq 0.05$).

3.3 Results

Expression of the progesterone receptor (PR) is often decreased or absent in human ovarian cancer tissue samples (see Introduction). Therefore, we began our studies by screening a panel of eight distinct and commonly-used ovarian cancer cell lines of epithelial origin for PR expression. Regardless of histologic sub-type (adenocarcinoma = OVCAR-5, SKOV-3, CAOV-3; clear cell carcinoma = ES-2, TOV-21G; papillary adenocarcinoma = OVCAR-3; papillary cystadenocarcinoma = HEY; endometrioid carcinoma = TOV-112D), PR protein expression was undetectable in every ovarian cancer cell line studied (Fig. 1A). Additionally, quantitative-PCR (qPCR) analysis detected only negligible amounts of PR mRNA present in these cell lines (Fig. 1B). However, because PR mRNA was at least minimally present, the loss of PR expression in these cell lines is likely not due to a complete deletion of the PR gene (ch. 11q23.3-24.3) but may be the result of a genetic loss of heterozygosity (LOH) as seen in approximately 75% of ovarian tumors [66-68]. Other possible explanations for reduced PR expression include a decreased responsiveness of ovarian cancer cells to estrogen-mediated PR transcription [123], hyper-methylation-induced silencing of the PR promoter [124], or other unidentified mechanisms (i.e. miRNAs, translational control, protein stability) all warranting further investigation

In order to investigate the impact PR expression and signaling may have on ovarian cancer cell biology, we created a PR expressing ovarian cancer cell line. ES-2 clear cell carcinoma cells were chosen as our model system because

of their inherently aggressive nature, ease of transfection, rapid growth rate, ability to form xenografted tumors, and potential to ultimately re-express PR based on their mRNA expression profile (Fig. 1B). ES-2 cells were transfected with a GFP-tagged PR-B construct and clonally selected for PR protein expression levels comparable to the T47D-YB breast cancer cell line (Fig. 2A). Transgenic PR protein functioned appropriately in these cells, as stimulation with the more potent, longer lasting synthetic progestin R5020 caused a significant increase in transcription from a progesterone response element (PRE) containing luciferase reporter construct (Fig. 2B). Increased PRE-mediated transcription was specific to PR stimulation, as a second ES-2 cell line stably expressing only a GFP construct (Fig. 2A) failed to respond to ligand and the response seen in PR expressing cells was inhibited by the competitive PR antagonist RU486 (Fig. 2B). Finally, PR, a well characterized steroid hormone binding nuclear transcription factor, became visually concentrated within the nucleus of cells following ligand stimulation (Fig. 2C). Additionally, we also witnessed an increase in the overall size of nuclei present within PR expressing cells exposed to R5020 for as little as 24 hours (Fig. 2C).

After establishing a functionally responsive PR expressing model cell line, we investigated how PR may affect the growth characteristics of ES-2 ovarian cancer cells. Prior studies have shown that progesterone exhibits anti-proliferative effects on the growth of ovarian cancer cells [74-75,125] particularly at higher concentration levels [11,63,126]. However, to avoid activating other

unrelated progesterone receptors (i.e. members of the membrane progesterone receptor family (mb-PR-α, -β, and –γ) and progesterone receptor membrane component-1 (PGRMC1)), that were present in our cells (data not shown) with progesterone, cells were stimulated with the PR specific agonist R5020. To study how PR impacts cell proliferation over extended periods of time, we used the MTT (3-(4,5-dimethylthiazol-2-yl)-2,5-diphenyltetrazolium bromide) cell proliferation assay as a readout. Taking measurements at 2-day intervals, we observed a significant increase in the number of viable cells present beginning at day 8 and continuing through day 12 in PR expressing cells stimulated with R5020 versus vehicle-treated cells (Fig. 3A). Interestingly, however, the proliferative rate of ligand-stimulated cells was never greater than that of vehicle-treated cells, rather cells in the R5020 cohort failed to die in a predictable manner over a long period of time without media replenishment (Fig. 3A). Furthermore, the continued proliferation of ligand-stimulated cells ceased by day 8 of treatment as the number of viable cells present through day 12 remained unchanged (Fig. 3A). These findings suggest that ligand-activated PR does not influence cellular proliferation, but instead may be promoting an increase in long-term cell survival as the initial increase in the number of R5020-treated cells failed to decrease over time like in vehicle-treated cells. Therefore, we investigated whether PR influences cell survival using poly (ADP)-ribose polymerase (PARP) cleavage as an indicator of apoptotic cell death. Beginning as early as day 4, the amount of cleaved-PARP was greater in vehicle-treated samples compared to R5020-treated samples, thus indicating that PR activation inhibits apoptosis of ES-2

ovarian cancer cells (Fig. 3B). However, these combined observations indicating that PR improves ovarian cancer cell survival are contrary to several previous reports demonstrating that the exposure of ovarian cancer cells to progesterone leads to an increase in apoptotic cell death [26-27,74-76,127].

The results of our MTT cell proliferation assay indicated that ligand activated PR did not affect the proliferative rate of cells grown on a two-dimensional matrix when growth factor supplementation was limiting (Fig. 3A). Therefore, we used a soft-agar based colony formation assay to better understand how PR impacts the proliferation of ES-2 ovarian cancer cells in an anchorage-independent manner. When grown under these conditions for four weeks, R5020 stimulation dramatically inhibited the formation of PR expressing cell colonies (Fig. 4A). Additionally, when an equal number of colonies were objectively sorted based on size by computer analysis, there were significantly more smaller colonies (0-25 pixels) present and significantly fewer large colonies (51-75 and 76-100 pixels) present in the ligand-stimulated group of PR expressing cells (Fig. 4B). Of great surprise, however, was that even after 4 weeks of growth, single- and two-celled PR expressing “colonies” were present and viable in the R5020 treated cohort (Fig. 4B, inset).

Contrary to an overwhelming amount of evidence demonstrating the pro-survival and pro-proliferative impact of PR on breast cancer cells, we were faced with explaining a pro-survival but anti-proliferative phenotype in PR expressing ES-2 ovarian cancer cells. However, this seemingly paradoxical scenario where

cells exist in a viable and metabolically active but non-proliferative state could potentially be explained by the phenomenon of cellular senescence. The exit of proliferating cells from the cell-cycle (i.e. into G_0) can be separated into a quiescent arm, where cells are capable of re-entering the cell-cycle once withdrawn growth factors are re-introduced, and a senescent arm that is classically defined as a state of permanent cell-cycle arrest [128-129]. Therefore, we analyzed whether PR expressing ES-2 ovarian cancer cells were undergoing a senescent transition following prolonged ligand stimulation based on three phenotypic criteria commonly used to identify cellular senescence. The first and most common means of detecting senescence is via senescence associated-β-galactosidase (SA-β-gal) activity; a lysosomal hydrolase with an optimum activity at pH = 6.0 [130-131]. Examining PR expressing cells after 12 days of R5020 exposure identified the presence of SA-β-gal positive cells (Fig. 5A, panel 2, arrowheads). (Note: These findings were confirmed in a second stable PR expressing clone not discussed herein). When compared to SA-β-gal negative cells present within the same culture (Fig. 5A, panel 2, asterisk), SA-β-gal positive cells were larger and more flattened in appearance; morphologic changes characteristic of senescent cells (Fig. 5A, panels 3 and 4, arrowheads) [132]. We also noticed that many SA-β-gal positive cells contained more than one nucleus (data not shown). Finally, in order to objectively quantify the percentage of PR expressing cells exiting the cell-cycle into the G_0 phase, we used flow cytometry to separate cells existing in G_0 from the G_0/G_1 compartment [120]. As a result, after 12 days of ligand exposure, we observed a significant

increase in the percentage of PR expressing cells exiting the cell-cycle into G_0 as compared to vehicle-treated cells, while the percentage of cells remaining in the G_1 phase was significantly decreased (Fig. 5B).

Separating the G_0 and G_1 phases of the cell-cycle by flow cytometry using the RNA-specific Pyronin Y stain is based on the transcriptional repression and reduced cellular RNA content commonly observed in cells that have exited the cell-cycle into G_0. In our studies, however, even though the percentage of cells in the G_1 phase of the cell-cycle was significantly decreased (Fig. 5B), dot plot contour analysis revealed a small population of R5020-treated cells present in G_1 that possessed higher cellular RNA levels than vehicle-treated G_1 cells (Fig. 5B, shaded region). This observation, combined with a decrease in the amount of tri-methylation at lysine 9 of histone H3 as seen in transcriptionally inactive heterochromatic foci (data not shown), suggests that PR-induced senescence is perhaps regulated by the increased expression of pro-senescence gene targets.

While the variety of mechanisms associated with cellular senescence is constantly expanding, there are two main signaling pathways involving cell-cycle control that are primarily responsible for regulating senescence induction. These two pathways include the p14-HDM2-p53-p21 and p16-CDK-pRb-E2F axes that when induced by a host of pro-senescence signaling molecules can independently achieve senescence growth arrest (Fig. 6A) [133]. Therefore, because known PR gene targets are included in these two pathways, and we observed increases in total RNA content present in ligand-stimulated cells (Fig.

5B), we explored each individual member of these pathways for changes in mRNA expression (Fig. 6B). Of all senescence gene targets analyzed, mRNA levels of the potent cell-cycle inhibitor p21 (a.k.a. CIP1, WAF1, CDKN1A) exhibited the greatest change in expression with an increase of greater than 50% in PR expressing cells exposed to R5020 for 4 days (Fig. 6B). Furthermore, p21 gene (Fig. 6C) and protein (Fig. 6D) expression were significantly increased after only 24 hours of ligand stimulation and were inhibited by the competitive PR antagonist RU486 (Fig. 6D). p21 is a well-known cell-cycle inhibitor best characterized for its ability to prevent the transition from the G_1 phase to the S phase by blocking cyclin E-CDK2 activity and to a lesser extent cyclin A-CDK1/2 and cyclin B1-CDK1 activities [134]. For this reason, increased p21 expression and activity have been directly linked to the induction of cellular senescence [135-137].

To better understand the time necessary for a majority of cells to achieve a state of senescence, we performed a 12 day timecourse examining SA-β-gal activity at 4 day intervals (Fig. 7A). Interestingly, the number of PR expressing cells that became SA-β-gal positive steadily increased over time with ligand stimulation in a manner reflective of the plateau in cellular proliferation seen by MTT assay (Fig. 3A). PR expressing cells exposed only to vehicle control remained SA-β-gal negative over time indicating that the induction of senescence occurs in a ligand-dependent fashion specific to PR expressing cells (Fig. 7A). Furthermore, p21 expression was significantly increased throughout our

timecourse studies in R5020 treated PR expressing cells at both the transcriptional (Fig. 7B) and protein (Fig. 7C) levels. Based on our findings that liganded PR promotes cellular senescence and causes a sustained increase in expression of the pro-senescence marker p21, we hypothesized that PR-induced senescence may occur in a p21-dependent manner.

However, before investigating the role of p21 in PR-mediated senescence further, we sought to extend our findings to sub-types of ovarian cancer other than clear cell carcinomas (i.e. ES-2 cells). Therefore, we similarly generated a stably expressing PR positive cell line using OVCAR-3 papillary adenocarcinoma cells as a model system (see Fig. 1). We clonally selected stably transfected OVCAR-3 cells, which are otherwise PR null, that displayed levels of PR expression comparable to our original PR positive ES-2 cell line (Fig. 8A). PR positive OVCAR-3 cells were analyzed for increased SA-β-gal activity and the development of senescence over a 12 day time period (Fig. 8B). As witnessed in our PR expressing ES-2 cells, PR positive OVCAR-3 cells underwent cellular senescence after exposure to ligand for 12 days while vehicle-treated cells displayed no signs of SA-β-gal activity (Fig. 8B). However, we noticed that senescence occurred in a less uniform fashion in ligand-activated PR expressing OVCAR-3 cells (Fig. 8B). The uneven distribution of senescent PR positive OVCAR-3 cells might be explained by recent descriptions of a senescence-messaging secretome and the influence senescent cells may have on non-senescent neighbors [138]. Nevertheless, the fact that cells of another histologic

sub-type also senesce supports the possibility that PR-mediated senescence is an anti-proliferative mechanism common to all ovarian cancer cells regardless of their origin.

Previous work in breast cancer cells has shown that PR stimulation increases p21 transcription and expression [119,139]. However, PR is also known to: 1.) increase the expression of signal transducer and activator of transcription (STAT) family members [119], 2.) form associations with STAT3 in PR-STAT3 complexes [140], and 3.) cause STAT transcriptional activation [140-141] which leads to STAT-mediated increases in p21 expression [142]. Therefore, to identify the mechanism behind PR-induced p21 expression in senescent ovarian cancer cells, we began by screening each STAT family member for PR-mediated changes in mRNA expression (Fig. 9A). After 12 days of ligand exposure, a time when cellular senescence is achieved in PR expressing cells (Fig. 5A and 7A), STAT1 and STAT3 transcription was significantly increased while STAT5A and STAT5B mRNA levels were unchanged (Fig. 9A). However, the nearly 2.5-fold relative increase in STAT3 expression was also significantly greater than the 1.6-fold increase in STAT1 mRNA levels (Fig. 9A). In addition to increasing STAT3 expression, ligand-activated PR also led to a time-dependent increase in STAT3 activation peaking at 24 hours of stimulation (Fig. 9B). Finally, both p21 and STAT3 mRNA levels were significantly increased by PR in response to progestin at each 4 day interval used to analyze the progression of cellular senescence (Fig. 9C).

Based on the observations that PR increases both p21 and STAT3 expression while promoting STAT3 phosphorylation, a known regulator of p21 transcription, we investigated whether increased p21 expression required PR-induced STAT3 activation. To address this question, we created a stable shRNA-mediated STAT3 knock-down cell line (STAT3-shRNA) using our PR expressing ES-2 ovarian cancer cells as a model system (Fig. 10A). For control purposes, a PR positive cell line stably expressing a non-specific, non-targeting shRNA sequence was also established (Control-shRNA) (Fig. 10A). Clonal cell lines were screened for significant STAT3 downregulation and selected based on PR and STAT3 expression consistent with the previously characterized control (Control-GFP) and PR (PR-GFP) expressing cell lines (Fig. 10A). A PRE-based luciferase reporter assay confirmed that ligand-induced PR transcriptional activity was unaltered in these newly generated double transgenic cell lines (Fig. 10B). Additional characterization of STAT3 knock-down cells (STAT3-shRNA) demonstrated PR nuclear translocation and retention as well as an increase in nuclear size after 24 hours of ligand exposure similar to that seen in control PR expressing cells (Control-shRNA) (Fig. 10C).

Based on reports implicating STAT3 as a positive regulator of p21 transcription [119,142], we predicted that in the setting of decreased STAT3 expression PR would be unable to increase p21 expression to a degree necessary for inducing cellular senescence. Therefore, when we examined PR expressing STAT3 knock-down cells treated with R5020 for 8 days, we were

surprised to see that a majority of cells were strongly SA-β-gal positive (Fig. 11A, panel 2) while the remaining minority were mildly SA-β-gal positive (Figure. 11A, panel 2, asterisk). Progestin-stimulated STAT3 knock-down cells exhibited a larger and more flattened morphology as seen before in senescent PR expressing cells possessing normal STAT3 levels (Fig. 11A, panels 3 and 4). A majority of senescent cells were again also multi-nucleated (data not shown). Previous observations demonstrated an increase in the percentage of ligand-induced PR expressing cells with normal STAT3 levels present in the G_0 phase of the cell-cycle (Fig. 5B). However, following 12 days of progestin-stimulation, we observed a significant decrease in the percentage of STAT3 knock-down cells present in the G_0 fraction and a significant increase in the percentage of these cells in the G_1 fraction (Fig. 11B). These seemingly discordant findings are explainable by the fact that senescent cells can exist in phases of the cell-cycle other than G_0 [133]. Therefore, knowing that our senescent cell population was more transcriptionally active and resided in G_1, we returned our attention to p21 whose main function is to arrest cells in G_1 by preventing S phase transition [134].

Surprisingly, when we analyzed p21 mRNA levels in PR expressing STAT3 knock-down cells, there was a significant increase in p21 mRNA levels after 24 hours of ligand stimulation when compared to control-treated cells (Fig. 12A). Additionally, we also observed a significant increase of PR-induced p21 levels in R5020-treated STAT3 knock-down cells (STAT3-shRNA) versus R5020-

treated control PR positive cells (Control-shRNA) (Fig. 12A). Increased p21 transcription also translated into upregulated p21 protein expression that was again blocked by the competitive PR antagonist RU486 (Fig. 12B). However, in order to determine whether the differences in PR-induced p21 mRNA levels between cell lines was the result of increased transcription and not differences in basal p21 expression from cell line variation, we transfected cells with a luciferase reporter construct containing the proximal region of the p21 promoter (Fig. 11C). Ligand-induced, PR-mediated transcription of the p21 promoter was significantly enhanced in cells exhibiting down-regulated STAT3 expression (STAT3-shRNA) when compared to cells possessing normal levels of STAT3 expression (Control-shRNA) (Fig. 12C).

Based on the amplification of PR-induced p21 expression observed in STAT3 knock-down cells, we examined whether the development of cellular senescence would also be altered. As a result, when STAT3 expression was downregulated, SA-β-gal activity revealed a dramatic acceleration in the time required for progestin-stimulated PR expressing cells to become senescent (Fig. 13A). While the number of SA-β-gal positive PR expressing control cells (Control-shRNA) gradually increased every four days with ligand exposure, a majority of PR expressing STAT3 knock-down cells were senescent after only 4 days of treatment with R5020 (Fig. 13A). Furthermore, the accelerated rate of senescence in STAT3 knock-down cells (STAT3-shRNA) exposed to ligand for 4 days correlated with a significantly enhanced relative fold-increase in p21 mRNA

levels versus control PR expressing cells (Control-shRNA) (Fig. 13B). Additionally, after 8 days of ligand stimulation, p21 protein levels were upregulated in both PR expressing cell lines (Fig. 13C). However, compared to basal p21 protein expression in vehicle-treated cells, progestin-mediated p21 induction was greater in STAT3 knock-down cells (STAT3-shRNA) (Fig. 13C).

Although STAT3 is most commonly seen as a positive regulator of p21 transcription, our observations suggest that STAT3 negatively regulates PR-induced p21 transcription, and when downregulated, leads to enhanced cellular senescence because of a substantial increase in p21 expression. Therefore, we performed chromatin immunoprecipitation (ChIP) assays of the p21 promoter to more clearly define the relationship between PR, STAT3, and the control of p21 transcription. In vehicle-treated PR expressing cells (PR-GFP), we found that both PR and STAT3 are tonically associated with the same region of the p21 promoter previously characterized to contain four Sp1 transcription factor binding sites (Fig. 14A) [143]. Secondly, after 1 hour of ligand stimulation, additional PR molecules were not recruited to the p21 promoter in PR expressing cells (PR-GFP) even though STAT3 became disassociated (Fig. 14A). However, the recruitment of PR to the p21 promoter was greatly enhanced in PR expressing STAT3 knock-down cells (STAT3-shRNA) after 1 hour of ligand exposure (Fig. 14A). These findings were confirmed visually, as nuclear translocation and retention of PR-GFP was more pronounced in STAT3 knock-down cells; these cells also displayed a more uniform and less punctuate distribution of PR-GFP

throughout the nucleus (Fig. 14B). When normalized to total input DNA levels, the amount of PR recruited to the p21 promoter following R5020 exposure was unchanged in PR positive cells expressing normal STAT3 levels (Control-shRNA), while the amount of ligand-activated PR bound to the p21 promoter increased greater than 1.5-fold when STAT3 expression was downregulated (Fig. 14C).

Taken together, these findings regarding PR, STAT3, and p21 transcription have allowed us to develop a working model to explain how PR promotes cellular sensescence via STAT3-regulated p21 induction (Fig. 14D). 1.) Progesterone can stimulate either PR within the cytoplasm causing its nuclear translocation and retention or unliganded PR already present within the nucleus; both leading to the binding of PR to the p21 promoter. 2.) STAT3 is tonically bound to the same site on the p21 promoter as PR and prevents both additional PR recruitment and PR-induced p21 transcription. 3.) Removal of STAT3 from the p21 promoter allows for additional PR molecules to be recruited and for PR-induced p21 transcription to proceed. 4.) When STAT3 expression is downregulated, a substantial enhancement of PR-mediated p21 expression forces PR expressing cells to more rapidly senesce and arrest in the G_1 phase of the cell-cycle. 5.) When STAT3 is expressed at normal levels, moderate increases in PR-dependent p21 expression cause PR expressing cells to gradually undergo cellular senescence by exiting the cell-cycle into G_0.

After establishing that ligand stimulation causes PR expressing ovarian cancer cells to become senescent while increasing STAT3-regulated p21 expression, we sought to determine whether this response was dependent upon p21 cell-cycle inhibition. Therefore, using PR expressing ES-2 cells, we created a shRNA-mediated cell line exhibiting stably downregulated p21 expression. Stable knock-down of p21 expression occurred at both the transcriptional (p21 qPCR, Fig. 15A) and protein (p21 Western blot, Fig. 15B) levels. However, knowing that activated PR increases p21 expression in ES-2 ovarian cancer cells, we confirmed that p21 protein levels in our knock-down cells would remain downregulated following prolonged ligand stimulation (i.e. 8 days) compared to Control-shRNA cells (Fig. 15B). Finally, we analyzed how p21 downregulation would impact PR-mediated senescence over time based on SA-β-gal activity. Based on our hypothesis and prior findings, we expected to observe absent, reduced, or delayed senescence when p21 induction was blocked. Instead, we witnessed a reduction in the time required for senescence to occur and a dramatic increase in the degree of senescence induction (Fig. 15C). Although unexpected, these findings do however demonstrate that ligand-activated PR induces ovarian cancer cell senescence in association with or in the absence of p21 upregulation.

3.4 Discussion

While progesterone receptor (PR) signaling and action is well characterized for breast cancer cells, very little is known about the actions of PR in ovarian cancer. The fact that PR expression is commonly lost during ovarian cancer development and that patients with PR negative tumors have significantly worse outcomes suggests that PR possesses tumor-suppressive properties. However, PR signaling and its impact on ovarian cancer tumor cell biology is virtually unstudied. Therefore, the goal of our studies was to define PR as an ovarian cancer cell tumor suppressor and characterize the signaling mechanisms responsible for tumor cell inhibition. The further exploitation of these pathways may lead to the discovery and development of novel therapies effective in treating both PR positive and PR null ovarian tumors.

After successfully establishing multiple stable clones of PR expressing ES-2 ovarian cancer cells, we observed significant changes in tumor cell behavior. Ligand-activated PR promoted a pro-survival but anti-proliferative phenotype in ovarian cancer cells. Interestingly, the phenomenon of cellular senescence was able to explain these findings. Cellular senescence, defined as a state of permanent cell-cycle arrest, is being increasingly accepted as an inherent cellular mechanism for inhibiting oncogenesis [129,133,144-146]. We were able to definitively demonstrate that in the presence of ligand, PR expressing cells became senescent based on the gradual increase over time in senescence-associated β-galactosidase (SA-β-gal) activity, larger and more flattened morphologic changes, and increased cell-cycle exit into the G_0 phase.

However, flow-cytometry cell-cycle analysis, which allowed us to separate the G_0 and G_1 phases from the G_0/G_1 compartment, revealed the presence of ligand-treated cells with increased cellular RNA content. This obscure finding was a key starting point to understanding how PR expressing cells undergo senescence, as it suggested that PR regulates the expression of key senescence-associated target genes.

Screening each member of the two major senescence signaling pathways for changes in gene expression led to the identification of p21 as a PR target gene in senescent ovarian cancer cells. This observation was significant because not only is p21 defined as a major negative regulator of the cell-cycle (via CDK1/2 inhibition), but p21 activity has also been linked to promoting cellular senescence [135-137]. Previous work in breast cancer cells has shown that PR stimulation leads to an increase in p21 gene transcription [119]. Additional studies have shown that p21 transcription is also positively regulated by STAT3, a member of the STAT family of transcription factors [142]. Therefore, when we observed increases of both p21 and STAT3 in senescent ovarian cancer cells and increased STAT3 phosphorylation following ligand stimulation, we hypothesized that p21 induction via PR was dependent upon STAT3. However, when we generated a PR expressing ovarian cancer cell line stably downregulating STAT3 expression, we were surprised to find that ligand-induced p21 transcription was significantly increased. This finding thus suggested that STAT3 acts to inhibit PR-mediated p21 induction.

While STAT3 is widely accepted as a positive regulator of p21 transcription [119,142], one report characterizes STAT3 as a transcriptional repressor of both p53 and p21 in melanoma cells [147]. Furthermore, more recent work demonstrates that STAT3 is constitutively active in ovarian cancer tissue samples [148]. These observations thus led us to hypothesize that STAT3 limits the induction of p21 transcription by ligand-activated PR. Chromatin immunoprecipitation (ChIP) studies supported our hypothesis, as we observed a significant increase in the amount of PR bound to the p21 promoter in STAT3 knock-down cells when progestin was present. However, additional PR molecules were not recruited following ligand stimulation of PR expressing cells possessing normal STAT3 levels; a discrepancy that might be explained by the presence of discrete PR-containing nuclear bodies. After only one hour of ligand stimulation, PR became evenly distributed throughout the nucleus in STAT3 knock-down cells while a majority of nuclei in PR expressing cells with normal STAT3 levels still possessed punctuate PR foci. Therefore, the combination of our ChIP and PR localization results with an enhanced p21 expression response raises the possibility that STAT3 inhibits PR-mediated p21 transcription by sequestering nuclear PR in transcriptionally inactive PR-STAT3 complexes.

However, if STAT3 serves to block PR-mediated transcription, why in turn does PR cause an increase in STAT3 expression (Fig. 9A) and phosphorylation (Fig. 9B)? One possible explanation for this observation is that PR may use STAT3 to regulate its own transcriptional activity. When present, STAT3 limits

the amount of PR-induced p21 expression causing a gradual development of cellular senescence (Fig. 7A). When STAT3 is absent, however, PR transcriptional activity is uncontrolled leading to significantly enhanced p21 induction and accelerated cellular senescence (Fig. 13A). Therefore, we hypothesize that PR regulates its p21 gene dosage effects by directly increasing STAT3 transcription [119] and by indirectly activating STAT3 via IL-6 transcription and secretion (preliminary data not shown).

Finally, in an effort to demonstrate that the induction of cellular senescence by PR occurs in a p21-dependent manner, we generated a PR positive ovarian cancer cell line exhibiting stable downregulation of p21 expression. According to our hypothesis, in the face of decreased p21 levels, PR would be unable to cause ovarian cancer cell senescence. However, as occurred with STAT3 downregulation, ligand stimulation of PR expressing p21 knock-down cells caused a faster and more complete senescence response. At first glance, these results suggest that p21 is not responsible for mediating PR-induced senescence. However, a negative result in this scenario does not exclude p21 from being the primary mediator of PR-induced senescence, because in the absence of p21, PR may simply employ other mechanisms to promote cellular senescence. For example, PR could alter the expression of other undefined pro-senescence-associated gene targets, or acquire increased transcriptional activity due to unopposed CDK2 phosphorylation [149-150], or activate other known or unknown pro-senescence signaling pathways. Therefore, when p21 expression

is lost in ovarian cancer, these PR signaling alternatives may represent tumor suppressive fail-safe mechanisms which may cause senescence to occur more rapidly and thoroughly.

Nevertheless, the following observations suggest that PR-induced senescence prefers to utilize p21 as the primary mediator of cellular senescence. Firstly, of all mediators belonging to the two major senescence signaling pathways, p21 demonstrated the greatest change in expression and was significantly increased with ligand-activated PR throughout the gradual and accelerated progression of cellular senescence. Secondly, enhanced p21 upregulation (via STAT3 downregulation) caused a more robust senescence response. Lastly, PR activation led to cell-cycle exit into G_0, cell-cycle arrest in G_1, and cytokinetic defects in the G2/M transition; all characteristic effects of p21-mediated cell-cycle control [134,151-152]. Therefore, based on our results, we believe that PR-mediated senescence of ES-2 ovarian cancer cells preferentially occurs in a p21-dependent manner.

In summary, our work has shown that ligand-activated PR inhibits ovarian cancer cell proliferation by inducing a state of cellular senescence along with an associated increase in p21 expression. We have also found that STAT3 is an endogenous inhibitor of PR-mediated p21 transcription in ovarian cancer cells. Furthermore, when STAT3 transcriptional repression is removed, p21 induction is enhanced and accelerates PR-mediated senescence. This process may represent a new paradigm describing the ability of PR to “titrate” its own

transcriptional activity and gene dosage effects. Finally, PR stimulation also induces accelerated senescence in the absence of p21, thus suggesting that PR may be capable of activating multiple pro-senescence mechanisms. Each of these observations regarding PR-mediated cellular senescence is unique in its own right and has generated additional related lines of research warranting further investigation.

3.5 Acknowledgements

This work was supported by a grant from the Minnesota Ovarian Cancer Alliance (MOCA). We would like to thank Dr's. Amy Skubitz and Sundaram Ramakrishnan from the University of Minnesota Masonic Cancer Center for providing us with the ovarian cancer cell lines used herein, and members of the University of Minnesota Masonic Cancer Center's flow cytometry facility and Biomedical Image Processing Lab (BIPL) for their assistance in data collection. We would also like to thank Dr. Judith Campisi from Lawrence Berkeley National Laboratories (Life Sciences Division) and the Buck Institute for Age Research for sharing with us her expert opinions on the field of cellular senescence with respect to the results discussed herein.

3.6 Conflict of Interest

The authors declare that they have no conflict of interest.

3.7 Figure Legends

Figure 1 Progesterone receptor (PR) expression is absent in ovarian cancer cell lines. A.) Protein expression of the two PR isoforms (PR-A and PR-B) was absent in eight distinct ovarian cancer cell lines as determined by Western blot analysis compared to the T47D breast cancer cell line. **B.)** Quantitative-PCR detected insignificant amounts of PR-A and PR-B mRNA expression in a panel of eight ovarian cancer cell lines relative to the T47-D breast cancer cell line (all values were normalized to beta-actin levels, mean ± SD, n = 3).

Figure 2 Stable expression of the progesterone receptor (PR) in the ES-2 ovarian cancer cell line. A.) Western blot analysis demonstrated stable expression of GFP-tagged PR-B in ES-2 cells (PR-GFP) as compared to the ES-2 parental cell line (ES-2), ES-2 cells stably expressing only the GFP tagging construct (Control-GFP), and the PR-B expressing T47D-YB breast cancer cell line (T47D-YB). **B.)** Stimulation of PR-GFP expressing ES-2 cells for 48 hours with R5020 (10 nM) significantly increased (*) transcription from a transiently transfected progesterone response element (PRE) containing luciferase reporter construct which was specifically inhibited (#) by the PR antagonist RU486 (1 uM) (all values normalized to constitutive *Renilla* luciferase expression, mean ± SD, n = 4, $^{*,\#}p \leq 0.05$). **C.)** Fluorescence microscopy revealed increased nuclear co-

localization of PR-GFP with DAPI nuclear stain after 24 hours of stimulation with R5020 (10 nM) when compared to vehicle-treated PR-GFP and Control-GFP cells. All images were acquired at 200X magnification.

Figure 3 Ligand-stimulated progesterone receptor (PR) increases ES-2 ovarian cancer cell survival. A.) Continuously stimulating PR-GFP cells with R5020 (10 nM) significantly increased the number of cells present at 8, 10, and 12 days as measured by MTT assay (all values normalized to Day 0 readings, mean ± SD, n = 3, $*p \leq 0.05$). **B.)** Western blot studies of PR-GFP cells revealed decreased PARP cleavage levels compared to vehicle treated cells when treated over time with R5020 (10 nM).

Figure 4 Progesterone receptor (PR) activation inhibits ES-2 ovarian cancer cell colony formation. A.) PR-GFP expressing cells grown in soft-agar demonstrated an overall reduction in colony formation when stimulated with R5020 (10 nM) for 4 weeks compared to vehicle-treated and Control-GFP cells. **B.)** Quantifying equal numbers of colonies grown in soft-agar for 4 weeks revealed a significant increase (*) in the percentage of small colonies (0-25 pixels) and a significant decrease (#) in the percentage of larger colonies (51-75 and 76-100 pixels) relative to vehicle-treated samples (mean ± SD, n = 3 fields/sample, 10^2 colonies/field, $^{*,\#}p \leq 0.05$). **Inset:** Representative live-colony image taken at 100X magnification demonstrating the presence of viable, single- and two-celled colonies in 4-week long R5020 (10 nM) treated PR-GFP samples.

Figure 5 Ligand-activated progesterone receptor (PR) promotes cellular senescence and cell-cycle exit of ES-2 ovarian cancer cells. A.) Exposure of PR-GFP cells to R5020 (10 nM) for 12 days induced cellular senescence as indicated by cells (arrowheads) with increased senescence-associated beta-galactosidase (SA-β-gal) activity, while non-senescent cells (asterisk) remain SA-β-gal negative. Senescent PR-GFP cells also develop a characteristically larger, more flattened morphology as revealed by TRITC-labeled wheat germ agglutinin (WGA-TRITC) cell membrane staining. Nuclei were identified by DAPI counterstaining. All images were acquired at 40X magnification. **B.)** Flow cytometric analysis of PR-GFP cells treated with R5020 (10 nM) for 12 days revealed a significant increase (*) in the percentage of total cells exiting the cell cycle into G_0 and a significant decrease (#) in the percentage of total cells present in the G_1 phase of the cell cycle (mean ± SD, n = 3, ~10^3 cells/sample, $^{*,\#}p \leq 0.05$). Shaded region in R5020 treated samples highlights cells in the G_1 phase of the cell with increased RNA content.

Figure 6 Ligand-activated progesterone receptor (PR) induces expression of the pro-senescence mediator p21 in ES-2 ovarian cancer cells. A.) Diagrammatic representation of the two major signaling pathways and intermediates involved with the development of senescence growth arrest (CDK's = cyclin-dependent kinases) (adapted from [133]). **B.)** Quantitative-PCR analysis of positive and negative senescence regulators in PR-GFP expressing cells identified p21 as having the greatest change in mRNA expression when treated

with R5020 (10 nM) for 24 hours (all values normalized to GAPDH expression, mean ± SD, n = 4). **C.)** PR-GFP expressing cells transiently transfected with a p21 promoter containing luciferase reporter construct demonstrated a significant increase in transcription when stimulated with R5020 (10 nM) for 24 hours (all values normalized to constitutive *Renilla* luciferase expression, mean ± SD, n = 3, *p ≤ 0.05). **D.)** Western blot analysis of PR-GFP expressing ES-2 cells demonstrated an increase in p21 protein expression when stimulated with R5020 (10 nM) for 24 hours which was inhibited by the PR antagonist RU486 (100 nM).

Figure 7 Stimulating the progesterone receptor (PR) with ligand induces a time-dependent increase in cellular senescence of ES-2 ovarian cancer cells while maintaining elevated p21 expression levels. A.) Compared to Control-GFP and vehicle-treated cells, the continuous exposure of PR-GFP expressing cells to R5020 (10 nM) caused a relative and time-dependent increase in cellular senescence as measured by senescence associated β-galactosidase (SA-β-gal) activity. All images were acquired at 100X magnification. **B.)** Significantly increased p21 mRNA levels in PR-GFP expressing cells was maintained for 4 days by R5020 (10 nM) stimulation compared to vehicle-treated cells as measured by quantitative-PCR (values normalized to GAPDH levels, mean ± SD, n = 3, *p ≤ 0.05). **C.)** Western blot analysis demonstrated that p21 protein levels remained increased for 8 days in PR-GFP expressing cells stimulated with R5020 (10 nM) versus Control-GFP and vehicle-treated cells.

Figure 8 Following prolonged ligand stimulation, stable progesterone receptor (PR) expression in the OVCAR-3 ovarian cancer cell line causes cellular senescence. A.) Western blot analysis demonstrated stable expression of GFP-tagged PR-B in OVCAR-3 cells (OVCAR-3-PR-GFP) as compared to the OVCAR-3 parental cell line (OVCAR-3), ES-2 cells stably expressing GFP-tagged PR-B (PR-GFP), and the PR-B expressing T47D-YB breast cancer cell line (T47D-YB). **B.)** OVCAR-3-PR-GFP cells exposed to R5020 (10 nM) ligand for 12 days underwent cellular senescence as measured by increased senescence-associated beta-galactosidase (SA-β-gal) activity, while vehicle-treated cells remained SA-β-gal negative. All images were acquired at 100X magnification

Figure 9 Ligand-activated progesterone receptor (PR) promotes STAT3 phosphorylation and expression in ES-2 ovarian cancer cells. A.) Quantitative-PCR analysis of PR-GFP expressing cells exposed to R5020 (10 nM) for 12 days identified STAT3 as having a significantly greater relative fold-change in mRNA levels versus other members of the STAT gene family (values normalized to GAPDH levels, mean ± SD, n = 3, *p ≤ 0.05). **B.)** PR-GFP expressing cells stimulated with R5020 (10 nM) demonstrated an increase in STAT3 phosphorylation after 24 hours, but not after 6 hours as determined by Western blot analysis. **C.)** Over time, a significant increase in both p21 and STAT3 mRNA levels was sustained in PR-GFP cells exposed to R5020 (10 nM)

as measured by quantitative-PCR (values normalized to GAPDH levels, mean ± SD, n = 3, *p ≤ 0.05).

Figure 10 The functional characteristics of the progesterone receptor (PR) are not altered following stable downregulation of STAT3 expression in ES-2 ovarian cancer cells. A.) Western blot analysis confirmed stable shRNA-mediated downregulation of STAT3 protein levels (STAT3-shRNA) in PR-GFP expressing ES-2 cells compared to non-PR-expressing cells (Control-GFP) and PR-expressing cells with (Control-shRNA) and without (PR-GFP) stable expression of a non-targeting shRNA construct. **B.)** Transient transfection of PR-GFP, STAT3-shRNA cells with a progesterone response element (PRE) containing luciferase reporter construct demonstrated no differences in the significantly increased PR transcriptional activity compared to other cell lines after stimulation with R5020 (10 nM) for 30 hours (all values normalized to constitutive *Renilla* luciferase expression, mean ± SD, n = 3, *p ≤ 0.05). **C.)** The translocation of PR-GFP into nuclei stained with DAPI following 24 hours of R5020 (10 nM) stimulation is unaltered in PR-GFP, STAT3-shRNA expressing cells compared to PR-GFP cells stably expressing a non-targeting shRNA construct (Control-shRNA). All images were acquired at 200X magnification.

Figure 11 Stimulating the progesterone receptor (PR) with ligand promotes cellular senescence and cell-cycle arrest of ES-2 ovarian cancer cells possessing decreased STAT3 expression levels. A.) Exposure of PR-GFP, STAT3-shRNA cells to R5020 (10 nM) for 8 days induced cellular senescence as

indicated by cells with strongly increased senescence-associated beta-galactosidase (SA-β-gal) activity, while remaining incompletely senesced cells (asterisk) were mildly SA-β-gal positive. Completely senesced PR-GFP, STAT3-shRNA cells exhibit a characteristically larger, more flattened morphology as revealed by TRITC-labeled wheat germ agglutinin (WGA-TRITC) cell membrane staining that was exaggerated compared to incompletely senesced cells (asterisk). Nuclei were identified by DAPI counterstaining. All images were acquired at 400X magnification. **B.)** Flow cytometric analysis of PR-GFP, STAT3-shRNA cells treated with R5020 (10 nM) for 12 days revealed a significant decrease (*) in the percentage of total cells that exit the cell cycle into G_0 and a significant increase (#) in the percentage of total cells that move into and become fixed in the G_1 phase of the cell cycle (mean ± SD, n = 3, ~20^3 cells/sample, $^{*,\#}p \leq 0.05$).

Figure 12 Increased p21 expression due to progesterone receptor (PR) stimulation is enhanced in ES-2 ovarian cancer cells when STAT3 expression is downregulated. A.) As measured by quantitative-PCR, the relative fold-increase of p21 mRNA levels in PR-GFP expressing cells was significantly greater after 24 hours of R5020 (10 nM) stimulation in cells exhibiting stable downregulation of STAT3 expression (STAT3-shRNA) versus cells stably expressing a non-targeting control shRNA construct (Control-shRNA) (values normalized to GAPDH levels, mean ± SD, n = 4, *p ≤ 0.05). **B.)** Western blot analysis determined that increased p21 protein expression in PR-GFP cells

exhibiting stable downregulation of STAT3 expression (STAT3-shRNA) after 24 hours of R5020 (10 nM) stimulation was specific to PR as p21 induction was blocked in the presence of the PR antagonist RU486 (100 nM). **C.)** PR-GFP cells exhibiting a stable downregulation of STAT3 expression (STAT3-shRNA) and transiently transfected with a p21 promoter containing luciferase reporter construct exhibited a significant enhancement (◊) of the increased (*) transcriptional response to 20 hours of R5020 (10 nM) stimulation (inhibitable (#) by the PR antagonist RU486 (100 nM)) compared to PR-GFP cells stably expressing a non-targeting control shRNA construct (Control-shRNA) (all values normalized to constitutive *Renilla* luciferase expression, mean ± SD, n = 3, $^{\lozenge,*,\#}p \leq 0.05$).

Figure 13 When STAT3 expression is downregulated, ligand-activated progesterone receptor (PR) enhances the development of cellular senescence and further increases elevated p21 expression levels in ES-2 ovarian cancer cells. A.) Compared to PR-GFP positive cells stably expressing a non-targeting control shRNA construct (Control-shRNA), the continuous exposure to R5020 (10 nM) of PR-GFP cells demonstrating stable downregulation of STAT3 expression caused a relative decrease in the time required to undergo cellular senescence as measured by senescence associated β-galactosidase (SA-β-gal) activity. All images were acquired at 100X magnification. **B.)** The relative fold-increase of p21 mRNA levels after 4 days of R5020 (10 nM) stimulation was significantly increased in PR-GFP expressing

cells with stable downregulation of STAT3 expression (STAT3-shRNA) compared to PR-GFP positive cells stably expressing a non-targeting control shRNA construct (Control-shRNA) as measured by quantitative-PCR (values normalized to GAPDH levels, mean ± SD, n = 3, *p ≤ 0.05). **C.)** Western blot analysis demonstrated that when compared to vehicle-treated cells, the relative increase in p21 protein levels caused by 8 days of R5020 (10 nM) stimulation was greater in PR-GFP cells stably downregulating STAT3 expression (STAT3-shRNA) versus PR-GFP positive cells stably expressing a non-targeting shRNA construct (Control-shRNA).

Figure 14 Decreased STAT3 expression promotes ligand-induced localization of the progesterone receptor (PR) to the p21 promoter in ES-2 ovarian cancer cells. A.) Compared to PR-GFP expressing cells, chromatin immunoprecipitation (ChIP) demonstrated a relative increase in the binding of PR to the p21 promoter after 1 hour of R5020 (10 nM) stimulation (+) in PR-GFP cells stably downregulating STAT3 expression (STAT3-shRNA) (No Ab = IP negative control, mIgG = IP specificity control). **B.)** The nuclear localization of PR-GFP after 1 hour of R5020 treatment was greater and more diffuse in PR-GFP cells stably downregulating STAT3 expression (STAT3-shRNA) as compared to PR-GFP cells expressing normal amounts of STAT3 (PR-GFP). **C.)** Following 1 hour of R5020 (10 nM) stimulation, quantitative-PCR analysis determined that there was a greater than 1.5-fold increase in the amount of PR bound to the p21 promoter in PR-GFP cells stably downregulating STAT3

expression (STAT3-shRNA) (values normalized to respective input DNA levels, n = 1). **D.)** Proposed model of progesterone receptor (PR)-mediated cellular senescence in ES-2 ovarian cancer cells. 1.) Progesterone (P) activates both cytoplasmic PR causing nuclear translocation/retention and PR already present within the nucleus. 2.) STAT3 located on the p21 promoter inhibits PR-mediated p21 transcription by blocking the binding of additional PRs to the p21 promoter. 3.) The eventual displacement of STAT3 from the p21 promoter allows for PR-mediated p21 transcription; a process enhanced by downregulating STAT3 expression. 4.) When STAT3 expression is reduced, p21 causes cellular senescence by arresting cells in the G_1 phase of the cell-cycle. 5.) In the presence of normal STAT3 expression, increased p21 causes cellular senescence by promoting cell-cycle exit into G_0.

Figure 15 Stimulation of the progesterone receptor (PR) with ligand accelerates cellular senescence in ES-2 ovarian cancer cells with decreased p21 expression levels. A.) Quantitative-PCR analysis confirmed that p21 mRNA levels were significantly decreased in PR-GFP positive ES-2 cells stably expressing a p21 shRNA construct (p21-shRNA) compared to PR-GFP cells stably expressing a non-targeting control shRNA construct (Control-shRNA) (values normalized to GAPDH levels, mean ± SD, n = 4, *p ≤ 0.05). **B.)** PR-GFP cells stably expressing a non-targeting shRNA construct (Control-shRNA) displayed a decrease in basal p21 levels and an upregulation of p21 protein by Western blot analysis after 8 days of R5020 (10 nM) stimulation, while

basal p21 expression was decreased and remained unchanged throughout in PR-GFP, p21-shRNA cells (p21-shRNA). **C.)** Compared to PR-GFP positive cells stably expressing a non-targeting control shRNA construct (Control-shRNA), the continuous exposure to R5020 (10 nM) of PR-GFP cells exhibiting a stable downregulation of p21 expression (p21-shRNA) caused a relative decrease in the time required to undergo cellular senescence as measured by senescence associated β-galactosidase (SA-β-gal) activity. All images were acquired at 100X magnification.

3.8 Figures

Ch. 3 – Figure 1

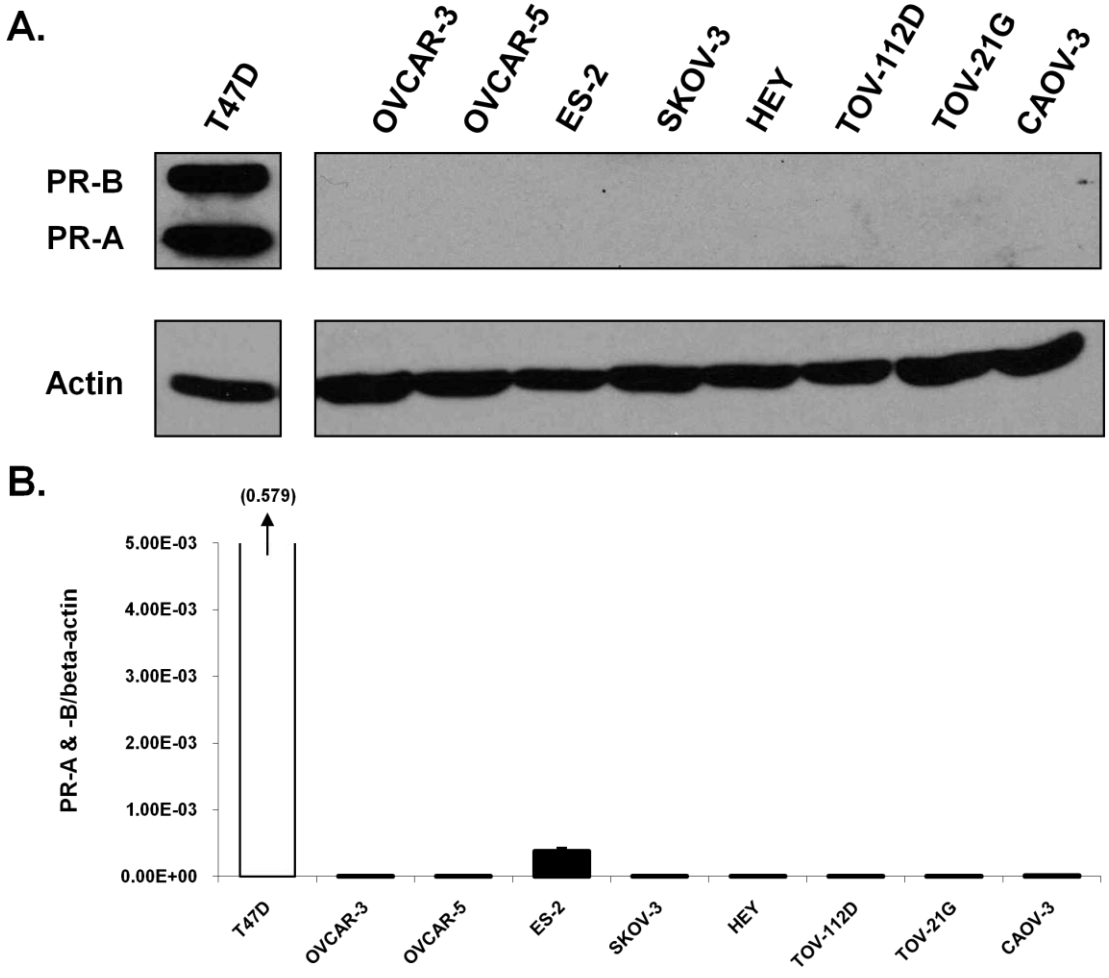
A.
T47D
OVCAR-3
OVCAR-5
ES-2
SKOV-3
HEY
TOV-112D
TOV-21G
CAOV-3
PR-B
PR-A
Actin
B.
(0.579)
5.00E-03
4.00E-03
3.00E-03
2.00E-03
1.00E-03
0.00E+00
PR-A & -B/beta-actin
T47D
OVCAR-3
OVCAR-5
ES-2
SKOV-3
HEY
TOV-112D
TOV-21G
CAOV-3

Ch. 3 – Figure 2

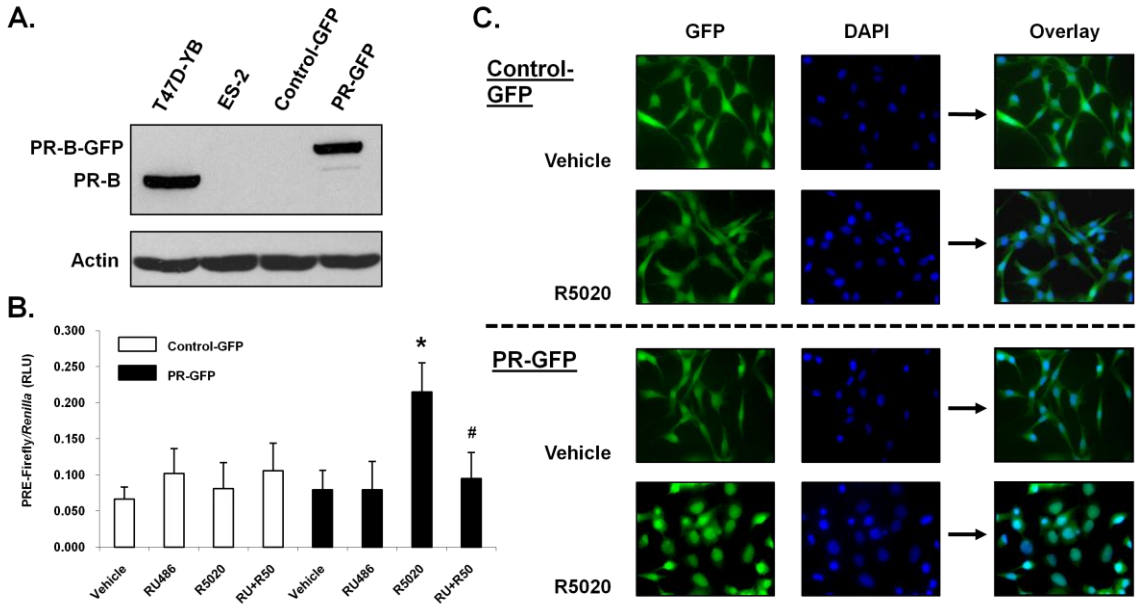
A.
T47D-YB
ES-2
Control-GFP
PR-GFP
PR-B-GFP
PR-B
Actin
B.
PRE-Firefly/Renilla (RLU)
0.300
0.250
0.200
0.150
0.100
0.050
0.000
Control-GFP
PR-GFP
*
#
Vehicle
RU486
R5020
RU+R50
Vehicle
RU486
R5020
RU+R50
C.
GFP
DAPI
Overlay
Control-GFP
Vehicle
R5020
PR-GFP
Vehicle
R5020

Ch. 3 – Figure 3

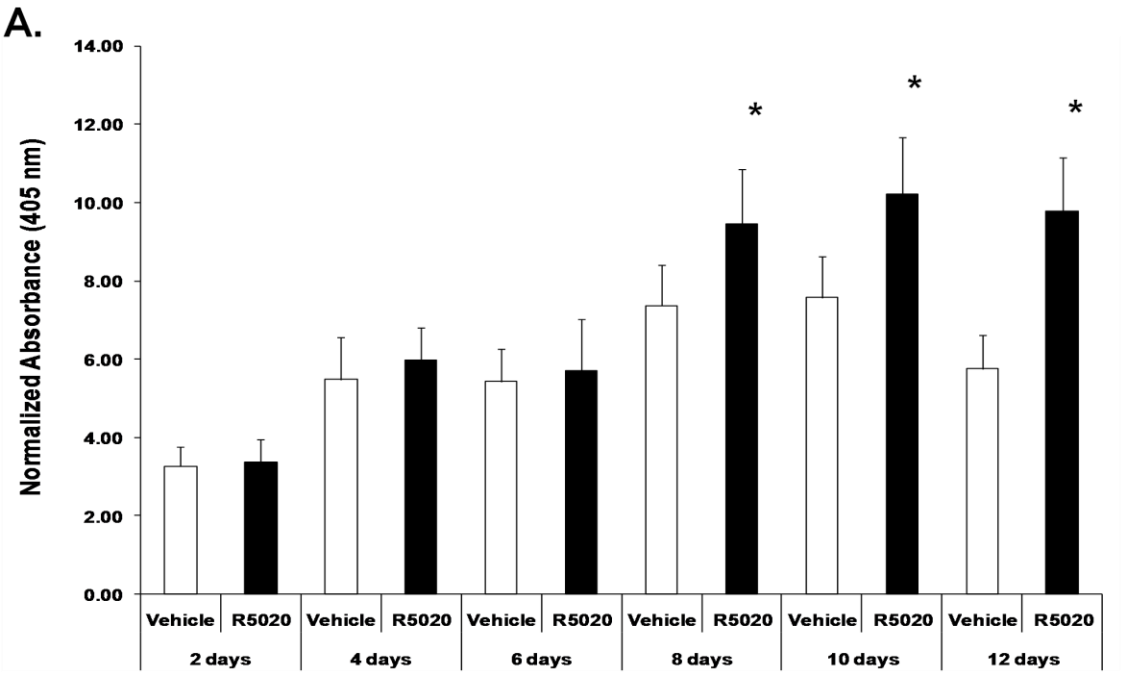
A.
Normalized Absorbance (405 nm)
14.00
12.00
10.00
8.00
6.00
4.00
2.00
0.00
*
*
*
Vehicle
R5020
2 days
4 days
6 days
8 days
10 days
12 days

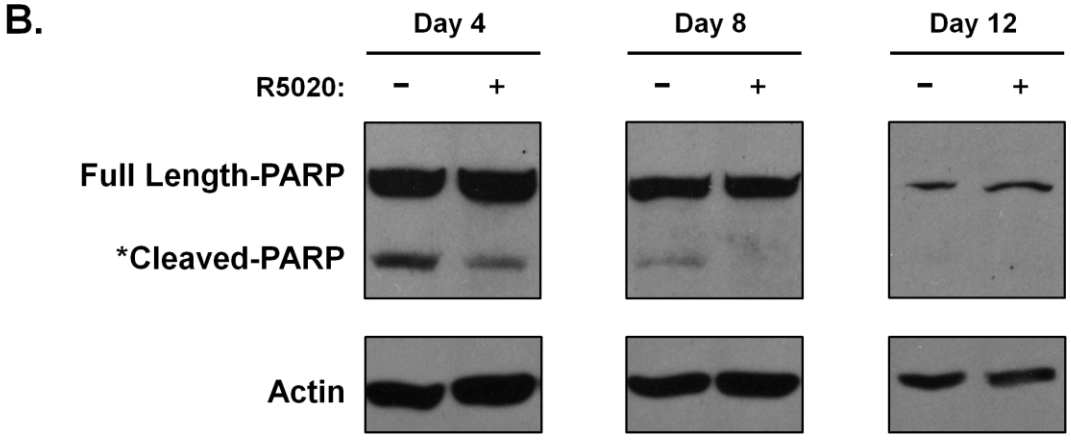
B.
Day 4
Day 8
Day 12
R5020:
–
+
Full Length-PARP
*Cleaved-PARP
Actin

Ch. 3 – Figure 4

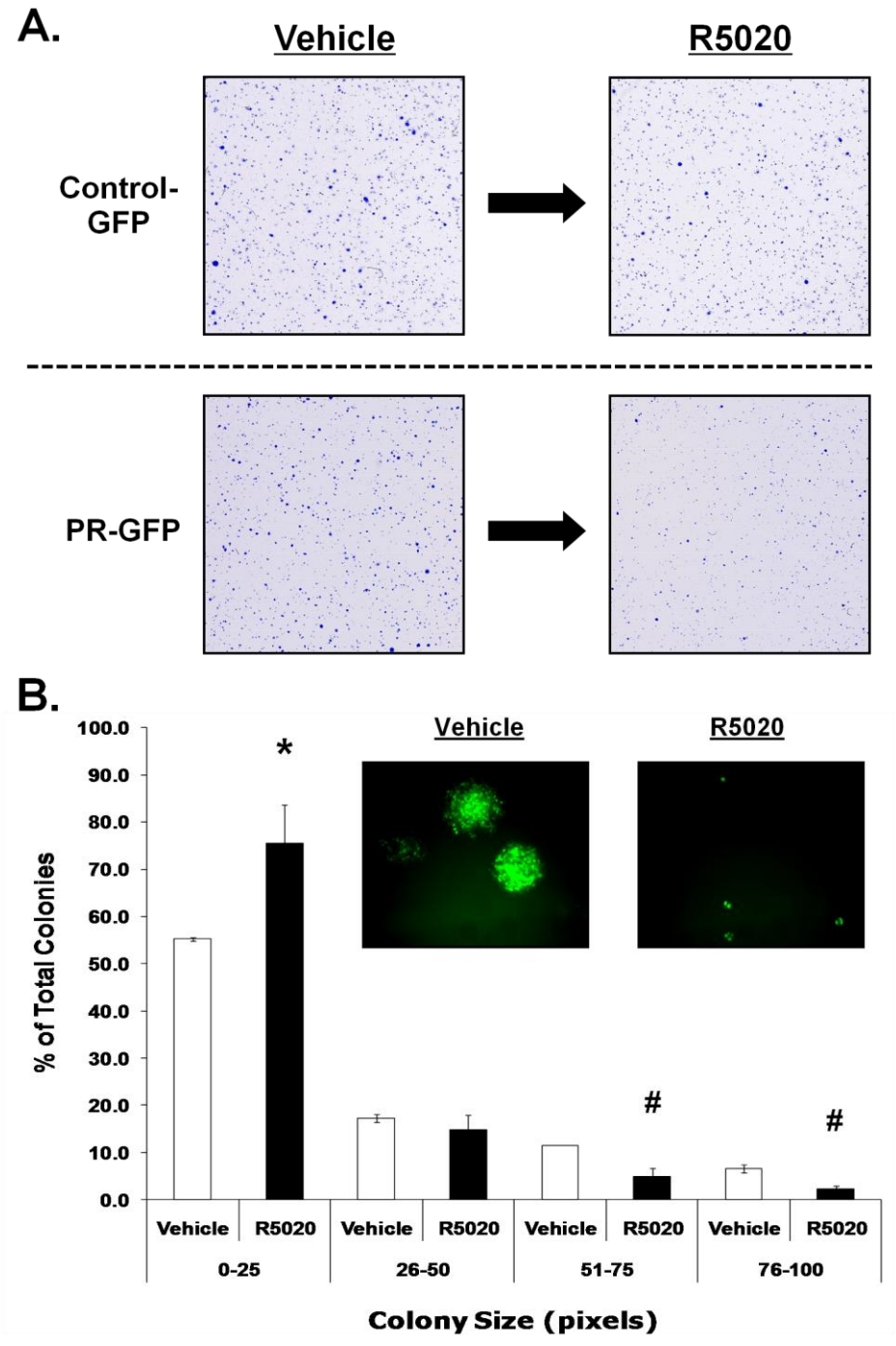
A.
Vehicle
R5020
Control-GFP
PR-GFP
B.
Vehicle
R5020
% of Total Colonies
100.0
90.0
80.0
70.0
60.0
50.0
40.0
30.0
20.0
10.0
0.0
*
#
#
Vehicle
R5020
Vehicle
R5020
Vehicle
R5020
Vehicle
R5020
0-25
26-50
51-75
76-100
Colony Size (pixels)

Ch. 3 – Figure 5

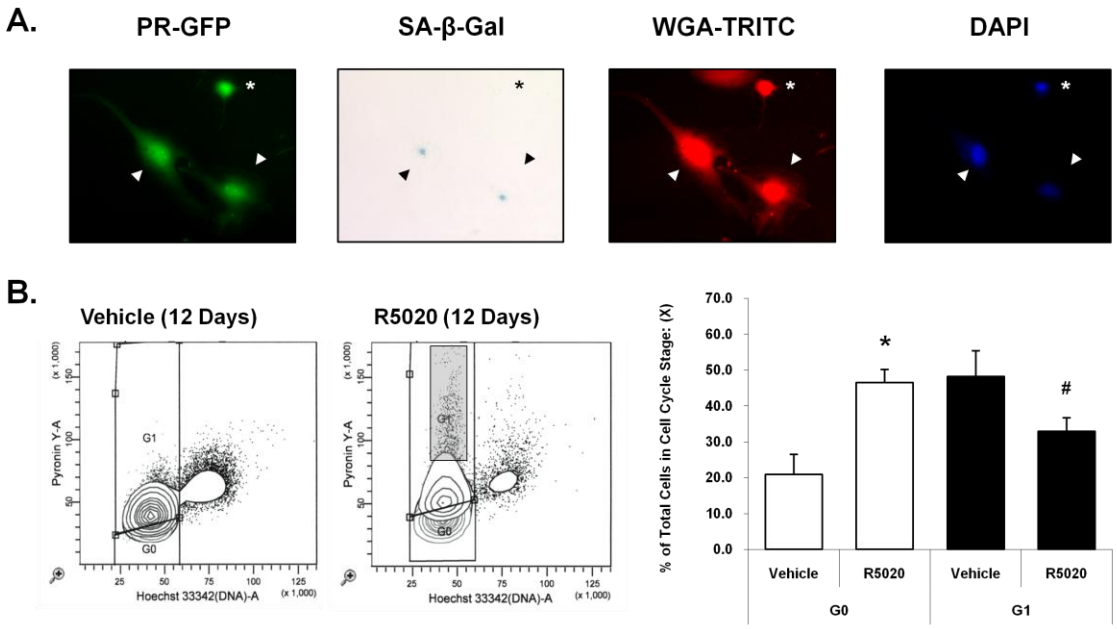
A.
PR-GFP
SA-β-Gal
WGA-TRITC
DAPI
B.
Vehicle (12 Days)
R5020 (12 Days)
Pyronin Y-A
Hoechst 33342(DNA)-A
G1
G0
% of Total Cells in Cell Cycle Stage: (X)
70.0
60.0
50.0
40.0
30.0
20.0
10.0
0.0
*
#
Vehicle
R5020
Vehicle
R5020
G0
G1

Ch. 3 – Figure 6

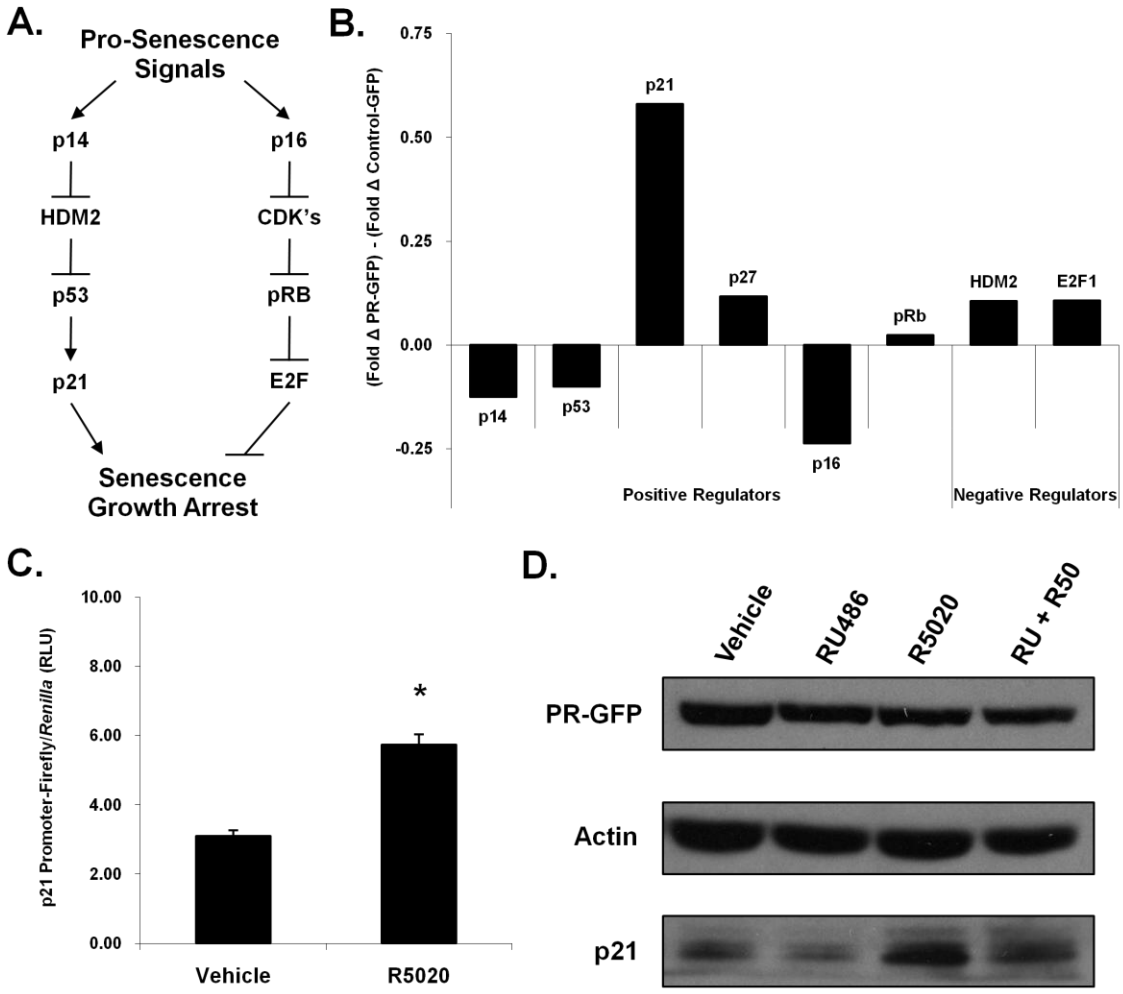
A.
Pro-Senescence Signals
p14
p16
HDM2
CDK's
p53
pRB
p21
E2F
Senescence Growth Arrest
B.
(Fold Δ PR-GFP) - (Fold Δ Control-GFP)
0.75
0.50
0.25
0.00
-0.25
p14
p53
p21
p27
p16
pRb
HDM2
E2F1
Positive Regulators
Negative Regulators
C.
p21 Promoter-Firefly/Renilla (RLU)
10.00
8.00
6.00
4.00
2.00
0.00
*
Vehicle
R5020
D.
Vehicle
RU486
R5020
RU + R50
PR-GFP
Actin
p21

Ch. 3 – Figure 7

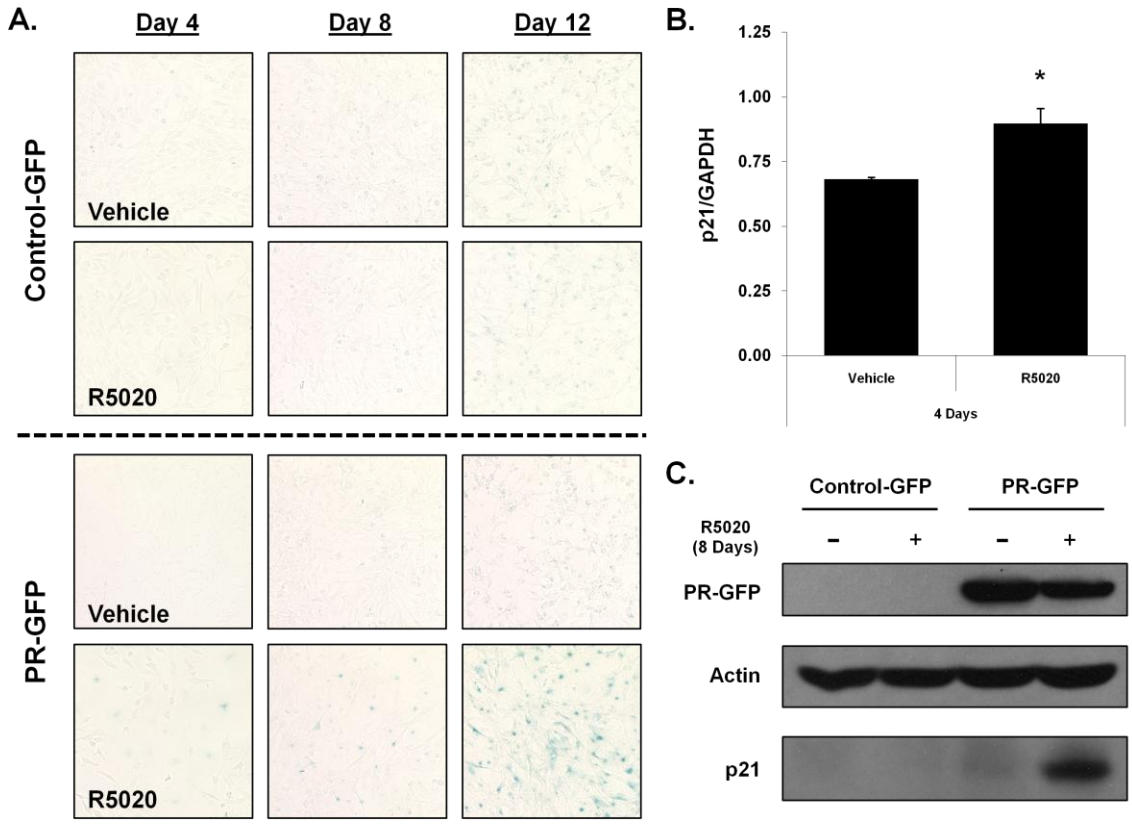
A.
Day 4
Day 8
Day 12
Control-GFP
Vehicle
R5020
PR-GFP
Vehicle
R5020
B.
p21/GAPDH
1.25
1.00
0.75
0.50
0.25
0.00
*
Vehicle
R5020
4 Days
C.
Control-GFP
PR-GFP
R5020
(8 Days)
-
+
-
+
PR-GFP
Actin
p21

Ch. 3 – Figure 8

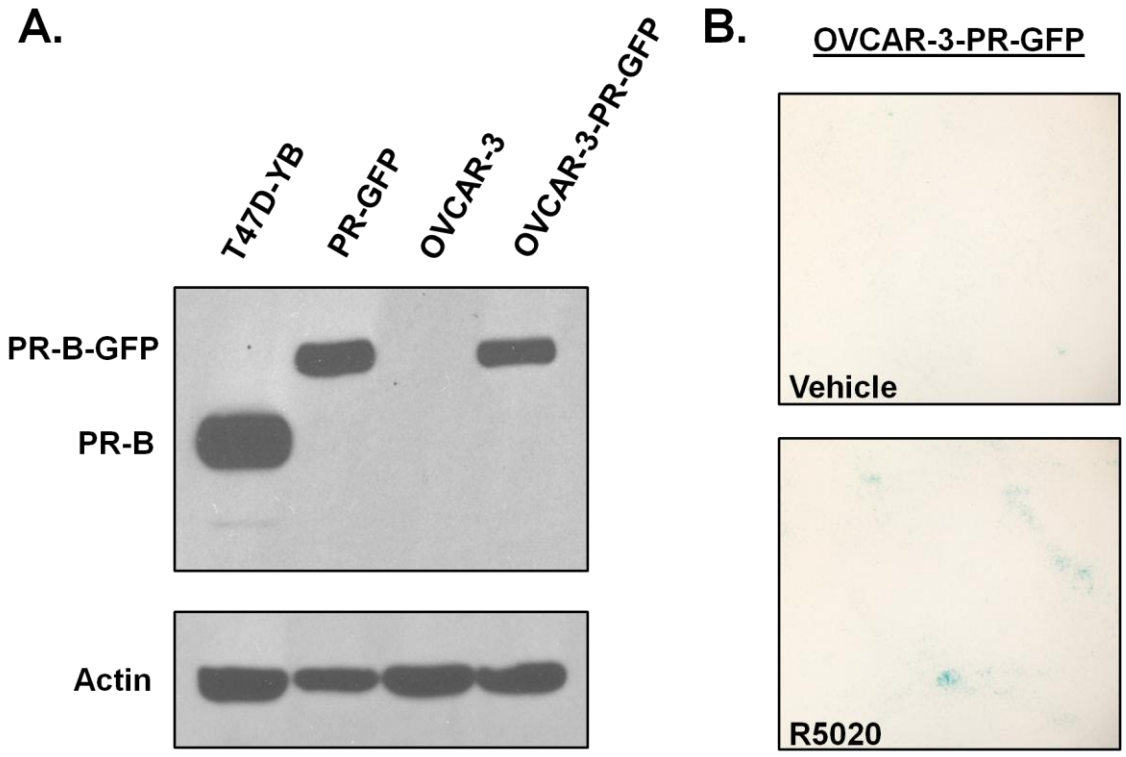
A.
T47D-YB
PR-GFP
OVCAR-3
OVCAR-3-PR-GFP
PR-B-GFP
PR-B
Actin
B.
OVCAR-3-PR-GFP
Vehicle
R5020

Ch. 3 – Figure 9

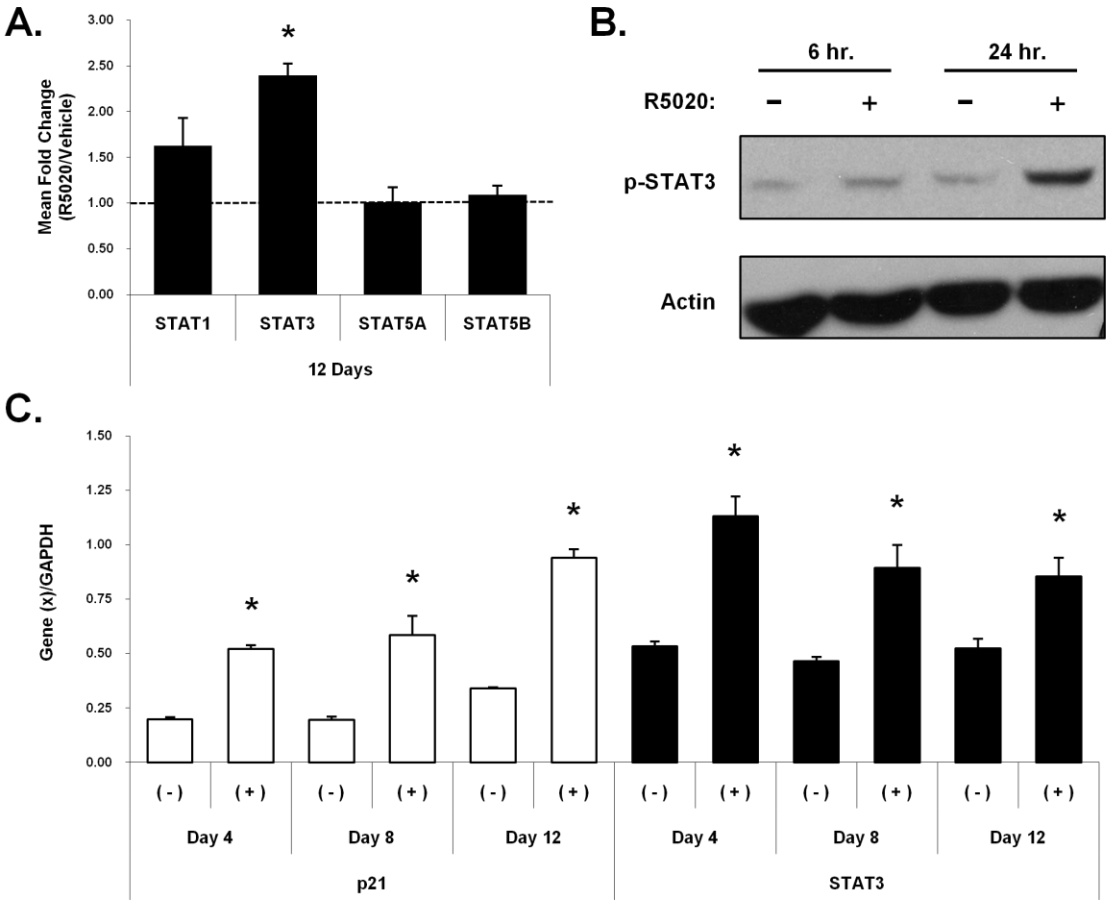
A.
Mean Fold Change (R5020/Vehicle)
3.00
2.50
2.00
1.50
1.00
0.50
0.00
*
STAT1
STAT3
STAT5A
STAT5B
12 Days
B.
6 hr.
24 hr.
R5020:
-
+
-
+
p-STAT3
Actin
C.
Gene (x)/GAPDH
1.50
1.25
1.00
0.75
0.50
0.25
0.00
(-)
(+)
Day 4
Day 8
Day 12
p21
STAT3

Ch. 3 – Figure 10

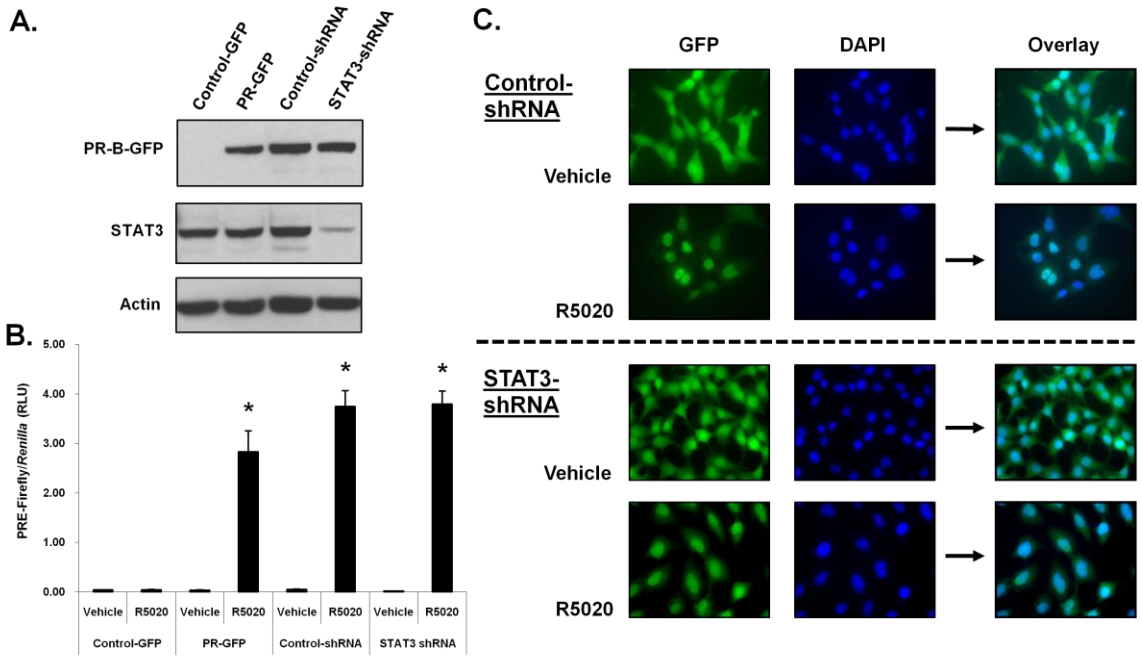

Ch. 3 – Figure 11

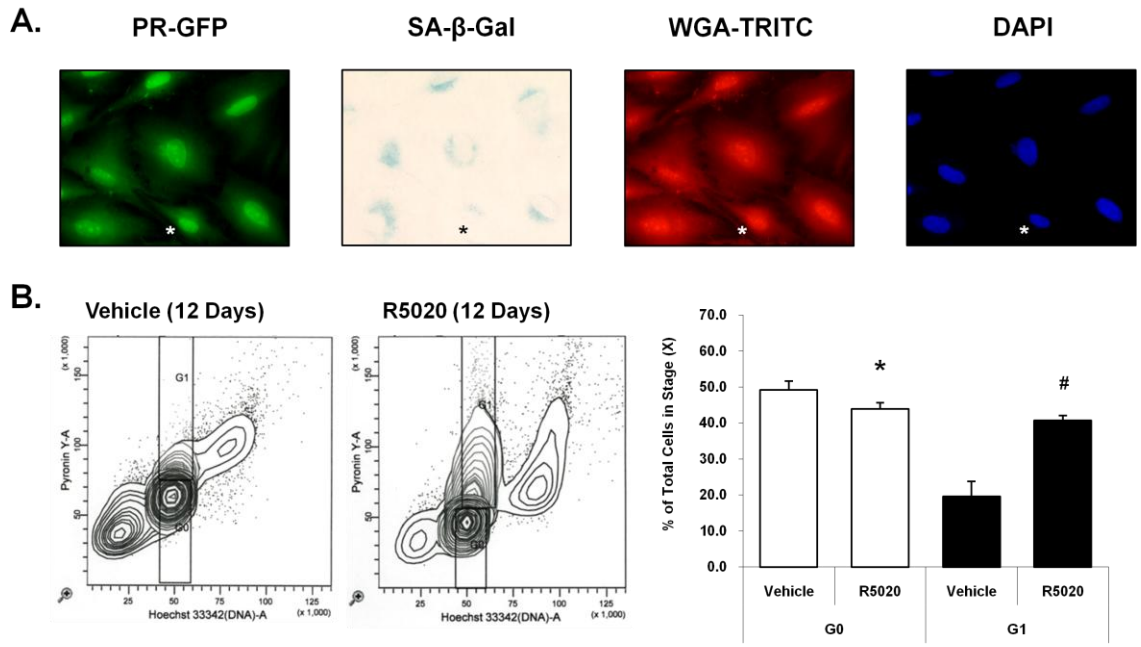

Ch. 3 – Figure 12

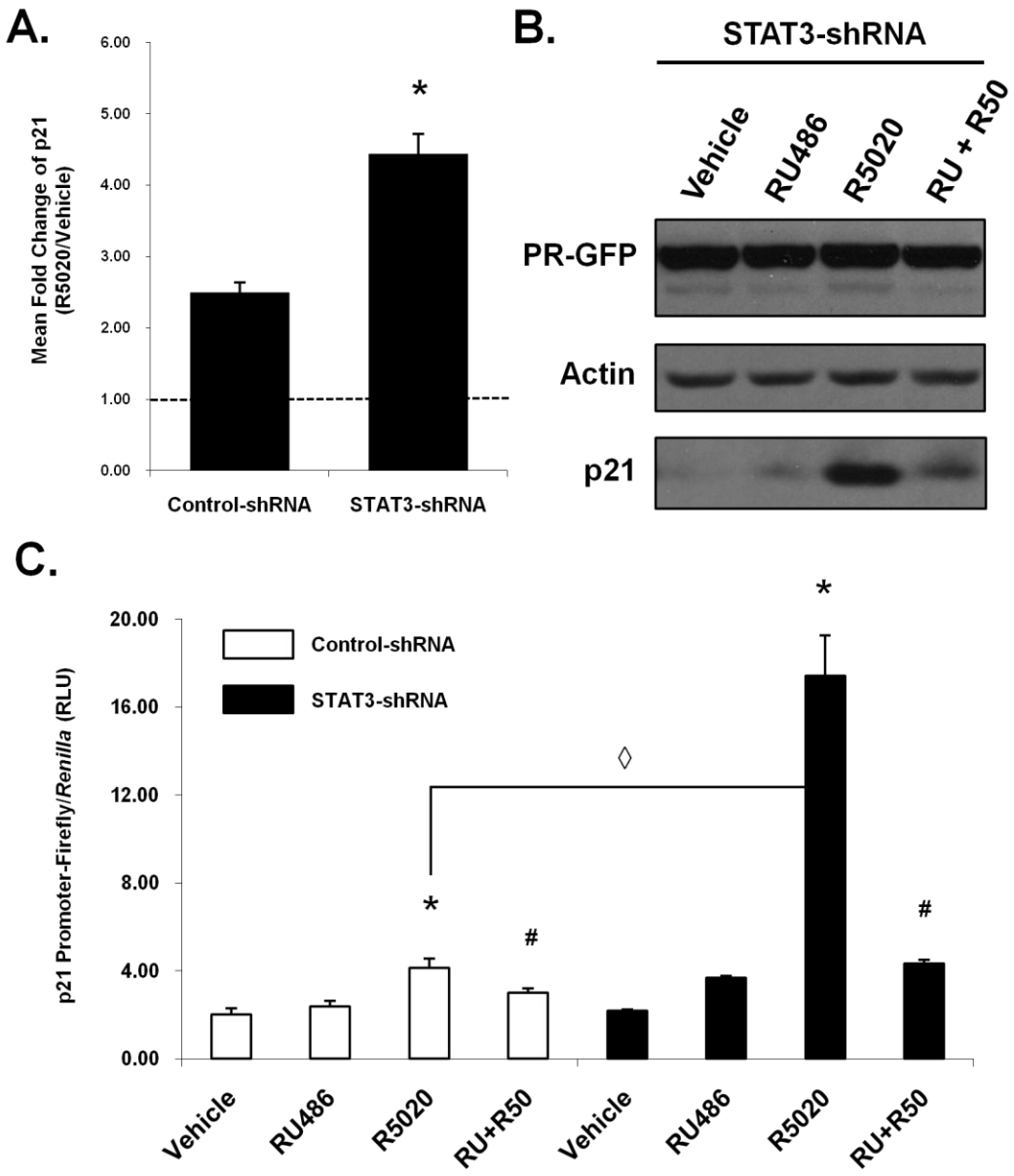

Ch. 3 – Figure 13

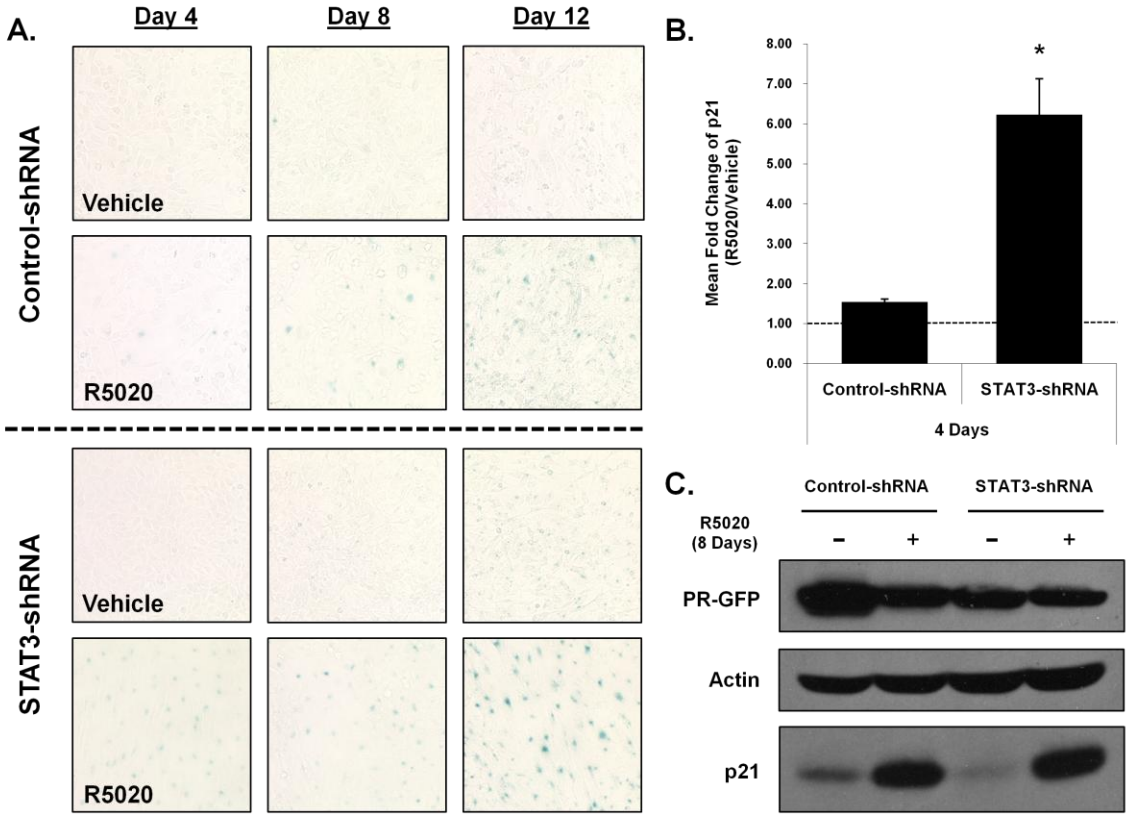

Ch. 3 – Figure 14

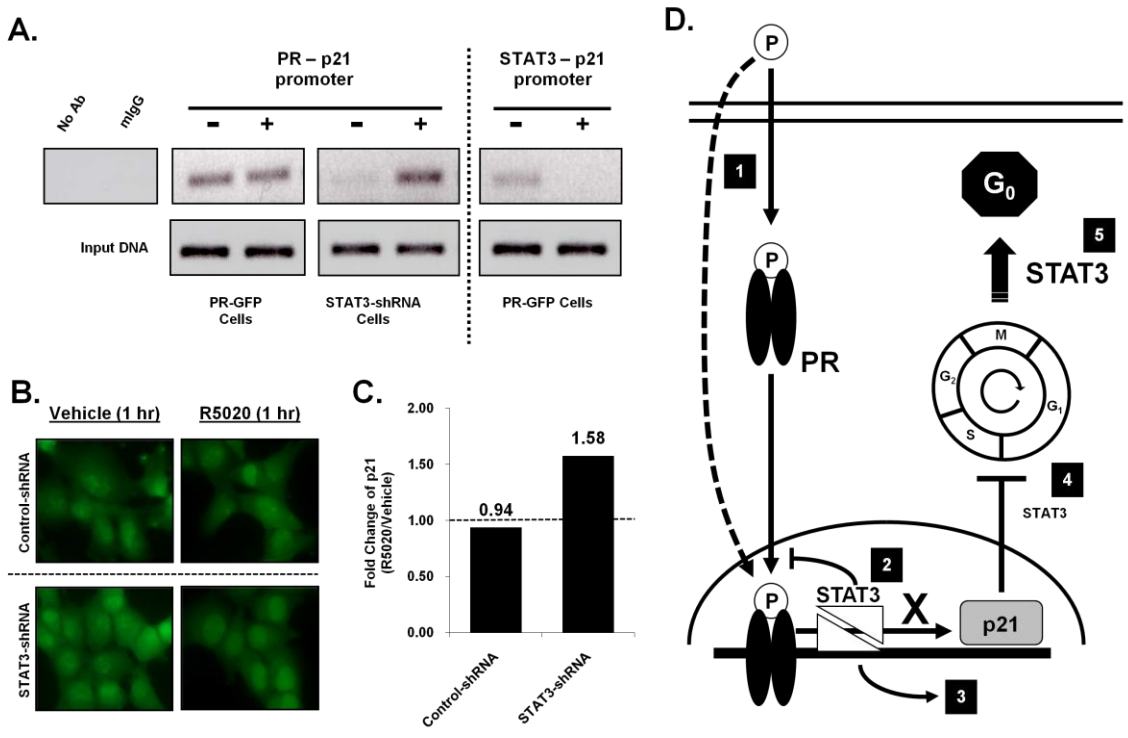

Ch. 3 – Figure 15

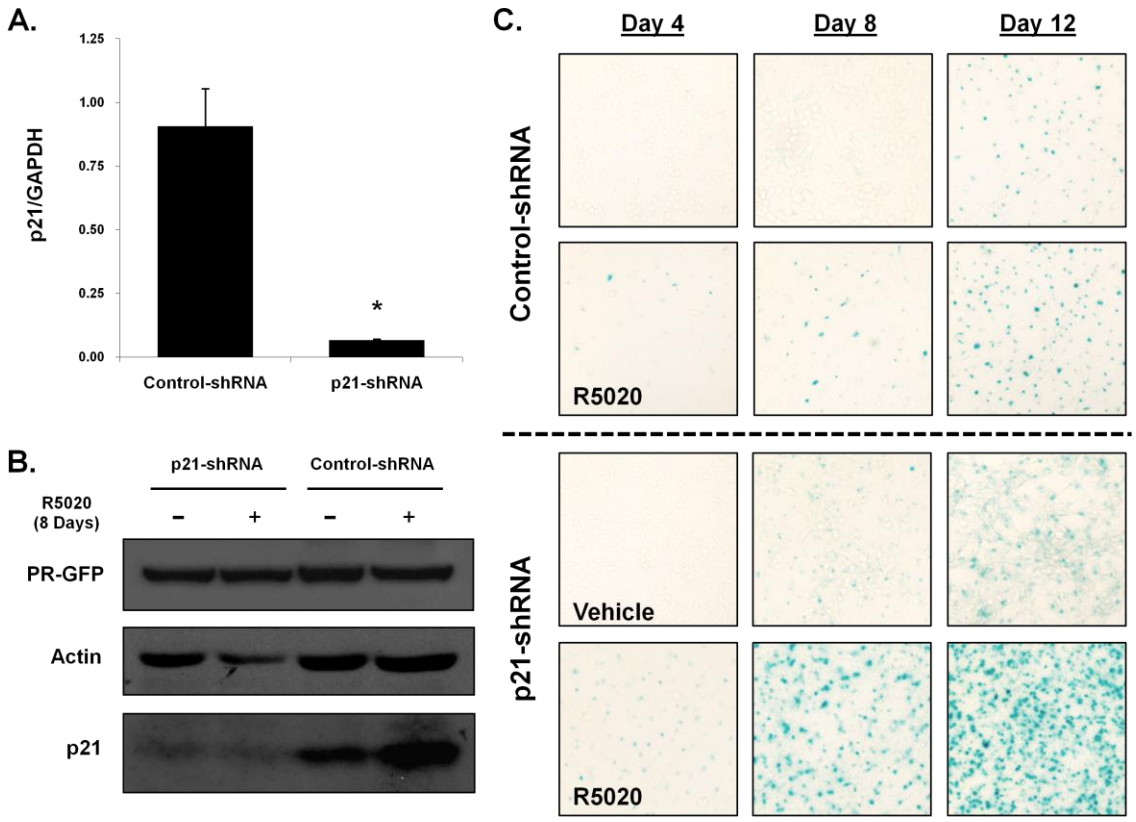

CHAPTER 4

SUMMARY AND CONCLUSIONS

4.1 Discussion

Between changes in circulating progesterone levels and alterations in progesterone receptor (PR) expression, there exists a substantial amount of clinical evidence to suggest that progesterone-mediated signaling inhibits ovarian carcinogenesis (see Introduction). However, questions regarding the therapeutic potential of a progesterone-based strategy for successfully treating ovarian cancer patients remain unanswered. While the success of *in vitro* and *in vivo* studies in support of this concept is encouraging, there have been relatively few published clinical trials investigating the efficacy of progesterone as an ovarian cancer chemotherapeutic (summarized by Zheng *et al.* [153]).

When progesterone-based therapy (i.e. megestrol acetate (MA) or medroxyprogesterone acetate (MPA)) was used to treat ovarian cancer patients with refractory or recurrent disease, results combined from 13 trials revealed a complete response rate of 2.3%, a partial response rate of 4.9%, and disease stabilization in 10.9% [108,154-165]. Additional studies have shown an improvement in disease stabilization and patient prognosis for advanced-stage cancer when progesterone was combined with either tamoxifen, platinum-based agents, or ethinyl estradiol [108-109,166-167]. Finally, when used as a first-line approach following surgery or radiation, progesterone-based therapy led to an overall response rate of 53.5% [168]. Curiously, in contrast to trials reporting moderate or no improvements in clinical course [169-171], this final study was one of the only ones to thoroughly analyze and correlate residual PR expression

to response rates after prolonged therapy [168]. These authors thus reported that PR and estrogen receptor (ER) positive tumors exhibited the greatest incidence of tumor regression (68%) [168].

While these clinical trial results make it difficult for any definitive conclusions to be made regarding progesterone therapy, there couldn't be a greater need for the discovery of new and effective treatment strategies. As mentioned previously, ovarian cancer mortality rates have not changed in over 70 years since statistics first started being kept [56]. Furthermore, the chemotherapeutic regimen of platinum plus paclitaxel, compounds first discovered 45 years ago, remains the gold standard for treating ovarian cancer. Even though this combination yields greater than 80% response rates, most patients relapse with a median progression-free survival of 18 months [172]. Ultimately, patient response rates gradually decrease with each subsequent relapse as tumors progress from a platinum-sensitive state to either platinum-resistant or –refractory disease [173]. These latter two groups of patients subsequently receive treatment with other agents such as doxorubicin, gemcitabine, topotecan, or etoposide until tumors become completely drug-resistant [172]. However, the lack of success these compounds display makes our observations regarding progesterone-mediated cellular senescence so exciting.

As the signaling intermediates and pathways have been better defined over the past 10 years, it has become increasingly evident that cellular

senescence evolved as an inherent tumor-suppressive mechanism [129,133,145,174-175]. Cancer progression requires the uncontrolled growth and proliferation of malignant cells [176] while senescence exists as a state of permanent cell-cycle arrest [133]. Therefore, by definition, cellular senescence is inhibitory towards further tumor progression. A senescent state is caused by a variety of both intrinsic mechanisms including telomere dysfunction, DNA damage, chromatin perturbation, sustained cellular stress, and oncogene-mediated mitogenic signaling as well as extrinsic mechanisms most notably from persistent cytokine (i.e IL-6, IL-8, C/EBPβ, and NF-κB) stimulation [133,177]. However, not until recently have there been any reports suggesting that naturally produced hormones are capable of inducing senescence arrest [117].

We believe that our observations demonstrating that progesterone treatment causes ovarian cancer cells to senesce possesses legitimate therapeutic potential. It has been well-documented using transgenic and knock-out mouse models that cellular senescence is not limited to the *in vitro* cell culture environment [178]. However, recent studies have also identified senescent cells in human tumor samples [179-185]. Therefore, to determine the translational and therapeutic potential of our *in vitro* findings, we extended our studies to include primary human ovarian cancer cell isolates. To first gain a firmer grasp on the often contentious results surrounding ovarian cancer PR expression when determined by immunohistochemistry, we established a collaboration with Dr. Blake Gilks, Head of the University of British Columbia's

Ovarian Cancer Research Team (OvCaRe). With their help and expertise, we determined the percentage of PR positive tumors from each major histologic sub-type in a cohort of 504 ovarian cancer tissue samples (Fig. 1A). While percentages varied between sub-types, we were encouraged to see that every group contained PR positive tumors and that the overall percentage of PR positive tumors was 34.5%; a value higher than reported by many studies with much smaller sample sizes. As a result, high-dose progesterone therapy, whose side effects are no worse than standard chemotherapeutics, may apply to more ovarian cancer patients than originally thought. To investigate the potential benefit progesterone therapy might have on treating ovarian cancer, we isolated PR expressing metastatic ovarian cancer cells from a case of Stage III disease (Fig. 1B). As before, we evaluated the ability of PR activity to upregulate p21 expression in these cells and saw a significant increase in p21 protein levels after 8 days of stimulation (Fig. 1C). However, of greatest interest was our observation that prolonged PR activity caused primary human ovarian cancer cells to undergo senescence arrest (Fig. 1D).

We believe that the ability of PR to induce a state of permanent cell-cycle arrest in PR positive human ovarian cancer cells warrants further investigation as a novel chemotherapeutic option. Nevertheless, our studies characterizing the signaling mechanisms behind this response have provided additional molecular targets that could be manipulated in PR null ovarian cancers. One option would be to increase expression of the p21 cell-cycle inhibitor, which other studies have

also shown can be upregulated by progesterone in ovarian cancer cells [114,186]. Additionally, several clinical studies have revealed an association between increased p21 levels and prognostic improvements for ovarian cancer patients [187-189]. While *in vivo* p21 modulators are currently being investigated as chemotherapeutic agents [134], other groups are actively investigating inhibitors of the p21 targets CDK1 and CDK2 for their anti-tumorigenic properties [190]. CDK2 inhibition is an especially attractive target as recent *in vitro* evidence demonstrates that CDK2 can block the activity of cell-cycle inhibitors such as p15, p16, p21, and p27 [191]. Lastly, because of our observations describing the ability of STAT3 to inhibit PR-mediated p21 transcription, inhibiting the constitutive activity of STAT3 in ovarian cancer [148] may be the most effective approach. In support of this option are two recent gene array studies that identified a positive correlation between the expression of STAT3 gene targets with higher grade ovarian carcinomas [192] and discovered STAT3 is a central multi-pathway regulator in clear cell carcinoma of the ovary [193]. (Note: The ES-2 cell line used herein is of clear cell origin.) However, incidental observations made in our STAT3 knock-down cell line may have even greater significance.

The cell of origin of ovarian cancers has yet to be clearly defined and is a major reason why ovarian cancer cannot be cured by chemotherapy alone. Not being able to characterize the source of ovarian tumors has hindered the development of more effective and more tumor-specific agents. It has been a long-held belief that tumorigenesis arises from disorganized repair of ovarian

surface epithelial cells damaged by ovulation in a process termed “incessant ovulation” [194]. If correct, this theory might explain why ovarian cancer cells of epithelial origin senesce when exposed to high concentrations of progesterone (i.e. levels achieved and maintained by ovarian corpus luteal cells after ovulation). Recently, it has been shown that cellular senescence helps in the repair of damaged liver tissue [195] thus suggesting that senescence helps wound healing while permanently preventing aberrant cells from proliferating [146]. Therefore, is it possible that surface epithelial cells damaged during ovulation and wound healing lose PR expression (potentially due to a genetic LOH [65]) and are thus refractory to the pro-senescence tumor-suppressive influence of progesterone?

The scenario involving progesterone and senescence induction appears to support the epithelial cell of origin hypothesis. However, arguments made over the past decade, based solely on histologic observations, suggest that ovarian cancer cells are more similar to carcinomas of Müllerian origin (i.e. fallopian tube, endometrial, and endocervical cancers) than epithelial tumors derived from mesothelial cells [196-198]. Ironically, each position may be correct in its own right when one considers that a major characteristic of all cancer cells is their ability to adopt a less differentiated state as occurs with epithelial-to-mesenchymal (EMT) transition. Taking this into consideration, we were very surprised to see that when STAT3 expression was downregulated, ES-2 ovarian cancer cells underwent significant morphologic changes and adopted a cuboidal

cell phenotype (Fig. 2A) as exists for the single layer of surface epithelial cells normally lining the ovary. Even more surprising was that ES-2 STAT3 knock-down cells instinctively formed single-cell layer thick circular structures in 2-D culture (Fig. 2B). Therefore, is it possible that the constitutive expression and activity of STAT3 in ovarian cancer cells [148] is responsible for EMT and malignant transformation? This concept is supported by very recent studies showing that STAT3 downregulation causes differentiation of glioblastoma stem cells [199]. Interestingly, such EMT reversal may be augmented by long-term progesterone exposure which has been shown to promote ovarian cancer cell re-differentiation [186].

Of potentially greatest interest, however, are hints throughout the literature to suggest that membrane and nuclear progesterone receptors do not operate by mutually exclusive means. For example, it has been shown in human myometrial cells that both mPRα and mPRβ are capable of potentiating PR-B-mediated transcriptional activity of a glucocorticoid response element (GRE) following progesterone stimulation [34]. Additionally, as a result of mPR-regulated increases in cAMP (see Chapter 2, Figure 2), mPRs may enhance PR action due to transactivation caused by increased protein kinase A (PKA) activity as seen in breast cancer cells [200]. Lastly, mPRs have the ability to modulate expression of the PR transcriptional co-activator steroid receptor co-activator-2 (SRC-2) in human myometrial cells [34] which again may also alter PR transactivation and transcription. If these scenarios hold true for mPR and PR in ovarian cancer

cells, we would predict that cellular senescence may occur even faster and more completely with progesterone stimulation due to mPR-augmented PR activity.

Ovarian cancer has the highest mortality rate of all gynecologic malignancies [56]. While advancements in treatment techniques and strategies have improved 5-year survival rates, the overall cure rate remains unchanged at 30% [201]. As a result, the need for new and more effective chemotherapeutics is great, especially because ovarian cancers eventually become drug-resistant [173]. We believe that the natural steroid hormone progesterone holds promise for limiting ovarian tumorigenesis and controlling tumor progression. Based on our results and previous clinical and *in vitro* observations, we are confident in concluding that the progesterone receptor (PR) possesses tumor suppressive characteristics in ovarian cancer cells. Therefore, the induction of PR-mediated cellular senescence via high-dose progesterone therapy represents a novel and highly translatable approach to limiting the uncontrolled proliferation of ovarian cancer cells ultimately leading to improvements in overall patient survival.

4.2 Figure Legends

Figure 1 The progesterone receptor (PR) is expressed in human ovarian cancer tissue and its activity can promote cellular senescence of human ovarian cancer isolates. A.) PR expression was positively identified by immunohistochemistry (IHC) in human ovarian cancer tissues representing the five major cancer sub-types of ovarian surface epithelial (OSE) origin (n = 504).

B.) PR mRNA expression was significantly greater in cells from a human isolate of serous ovarian cancer than basal PR mRNA expression in the ES-2 ovarian cancer cell line as determined by quantitative-PCR analysis (values normalized to GAPDH levels, mean ± SD, n = 3, *p ≤ 0.05). **C.)** Exposure of primary human serous ovarian cancer cells to R5020 (10 nM) for 8 days lead to an increase in p21 protein expression as measured by Western blot analysis. **D.)** In the presence of R5020 (10 nM) for 10 days, primary serous ovarian cancer cells underwent cellular senescence identified by increased senescence-associated β-galactosidase (SA-β-gal) activity (upper panels) and changes in cellular morphology characteristic of cellular senescence (lower panels). All images were acquired at 10X magnification.

Figure 2 Decreased STAT3 expression causes cell morphology and growth pattern changes in progesterone receptor (PR) expressing ES-2 ovarian cancer cells. A.) PR expressing ES-2 cells growing in culture adopted a more cuboidal phenotype when STAT3 expression was stably downregulated (PR-GFP, STAT3-shRNA) as compared to the squamous and fibroblastic appearance of PR-GFP cells with normal STAT3 expression levels (PR-GFP). All images were acquired at 200X magnification. **B.)** Stably downregulating STAT3 expression caused PR-expressing ES-2 cells (PR-GFP, STAT3-shRNA) to form circular structures (asterisks) when growing in culture, while PR-GFP cells with normal STAT3 expression levels (PR-GFP) maintained the same growth pattern

as parental ES-2 ovarian cancer cells. All images were acquired at 50X magnification.

4.3 Figures

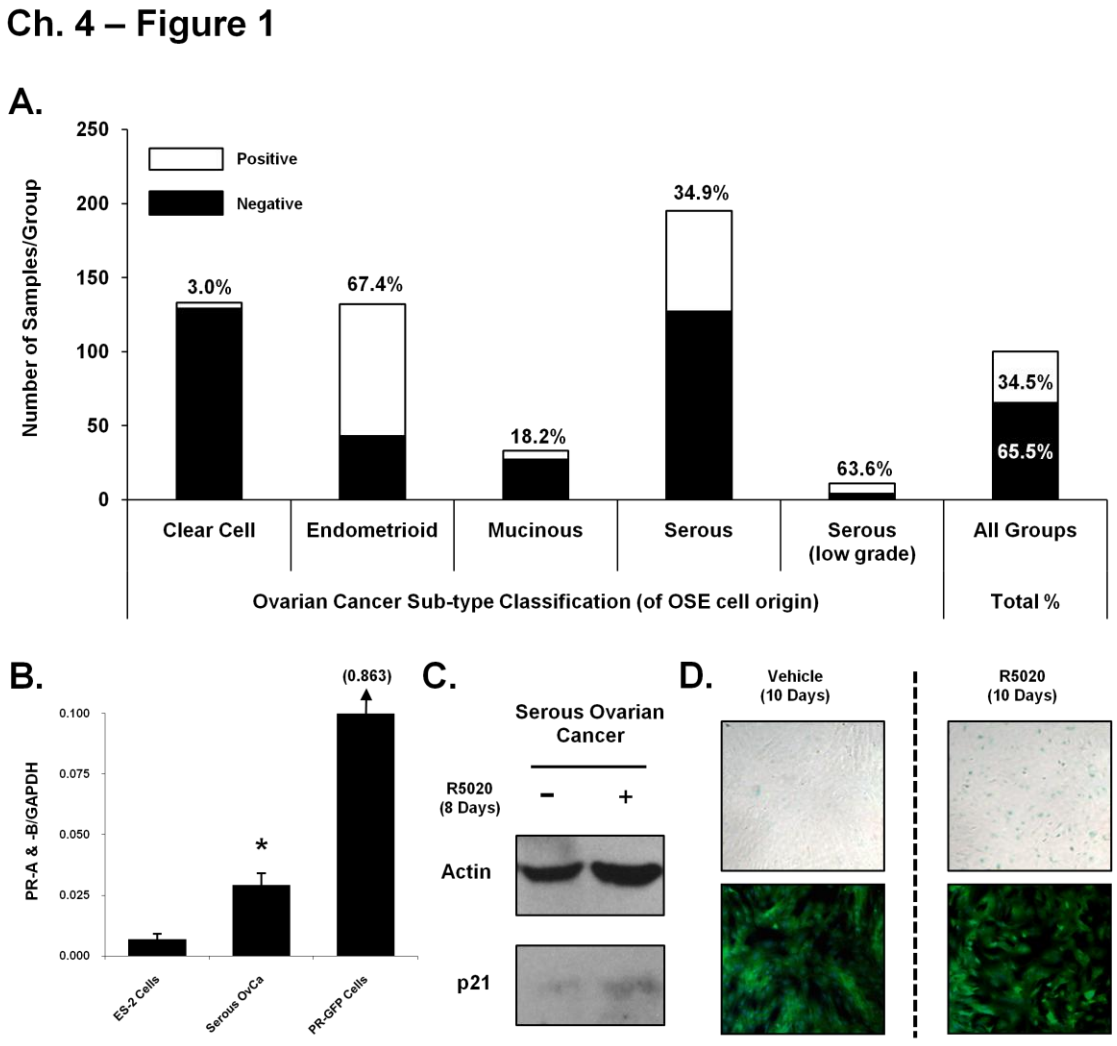

Ch. 4 – Figure 2

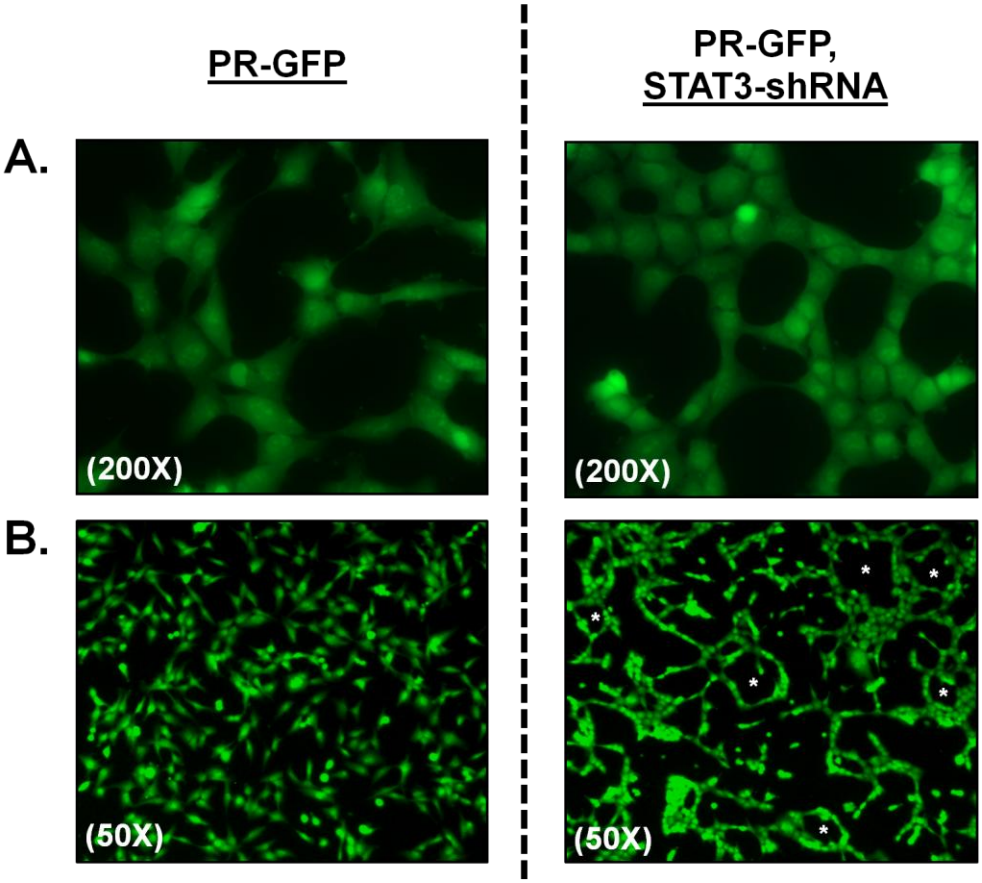

BIBLIOGRAPHY

1. Auersperg N, Wong AS, Choi KC, Kang SK, Leung PC (2001) Ovarian surface epithelium: biology, endocrinology, and pathology. Endocr Rev 22:255-288
2. Wong AS, Leung PC (2007) Role of endocrine and growth factors on the ovarian surface epithelium. J Obstet Gynaecol Res 33:3-16
3. Kruk PA, Uitto VJ, Firth JD, Dedhar S, Auersperg N (1994) Reciprocal interactions between human ovarian surface epithelial cells and adjacent extracellular matrix. Exp Cell Res 215:97-108
4. Murdoch WJ (1995) Programmed cell death in preovulatory ovine follicles. Biol Reprod 53:8-12
5. Bjersing L, Cajander S (1975) Ovulation and the role of the ovarian surface epithelium. Experientia 31:605-608
6. Osterholzer HO, Johnson JH, Nicosia SV (1985) An autoradiographic study of rabbit ovarian surface epithelium before and after ovulation. Biol Reprod 33:729-738
7. Eden JA, Jones J, Carter GD, Alaghband-Zadeh J (1990) Follicular fluid concentrations of insulin-like growth factor 1, epidermal growth factor, transforming growth factor-alpha and sex-steroids in volume matched normal and polycystic human follicles. Clin Endocrinol (Oxf) 32:395-405
8. Lindgren PR, Backstrom T, Cajander S, Damber MG, Mahlck CG, Zhu D, et al. (2002) The pattern of estradiol and progesterone differs in serum

and tissue of benign and malignant ovarian tumors. Int J Oncol 21:583-589

9. Wright JW, Toth-Fejel S, Stouffer RL, Rodland KD (2002) Proliferation of rhesus ovarian surface epithelial cells in culture: lack of mitogenic response to steroid or gonadotropic hormones. Endocrinology 143:2198-2207

10. Parrott JA, Doraiswamy V, Kim G, Mosher R, Skinner MK (2001) Expression and actions of both the follicle stimulating hormone receptor and the luteinizing hormone receptor in normal ovarian surface epithelium and ovarian cancer. Mol Cell Endocrinol 172:213-222

11. Syed V, Ulinski G, Mok SC, Yiu GK, Ho SM (2001) Expression of gonadotropin receptor and growth responses to key reproductive hormones in normal and malignant human ovarian surface epithelial cells. Cancer Res 61:6768-6776

12. Choi KC, Kang SK, Tai CJ, Auersperg N, Leung PC (2002) Follicle-stimulating hormone activates mitogen-activated protein kinase in preneoplastic and neoplastic ovarian surface epithelial cells. J Clin Endocrinol Metab 87:2245-2253

13. Choi JH, Choi KC, Auersperg N, Leung PC (2005) Gonadotropins upregulate the epidermal growth factor receptor through activation of mitogen-activated protein kinases and phosphatidyl-inositol-3-kinase in human ovarian surface epithelial cells. Endocr Relat Cancer 12:407-421

14. Davies BR, Finnigan DS, Smith SK, Ponder BA (1999) Administration of gonadotropins stimulates proliferation of normal mouse ovarian surface epithelium. Gynecol Endocrinol 13:75-81

15. Ivarsson K, Sundfeldt K, Brannstrom M, Hellberg P, Janson PO (2001) Diverse effects of FSH and LH on proliferation of human ovarian surface epithelial cells. Hum Reprod 16:18-23

16. Pon YL, Auersperg N, Wong AS (2005) Gonadotropins regulate N-cadherin-mediated human ovarian surface epithelial cell survival at both post-translational and transcriptional levels through a cyclic AMP/protein kinase A pathway. J Biol Chem 280:15438-15448

17. Ahmed N, Maines-Bandiera S, Quinn MA, Unger WG, Dedhar S, Auersperg N (2006) Molecular pathways regulating EGF-induced epithelio-mesenchymal transition in human ovarian surface epithelium. Am J Physiol Cell Physiol 290:C1532-1542

18. McClellan M, Kievit P, Auersperg N, Rodland K (1999) Regulation of proliferation and apoptosis by epidermal growth factor and protein kinase C in human ovarian surface epithelial cells. Exp Cell Res 246:471-479

19. Pierro E, Nicosia SV, Saunders B, Fultz CB, Nicosia RF, Mancuso S (1996) Influence of growth factors on proliferation and morphogenesis of rabbit ovarian mesothelial cells in vitro. Biol Reprod 54:660-669

20. Trolice MP, Pappalardo A, Peluso JJ (1997) Basic fibroblast growth factor and N-cadherin maintain rat granulosa cell and ovarian surface epithelial

cell viability by stimulating the tyrosine phosphorylation of the fibroblast growth factor receptors. Endocrinology 138:107-113

21. Parrott JA, Mosher R, Kim G, Skinner MK (2000) Autocrine interactions of keratinocyte growth factor, hepatocyte growth factor, and kit-ligand in the regulation of normal ovarian surface epithelial cells. Endocrinology 141:2532-2539

22. Gubbay O, Guo W, Rae MT, Niven D, Howie AF, McNeilly AS, et al. (2004) Anti-inflammatory and proliferative responses in human and ovine ovarian surface epithelial cells. Reproduction 128:607-614

23. Dabrow MB, Francesco MR, McBrearty FX, Caradonna S (1998) The effects of platelet-derived growth factor and receptor on normal and neoplastic human ovarian surface epithelium. Gynecol Oncol 71:29-37

24. Corps AN, Sowter HM, Smith SK (1997) Hepatocyte growth factor stimulates motility, chemotaxis and mitogenesis in ovarian carcinoma cells expressing high levels of c-met. Int J Cancer 73:151-155

25. Wong AS, Roskelley CD, Pelech S, Miller D, Leung PC, Auersperg N (2004) Progressive changes in Met-dependent signaling in a human ovarian surface epithelial model of malignant transformation. Exp Cell Res 299:248-256

26. Rodriguez GC, Nagarsheth NP, Lee KL, Bentley RC, Walmer DK, Cline M, et al. (2002) Progestin-induced apoptosis in the Macaque ovarian epithelium: differential regulation of transforming growth factor-beta. J Natl Cancer Inst 94:50-60

27. Rodriguez GC, Walmer DK, Cline M, Krigman H, Lessey BA, Whitaker RS, et al. (1998) Effect of progestin on the ovarian epithelium of macaques: cancer prevention through apoptosis? J Soc Gynecol Investig 5:271-276

28. Lange CA, Yee D (2008) Progesterone and breast cancer. Womens Health (Lond Engl) 4:151-162

29. Peluso JJ (2006) Multiplicity of progesterone's actions and receptors in the mammalian ovary. Biol Reprod 75:2-8

30. Zhu Y, Bond J, Thomas P (2003) Identification, classification, and partial characterization of genes in humans and other vertebrates homologous to a fish membrane progestin receptor. Proc Natl Acad Sci U S A 100:2237-2242

31. Zhu Y, Rice CD, Pang Y, Pace M, Thomas P (2003) Cloning, expression, and characterization of a membrane progestin receptor and evidence it is an intermediary in meiotic maturation of fish oocytes. Proc Natl Acad Sci U S A 100:2231-2236

32. Thomas P, Pang Y, Dong J, Groenen P, Kelder J, de Vlieg J, et al. (2007) Steroid and G protein binding characteristics of the seatrout and human progestin membrane receptor alpha subtypes and their evolutionary origins. Endocrinology 148:705-718

33. Perego P, Giarola M, Righetti SC, Supino R, Caserini C, Delia D, et al. (1996) Association between cisplatin resistance and mutation of p53 gene

and reduced bax expression in ovarian carcinoma cell systems. Cancer Res 56:556-562

34. Karteris E, Zervou S, Pang Y, Dong J, Hillhouse EW, Randeva HS, et al. (2006) Progesterone signaling in human myometrium through two novel membrane G protein-coupled receptors: potential role in functional progesterone withdrawal at term. Mol Endocrinol 20:1519-1534

35. Tubbs C, Thomas P (2009) Progestin signaling through an olfactory G protein and membrane progestin receptor-alpha in Atlantic croaker sperm: potential role in induction of sperm hypermotility. Endocrinology 150:473-484

36. Cai Z, Stocco C (2005) Expression and regulation of progestin membrane receptors in the rat corpus luteum. Endocrinology 146:5522-5532

37. Diaz FJ, Wiltbank MC (2004) Acquisition of luteolytic capacity: changes in prostaglandin F2alpha regulation of steroid hormone receptors and estradiol biosynthesis in pig corpora lutea. Biol Reprod 70:1333-1339

38. Romero-Sanchez M, Peiper SC, Evans B, Wang Z, Catasus L, Ribe A, et al. (2008) Expression profile of heptahelical putative membrane progesterone receptors in epithelial ovarian tumors. Hum Pathol 39:1026-1033

39. Meyer C, Schmid R, Scriba PC, Wehling M (1996) Purification and partial sequencing of high-affinity progesterone-binding site(s) from porcine liver membranes. Eur J Biochem 239:726-731

40. Falkenstein E, Meyer C, Eisen C, Scriba PC, Wehling M (1996) Full-length cDNA sequence of a progesterone membrane-binding protein from porcine vascular smooth muscle cells. Biochem Biophys Res Commun 229:86-89

41. Sasson R, Rimon E, Dantes A, Cohen T, Shinder V, Land-Bracha A, et al. (2004) Gonadotrophin-induced gene regulation in human granulosa cells obtained from IVF patients. Modulation of steroidogenic genes, cytoskeletal genes and genes coding for apoptotic signalling and protein kinases. Mol Hum Reprod 10:299-311

42. Peluso JJ, Fernandez G, Pappalardo A, White BA (2002) Membrane-initiated events account for progesterone's ability to regulate intracellular free calcium levels and inhibit rat granulosa cell mitosis. Biol Reprod 67:379-385

43. Peluso JJ, Pappalardo A, Losel R, Wehling M (2005) Expression and function of PAIRBP1 within gonadotropin-primed immature rat ovaries: PAIRBP1 regulation of granulosa and luteal cell viability. Biol Reprod 73:261-270

44. Kraus WL, Montano MM, Katzenellenbogen BS (1993) Cloning of the rat progesterone receptor gene 5'-region and identification of two functionally distinct promoters. Mol Endocrinol 7:1603-1616

45. Jacobsen BM, Richer JK, Schittone SA, Horwitz KB (2002) New human breast cancer cells to study progesterone receptor isoform ratio effects and ligand-independent gene regulation. J Biol Chem 277:27793-27800

46. Richer JK, Jacobsen BM, Manning NG, Abel MG, Wolf DM, Horwitz KB (2002) Differential gene regulation by the two progesterone receptor isoforms in human breast cancer cells. J Biol Chem 277:5209-5218

47. Mulac-Jericevic B, Lydon JP, DeMayo FJ, Conneely OM (2003) Defective mammary gland morphogenesis in mice lacking the progesterone receptor B isoform. Proc Natl Acad Sci U S A 100:9744-9749

48. Mulac-Jericevic B, Mullinax RA, DeMayo FJ, Lydon JP, Conneely OM (2000) Subgroup of reproductive functions of progesterone mediated by progesterone receptor-B isoform. Science 289:1751-1754

49. Dressing GE, Lange CA (2009) Integrated actions of progesterone receptor and cell cycle machinery regulate breast cancer cell proliferation. Steroids 74:573-576

50. Knotts TA, Orkiszewski RS, Cook RG, Edwards DP, Weigel NL (2001) Identification of a phosphorylation site in the hinge region of the human progesterone receptor and additional amino-terminal phosphorylation sites. J Biol Chem 276:8475-8483

51. Weigel NL (1996) Steroid hormone receptors and their regulation by phosphorylation. Biochem J 319 (Pt 3):657-667

52. Lange CA, Shen T, Horwitz KB (2000) Phosphorylation of human progesterone receptors at serine-294 by mitogen-activated protein kinase signals their degradation by the 26S proteasome. Proc Natl Acad Sci U S A 97:1032-1037

53. Rowan BG, Garrison N, Weigel NL, O'Malley BW (2000) 8-Bromo-cyclic AMP induces phosphorylation of two sites in SRC-1 that facilitate ligand-independent activation of the chicken progesterone receptor and are critical for functional cooperation between SRC-1 and CREB binding protein. Mol Cell Biol 20:8720-8730

54. Boonyaratanakornkit V, Scott MP, Ribon V, Sherman L, Anderson SM, Maller JL, et al. (2001) Progesterone receptor contains a proline-rich motif that directly interacts with SH3 domains and activates c-Src family tyrosine kinases. Mol Cell 8:269-280

55. Faivre EJ, Lange CA (2007) Progesterone receptors upregulate Wnt-1 to induce epidermal growth factor receptor transactivation and c-Src-dependent sustained activation of Erk1/2 mitogen-activated protein kinase in breast cancer cells. Mol Cell Biol 27:466-480

56. Jemal A, Siegel R, Ward E, Hao Y, Xu J, Thun MJ (2009) Cancer statistics, 2009. CA Cancer J Clin 59:225-249

57. Cho KR, Shih Ie M (2009) Ovarian cancer. Annu Rev Pathol 4:287-313

58. Leung PC, Choi JH (2007) Endocrine signaling in ovarian surface epithelium and cancer. Hum Reprod Update 13:143-162

59. Adami HO, Hsieh CC, Lambe M, Trichopoulos D, Leon D, Persson I, et al. (1994) Parity, age at first childbirth, and risk of ovarian cancer. Lancet 344:1250-1254

60. Thomas HV, Murphy MF, Key TJ, Fentiman IS, Allen DS, Kinlen LJ (1998) Pregnancy and menstrual hormone levels in mothers of twins compared to mothers of singletons. Ann Hum Biol 25:69-75

61. Salazar-Martinez E, Lazcano-Ponce EC, Gonzalez Lira-Lira G, Escudero-De los Rios P, Salmeron-Castro J, Hernandez-Avila M (1999) Reproductive factors of ovarian and endometrial cancer risk in a high fertility population in Mexico. Cancer Res 59:3658-3662

62. Tambyraja AL, Sengupta F, MacGregor AB, Bartolo DC, Fearon KC (2004) Patterns and clinical outcomes associated with routine intravenous sodium and fluid administration after colorectal resection. World J Surg 28:1046-1051; discussion 1051-1042

63. Fauvet R, Dufournet Etienne C, Poncelet C, Bringuier AF, Feldmann G, Darai E (2006) Effects of progesterone and anti-progestin (mifepristone) treatment on proliferation and apoptosis of the human ovarian cancer cell line, OVCAR-3. Oncol Rep 15:743-748

64. Modan B, Ron E, Lerner-Geva L, Blumstein T, Menczer J, Rabinovici J, et al. (1998) Cancer incidence in a cohort of infertile women. Am J Epidemiol 147:1038-1042

65. Gabra H, Langdon SP, Watson JE, Hawkins RA, Cohen BB, Taylor L, et al. (1995) Loss of heterozygosity at 11q22 correlates with low progesterone receptor content in epithelial ovarian cancer. Clin Cancer Res 1:945-953

66. Gabra H, Taylor L, Cohen BB, Lessels A, Eccles DM, Leonard RC, et al. (1995) Chromosome 11 allele imbalance and clinicopathological correlates in ovarian tumours. Br J Cancer 72:367-375

67. Davis M, Hitchcock A, Foulkes WD, Campbell IG (1996) Refinement of two chromosome 11q regions of loss of heterozygosity in ovarian cancer. Cancer Res 56:741-744

68. Gabra H, Watson JE, Taylor KJ, Mackay J, Leonard RC, Steel CM, et al. (1996) Definition and refinement of a region of loss of heterozygosity at 11q23.3-q24.3 in epithelial ovarian cancer associated with poor prognosis. Cancer Res 56:950-954

69. Gross TP, Schlesselman JJ, Stadel BV, Yu W, Lee NC (1992) The risk of epithelial ovarian cancer in short-term users of oral contraceptives. Am J Epidemiol 136:46-53

70. Rosenberg L, Palmer JR, Zauber AG, Warshauer ME, Lewis JL, Jr., Strom BL, et al. (1994) A case-control study of oral contraceptive use and invasive epithelial ovarian cancer. Am J Epidemiol 139:654-661

71. Ness RB, Grisso JA, Vergona R, Klapper J, Morgan M, Wheeler JE (2001) Oral contraceptives, other methods of contraception, and risk reduction for ovarian cancer. Epidemiology 12:307-312

72. Greer JB, Modugno F, Allen GO, Ness RB (2005) Short-term oral contraceptive use and the risk of epithelial ovarian cancer. Am J Epidemiol 162:66-72

73. Beral V, Doll R, Hermon C, Peto R, Reeves G (2008) Ovarian cancer and oral contraceptives: collaborative reanalysis of data from 45 epidemiological studies including 23,257 women with ovarian cancer and 87,303 controls. Lancet 371:303-314

74. Bu SZ, Yin DL, Ren XH, Jiang LZ, Wu ZJ, Gao QR, et al. (1997) Progesterone induces apoptosis and up-regulation of p53 expression in human ovarian carcinoma cell lines. Cancer 79:1944-1950

75. Yu S, Lee M, Shin S, Park J (2001) Apoptosis induced by progesterone in human ovarian cancer cell line SNU-840. J Cell Biochem 82:445-451

76. Syed V, Ho SM (2003) Progesterone-induced apoptosis in immortalized normal and malignant human ovarian surface epithelial cells involves enhanced expression of FasL. Oncogene 22:6883-6890

77. Syed V, Mukherjee K, Godoy-Tundidor S, Ho SM (2007) Progesterone induces apoptosis in TRAIL-resistant ovarian cancer cells by circumventing c-FLIPL overexpression. J Cell Biochem 102:442-452

78. Noguchi T, Kitawaki J, Tamura T, Kim T, Kanno H, Yamamoto T, et al. (1993) Relationship between aromatase activity and steroid receptor levels in ovarian tumors from postmenopausal women. J Steroid Biochem Mol Biol 44:657-660

79. Akahira J, Suzuki T, Ito K, Kaneko C, Darnel AD, Moriya T, et al. (2002) Differential expression of progesterone receptor isoforms A and B in the normal ovary, and in benign, borderline, and malignant ovarian tumors. Jpn J Cancer Res 93:807-815

80. Lee BH, Hecht JL, Pinkus JL, Pinkus GS (2002) WT1, estrogen receptor, and progesterone receptor as markers for breast or ovarian primary sites in metastatic adenocarcinoma to body fluids. Am J Clin Pathol 117:745-750

81. Akahira J, Inoue T, Suzuki T, Ito K, Konno R, Sato S, et al. (2000) Progesterone receptor isoforms A and B in human epithelial ovarian carcinoma: immunohistochemical and RT-PCR studies. Br J Cancer 83:1488-1494

82. Lee P, Rosen DG, Zhu C, Silva EG, Liu J (2005) Expression of progesterone receptor is a favorable prognostic marker in ovarian cancer. Gynecol Oncol 96:671-677

83. Hogdall EV, Christensen L, Hogdall CK, Blaakaer J, Gayther S, Jacobs IJ, et al. (2007) Prognostic value of estrogen receptor and progesterone receptor tumor expression in Danish ovarian cancer patients: from the 'MALOVA' ovarian cancer study. Oncol Rep 18:1051-1059

84. Yang XY, Xi MR, Yang KX, Yu H (2009) Prognostic value of estrogen receptor and progesterone receptor status in young Chinese ovarian carcinoma patients. Gynecol Oncol 113:99-104

85. Tangjitgamol S, Manusirivithaya S, Khunnarong J, Jesadapatarakul S, Tanwanich S (2009) Expressions of estrogen and progesterone receptors in epithelial ovarian cancer: a clinicopathologic study. Int J Gynecol Cancer 19:620-627

86. Munstedt K, Steen J, Knauf AG, Buch T, von Georgi R, Franke FE (2000) Steroid hormone receptors and long term survival in invasive ovarian cancer. Cancer 89:1783-1791

87. Ashley RL, Arreguin-Arevalo JA, Nett TM (2009) Binding characteristics of the ovine membrane progesterone receptor alpha and expression of the receptor during the estrous cycle. Reprod Biol Endocrinol 7:42

88. Ashley RL, Clay CM, Farmerie TA, Niswender GD, Nett TM (2006) Cloning and characterization of an ovine intracellular seven transmembrane receptor for progesterone that mediates calcium mobilization. Endocrinology 147:4151-4159

89. Thomas P (2008) Characteristics of membrane progestin receptor alpha (mPRalpha) and progesterone membrane receptor component 1 (PGMRC1) and their roles in mediating rapid progestin actions. Front Neuroendocrinol 29:292-312

90. Boulware MI, Weick JP, Becklund BR, Kuo SP, Groth RD, Mermelstein PG (2005) Estradiol activates group I and II metabotropic glutamate receptor signaling, leading to opposing influences on cAMP response element-binding protein. J Neurosci 25:5066-5078

91. Pierson-Mullany LK, Lange CA (2004) Phosphorylation of progesterone receptor serine 400 mediates ligand-independent transcriptional activity in response to activation of cyclin-dependent protein kinase 2. Mol Cell Biol 24:10542-10557

92. Dressing GE, Thomas P (2007) Identification of membrane progestin receptors in human breast cancer cell lines and biopsies and their potential involvement in breast cancer. Steroids 72:111-116

93. Milligan G (2009) G protein-coupled receptor hetero-dimerization: contribution to pharmacology and function. Br J Pharmacol 158:5-14

94. Shaw TJ, Keszthelyi EJ, Tonary AM, Cada M, Vanderhyden BC (2002) Cyclic AMP in ovarian cancer cells both inhibits proliferation and increases c-KIT expression. Exp Cell Res 273:95-106

95. Mayr B, Montminy M (2001) Transcriptional regulation by the phosphorylation-dependent factor CREB. Nat Rev Mol Cell Biol 2:599-609

96. Syed V, Mukherjee K, Lyons-Weiler J, Lau KM, Mashima T, Tsuruo T, et al. (2005) Identification of ATF-3, caveolin-1, DLC-1, and NM23-H2 as putative antitumorigenic, progesterone-regulated genes for ovarian cancer cells by gene profiling. Oncogene 24:1774-1787

97. Matsukawa J, Matsuzawa A, Takeda K, Ichijo H (2004) The ASK1-MAP kinase cascades in mammalian stress response. J Biochem 136:261-265

98. Miller WE, Lefkowitz RJ (2001) Expanding roles for beta-arrestins as scaffolds and adapters in GPCR signaling and trafficking. Curr Opin Cell Biol 13:139-145

99. Arafat WO, Gomez-Navarro J, Xiang J, Barnes MN, Mahasreshti P, Alvarez RD, et al. (2000) An adenovirus encoding proapoptotic Bax induces apoptosis and enhances the radiation effect in human ovarian cancer. Mol Ther 1:545-554

100. Marone M, Scambia G, Mozzetti S, Ferrandina G, Iacovella S, De Pasqua A, et al. (1998) bcl-2, bax, bcl-XL, and bcl-XS expression in normal and neoplastic ovarian tissues. Clin Cancer Res 4:517-524

101. Wu GS (2004) The functional interactions between the p53 and MAPK signaling pathways. Cancer Biol Ther 3:156-161

102. Fister S, Gunthert AR, Aicher B, Paulini KW, Emons G, Grundker C (2009) GnRH-II antagonists induce apoptosis in human endometrial, ovarian, and breast cancer cells via activation of stress-induced MAPKs p38 and JNK and proapoptotic protein Bax. Cancer Res 69:6473-6481

103. Kim BJ, Ryu SW, Song BJ (2006) JNK- and p38 kinase-mediated phosphorylation of Bax leads to its activation and mitochondrial translocation and to apoptosis of human hepatoma HepG2 cells. J Biol Chem 281:21256-21265

104. Mansouri A, Ridgway LD, Korapati AL, Zhang Q, Tian L, Wang Y, et al. (2003) Sustained activation of JNK/p38 MAPK pathways in response to cisplatin leads to Fas ligand induction and cell death in ovarian carcinoma cells. J Biol Chem 278:19245-19256

105. Lee LF, Li G, Templeton DJ, Ting JP (1998) Paclitaxel (Taxol)-induced gene expression and cell death are both mediated by the activation of c-Jun NH2-terminal kinase (JNK/SAPK). J Biol Chem 273:28253-28260

106. Givant-Horwitz V, Davidson B, Lazarovici P, Schaefer E, Nesland JM, Trope CG, et al. (2003) Mitogen-activated protein kinases (MAPK) as

predictors of clinical outcome in serous ovarian carcinoma in effusions. Gynecol Oncol 91:160-172

107. Chao KC, Wang PH, Yen MS, Chang CC, Chi CW (2005) Role of estrogen and progesterone in the survival of ovarian tumors--a study of the human ovarian adenocarcinoma cell line OC-117-VGH. J Chin Med Assoc 68:360-367

108. Belinson JL, McClure M, Badger G (1987) Randomized trial of megestrol acetate vs. megestrol acetate/tamoxifen for the management of progressive or recurrent epithelial ovarian carcinoma. Gynecol Oncol 28:151-155

109. Chen X, Feng Y (2003) Effect of progesterone combined with chemotherapy on epithelial ovarian cancer. Chin Med J (Engl) 116:388-391

110. Wei LL, Norris BM, Baker CJ (1997) An N-terminally truncated third progesterone receptor protein, PR(C), forms heterodimers with PR(B) but interferes in PR(B)-DNA binding. J Steroid Biochem Mol Biol 62:287-297

111. Migliaccio A, Castoria G, Di Domenico M, Ballare C, Beato M, Auricchio F (2005) The progesterone receptor/estradiol receptor association and the progestin-triggered S-phase entry. Ernst Schering Res Found Workshop:39-54

112. Migliaccio A, Castoria G, Di Domenico M, de Falco A, Bilancio A, Lombardi M, et al. (2000) Steroid-induced androgen receptor-oestradiol

receptor beta-Src complex triggers prostate cancer cell proliferation. EMBO J 19:5406-5417

113. Skildum A, Faivre E, Lange CA (2005) Progesterone receptors induce cell cycle progression via activation of mitogen-activated protein kinases. Mol Endocrinol 19:327-339

114. Zhou H, Luo MP, Schonthal AH, Pike MC, Stallcup MR, Blumenthal M, et al. (2002) Effect of reproductive hormones on ovarian epithelial tumors: I. Effect on cell cycle activity. Cancer Biol Ther 1:300-306

115. Lindgren P, Backstrom T, Mahlck CG, Ridderheim M, Cajander S (2001) Steroid receptors and hormones in relation to cell proliferation and apoptosis in poorly differentiated epithelial ovarian tumors. Int J Oncol 19:31-38

116. Horiuchi S, Kato K, Suga S, Takahashi A, Ueoka Y, Arima T, et al. (2005) Expression of progesterone receptor B is associated with G0/G1 arrest of the cell cycle and growth inhibition in NIH3T3 cells. Exp Cell Res 305:233-243

117. Takahashi A, Kato K, Kuboyama A, Inoue T, Tanaka Y, Kuhara A, et al. (2009) Induction of senescence by progesterone receptor-B activation in response to cAMP in ovarian cancer cells. Gynecol Oncol 113:270-276

118. Qiu M, Olsen A, Faivre E, Horwitz KB, Lange CA (2003) Mitogen-activated protein kinase regulates nuclear association of human progesterone receptors. Mol Endocrinol 17:628-642

119. Richer JK, Lange CA, Manning NG, Owen G, Powell R, Horwitz KB (1998) Convergence of progesterone with growth factor and cytokine signaling in breast cancer. Progesterone receptors regulate signal transducers and activators of transcription expression and activity. J Biol Chem 273:31317-31326

120. Darzynkiewicz Z, Juan G, Srour EF (2004) Differential staining of DNA and RNA. Curr Protoc Cytom Chapter 7:Unit 7 3

121. Gizard F, Robillard R, Barbier O, Quatannens B, Faucompre A, Revillion F, et al. (2005) TReP-132 controls cell proliferation by regulating the expression of the cyclin-dependent kinase inhibitors p21WAF1/Cip1 and p27Kip1. Mol Cell Biol 25:4335-4348

122. Prentice LM, Klausen C, Kalloger S, Kobel M, McKinney S, Santos JL, et al. (2007) Kisspeptin and GPR54 immunoreactivity in a cohort of 518 patients defines favourable prognosis and clear cell subtype in ovarian carcinoma. BMC Med 5:33

123. Fujimura M, Hidaka T, Kataoka K, Yamakawa Y, Akada S, Teranishi A, et al. (2001) Absence of estrogen receptor-alpha expression in human ovarian clear cell adenocarcinoma compared with ovarian serous, endometrioid, and mucinous adenocarcinoma. Am J Surg Pathol 25:667-672

124. Sasaki M, Dharia A, Oh BR, Tanaka Y, Fujimoto S, Dahiya R (2001) Progesterone receptor B gene inactivation and CpG hypermethylation in human uterine endometrial cancer. Cancer Res 61:97-102

125. Ivarsson K, Sundfeldt K, Brannstrom M, Janson PO (2001) Production of steroids by human ovarian surface epithelial cells in culture: possible role of progesterone as growth inhibitor. Gynecol Oncol 82:116-121

126. Keith Bechtel M, Bonavida B (2001) Inhibitory effects of 17beta-estradiol and progesterone on ovarian carcinoma cell proliferation: a potential role for inducible nitric oxide synthase. Gynecol Oncol 82:127-138

127. Hu Z, Deng X (2000) [The effect of progesterone on proliferation and apoptosis in ovarian cancer cell]. Zhonghua Fu Chan Ke Za Zhi 35:423-426

128. Blagosklonny MV (2003) Cell senescence and hypermitogenic arrest. EMBO Rep 4:358-362

129. Campisi J (2005) Senescent cells, tumor suppression, and organismal aging: good citizens, bad neighbors. Cell 120:513-522

130. Lee BY, Han JA, Im JS, Morrone A, Johung K, Goodwin EC, et al. (2006) Senescence-associated beta-galactosidase is lysosomal beta-galactosidase. Aging Cell 5:187-195

131. Dimri GP, Lee X, Basile G, Acosta M, Scott G, Roskelley C, et al. (1995) A biomarker that identifies senescent human cells in culture and in aging skin in vivo. Proc Natl Acad Sci U S A 92:9363-9367

132. Bayreuther K, Rodemann HP, Hommel R, Dittmann K, Albiez M, Francz PI (1988) Human skin fibroblasts in vitro differentiate along a terminal cell lineage. Proc Natl Acad Sci U S A 85:5112-5116

133. Campisi J, d'Adda di Fagagna F (2007) Cellular senescence: when bad things happen to good cells. Nat Rev Mol Cell Biol 8:729-740

134. Abbas T, Dutta A (2009) p21 in cancer: intricate networks and multiple activities. Nat Rev Cancer 9:400-414

135. Borgdorff V, Lleonart ME, Bishop CL, Fessart D, Bergin AH, Overhoff MG, et al. (2010) Multiple microRNAs rescue from Ras-induced senescence by inhibiting p21(Waf1/Cip1). Oncogene 29:2262-2271

136. Brown JP, Wei W, Sedivy JM (1997) Bypass of senescence after disruption of p21CIP1/WAF1 gene in normal diploid human fibroblasts. Science 277:831-834

137. Demidenko ZN, Blagosklonny MV (2008) Growth stimulation leads to cellular senescence when the cell cycle is blocked. Cell Cycle 7:3355-3361

138. Kuilman T, Peeper DS (2009) Senescence-messaging secretome: SMS-ing cellular stress. Nat Rev Cancer 9:81-94

139. Lange CA, Richer JK, Shen T, Horwitz KB (1998) Convergence of progesterone and epidermal growth factor signaling in breast cancer. Potentiation of mitogen-activated protein kinase pathways. J Biol Chem 273:31308-31316

140. Proietti C, Salatino M, Rosemblit C, Carnevale R, Pecci A, Kornblihtt AR, et al. (2005) Progestins induce transcriptional activation of signal transducer and activator of transcription 3 (Stat3) via a Jak- and Src-dependent mechanism in breast cancer cells. Mol Cell Biol 25:4826-4840

141. Stoecklin E, Wissler M, Schaetzle D, Pfitzner E, Groner B (1999) Interactions in the transcriptional regulation exerted by Stat5 and by members of the steroid hormone receptor family. J Steroid Biochem Mol Biol 69:195-204

142. Sinibaldi D, Wharton W, Turkson J, Bowman T, Pledger WJ, Jove R (2000) Induction of p21WAF1/CIP1 and cyclin D1 expression by the Src oncoprotein in mouse fibroblasts: role of activated STAT3 signaling. Oncogene 19:5419-5427

143. Owen GI, Richer JK, Tung L, Takimoto G, Horwitz KB (1998) Progesterone regulates transcription of the p21(WAF1) cyclin- dependent kinase inhibitor gene through Sp1 and CBP/p300. J Biol Chem 273:10696-10701

144. Campisi J (2001) Cellular senescence as a tumor-suppressor mechanism. Trends Cell Biol 11:S27-31

145. Campisi J (2005) Suppressing cancer: the importance of being senescent. Science 309:886-887

146. Adams PD (2009) Healing and hurting: molecular mechanisms, functions, and pathologies of cellular senescence. Mol Cell 36:2-14

147. Niu G, Wright KL, Ma Y, Wright GM, Huang M, Irby R, et al. (2005) Role of Stat3 in regulating p53 expression and function. Mol Cell Biol 25:7432-7440

148. Min H, Wei-hong Z (2009) Constitutive activation of signal transducer and activator of transcription 3 in epithelial ovarian carcinoma. J Obstet Gynaecol Res 35:918-925

149. Narayanan R, Adigun AA, Edwards DP, Weigel NL (2005) Cyclin-dependent kinase activity is required for progesterone receptor function: novel role for cyclin A/Cdk2 as a progesterone receptor coactivator. Mol Cell Biol 25:264-277

150. Moore NL, Narayanan R, Weigel NL (2007) Cyclin dependent kinase 2 and the regulation of human progesterone receptor activity. Steroids 72:202-209

151. Nakanishi M, Adami GR, Robetorye RS, Noda A, Venable SF, Dimitrov D, et al. (1995) Exit from G0 and entry into the cell cycle of cells expressing p21Sdi1 antisense RNA. Proc Natl Acad Sci U S A 92:4352-4356

152. Takahashi A, Ohtani N, Hara E (2007) Irreversibility of cellular senescence: dual roles of p16INK4a/Rb-pathway in cell cycle control. Cell Div 2:10

153. Zheng H, Kavanagh JJ, Hu W, Liao Q, Fu S (2007) Hormonal therapy in ovarian cancer. Int J Gynecol Cancer 17:325-338

154. Ahlgren JD, Ellison NM, Gottlieb RJ, Laluna F, Lokich JJ, Sinclair PR, et al. (1993) Hormonal palliation of chemoresistant ovarian cancer: three consecutive phase II trials of the Mid-Atlantic Oncology Program. J Clin Oncol 11:1957-1968

155. Geisler HE (1985) The use of high-dose megestrol acetate in the treatment of ovarian adenocarcinoma. Semin Oncol 12:20-22

156. Sikic BI, Scudder SA, Ballon SC, Soriero OM, Christman JE, Suey L, et al. (1986) High-dose megestrol acetate therapy of ovarian carcinoma: a phase II study by the Northern California Oncology Group. Semin Oncol 13:26-32

157. Veenhof CH, van der Burg ME, Nooy M, Aalders JG, Pecorelli S, Oliveira CF, et al. (1994) Phase II study of high-dose megestrol acetate in patients with advanced ovarian carcinoma. Eur J Cancer 30A:697-698

158. Wiernik PH, Greenwald ES, Ball H, Young JA, Vogl S (1998) High-dose megestrol acetate in the treatment of patients with ovarian cancer who have undergone previous treatment: Eastern Cooperative Oncology Group Study PD884. Am J Clin Oncol 21:565-567

159. Wilailak S, Linasmita V, Srisupundit S (2001) Phase II study of high-dose megestrol acetate in platinum-refractory epithelial ovarian cancer. Anticancer Drugs 12:719-724

160. Mangioni C, Franceschi S, La Vecchia C, D'Incalci M (1981) High-dose medroxyprogesterone acetate (MPA) in advanced epithelial ovarian cancer resistant to first- or second-line chemotherapy. Gynecol Oncol 12:314-318

161. Slayton RE, Pagano M, Creech RH (1981) Progestin therapy for advanced ovarian cancer: a phase II Eastern Cooperative Oncology Group trial. Cancer Treat Rep 65:895-896

162. Aabo K, Pedersen AG, Haid I, Dombernowsky P (1982) High-dose medroxyprogesterone acetate (MPA) in advanced chemotherapy-resistant ovarian carcinoma: a phase II study. Cancer Treat Rep 66:407-408

163. Trope C, Johnsson JE, Sigurdsson K, Simonsen E (1982) High-dose medroxyprogesterone acetate for the treatment of advanced ovarian carcinoma. Cancer Treat Rep 66:1441-1443

164. Hamerlynck JV, Maskens AP, Mangioni C, van der Burg ME, Wils JA, Vermorken JB, et al. (1985) Phase II trial of medroxyprogesterone acetate in advanced ovarian cancer: an EORTC Gynecological Cancer Cooperative Group Study. Gynecol Oncol 22:313-316

165. Malfetano J, Beecham JB, Bundy BN, Hatch KD (1993) A phase II trial of medroxyprogesterone acetate in epithelial ovarian cancers. A Gynecologic Oncology Group study. Am J Clin Oncol 16:149-151

166. Freedman RS, Saul PB, Edwards CL, Jolles CJ, Gershenson DM, Jones LA, et al. (1986) Ethinyl estradiol and medroxyprogesterone acetate in patients with epithelial ovarian carcinoma: a phase II study. Cancer Treat Rep 70:369-373

167. Fromm GL, Freedman RS, Fritsche HA, Atkinson EN, Scott W (1991) Sequentially administered ethinyl estradiol and medroxyprogesterone acetate in the treatment of refractory epithelial ovarian carcinoma in patients with positive estrogen receptors. Cancer 68:1885-1889

168. Rendina GM, Donadio C, Giovannini M (1982) Steroid receptors and progestinic therapy in ovarian endometrioid carcinoma. Eur J Gynaecol Oncol 3:241-246

169. Jakobsen A, Bertelsen K, Sell A (1987) Cyclic hormonal treatment in ovarian cancer. A phase-II trial. Eur J Cancer Clin Oncol 23:915-916

170. Markman M, Kennedy A, Webster K, Kulp B, Peterson G, Belinson J (2000) Phase I trial of paclitaxel plus megestrol acetate in patients with paclitaxel-refractory ovarian cancer. Clin Cancer Res 6:4201-4204

171. Senn HJ, Lei D, Castano-Almendral A, Brunner KW, Martz G, Obrecht P, et al. (1980) [Chemo-(hormonal)-therapy of advanced ovarian neoplasms in FIGO stages III and IV. Prospective SAKK-study 20/71]. Schweiz Med Wochenschr 110:1202-1208

172. Agarwal R, Kaye SB (2003) Ovarian cancer: strategies for overcoming resistance to chemotherapy. Nat Rev Cancer 3:502-516

173. Yap TA, Carden CP, Kaye SB (2009) Beyond chemotherapy: targeted therapies in ovarian cancer. Nat Rev Cancer 9:167-181

174. Sager R (1991) Senescence as a mode of tumor suppression. Environ Health Perspect 93:59-62

175. Braig M, Schmitt CA (2006) Oncogene-induced senescence: putting the brakes on tumor development. Cancer Res 66:2881-2884

176. Hanahan D, Weinberg RA (2000) The hallmarks of cancer. Cell 100:57-70

177. Soengas MS (2008) Cancer: Ins and outs of tumour control. Nature 454:586-587

178. Collado M, Serrano M (2010) Senescence in tumours: evidence from mice and humans. Nat Rev Cancer 10:51-57

179. Chen Z, Trotman LC, Shaffer D, Lin HK, Dotan ZA, Niki M, et al. (2005) Crucial role of p53-dependent cellular senescence in suppression of Pten-deficient tumorigenesis. Nature 436:725-730

180. Acosta JC, O'Loghlen A, Banito A, Guijarro MV, Augert A, Raguz S, et al. (2008) Chemokine signaling via the CXCR2 receptor reinforces senescence. Cell 133:1006-1018

181. Courtois-Cox S, Genther Williams SM, Reczek EE, Johnson BW, McGillicuddy LT, Johannessen CM, et al. (2006) A negative feedback signaling network underlies oncogene-induced senescence. Cancer Cell 10:459-472

182. Bartkova J, Rezaei N, Liontos M, Karakaidos P, Kletsas D, Issaeva N, et al. (2006) Oncogene-induced senescence is part of the tumorigenesis barrier imposed by DNA damage checkpoints. Nature 444:633-637

183. Fujita K, Mondal AM, Horikawa I, Nguyen GH, Kumamoto K, Sohn JJ, et al. (2009) p53 isoforms Delta133p53 and p53beta are endogenous regulators of replicative cellular senescence. Nat Cell Biol 11:1135-1142

184. Kuilman T, Michaloglou C, Vredeveld LC, Douma S, van Doorn R, Desmet CJ, et al. (2008) Oncogene-induced senescence relayed by an interleukin-dependent inflammatory network. Cell 133:1019-1031

185. Gray-Schopfer VC, Cheong SC, Chong H, Chow J, Moss T, Abdel-Malek ZA, et al. (2006) Cellular senescence in naevi and immortalisation in melanoma: a role for p16? Br J Cancer 95:496-505

186. Blumenthal M, Kardosh A, Dubeau L, Borok Z, Schonthal AH (2003) Suppression of the transformed phenotype and induction of differentiation-like characteristics in cultured ovarian tumor cells by chronic treatment with progesterone. Mol Carcinog 38:160-169

187. Werness BA, Freedman AN, Piver MS, Romero-Gutierrez M, Petrow E (1999) Prognostic significance of p53 and p21(waf1/cip1) immunoreactivity in epithelial cancers of the ovary. Gynecol Oncol 75:413-418

188. Geisler HE, Geisler JP, Miller GA, Geisler MJ, Wiemann MC, Zhou Z, et al. (2001) p21 and p53 in ovarian carcinoma: their combined staining is more valuable than either alone. Cancer 92:781-786

189. Schmider A, Gee C, Friedmann W, Lukas JJ, Press MF, Lichtenegger W, et al. (2000) p21 (WAF1/CIP1) protein expression is associated with prolonged survival but not with p53 expression in epithelial ovarian carcinoma. Gynecol Oncol 77:237-242

190. Chien JR, Aletti G, Bell DA, Keeney GL, Shridhar V, Hartmann LC (2007) Molecular pathogenesis and therapeutic targets in epithelial ovarian cancer. J Cell Biochem 102:1117-1129

191. Campaner S, Doni M, Hydbring P, Verrecchia A, Bianchi L, Sardella D, et al. (2010) Cdk2 suppresses cellular senescence induced by the c-myc oncogene. Nat Cell Biol 12:54-59; sup pp 51-14

192. Meinhold-Heerlein I, Bauerschlag D, Hilpert F, Dimitrov P, Sapinoso LM, Orlowska-Volk M, et al. (2005) Molecular and prognostic distinction between serous ovarian carcinomas of varying grade and malignant potential. Oncogene 24:1053-1065

193. Yamaguchi K, Mandai M, Oura T, Matsumura N, Hamanishi J, Baba T, et al. (2010) Identification of an ovarian clear cell carcinoma gene signature that reflects inherent disease biology and the carcinogenic processes. Oncogene 29:1741-1752

194. Ho SM (2003) Estrogen, progesterone and epithelial ovarian cancer. Reprod Biol Endocrinol 1:73

195. Krizhanovsky V, Yon M, Dickins RA, Hearn S, Simon J, Miething C, et al. (2008) Senescence of activated stellate cells limits liver fibrosis. Cell 134:657-667

196. Dubeau L (1999) The cell of origin of ovarian epithelial tumors and the ovarian surface epithelium dogma: does the emperor have no clothes? Gynecol Oncol 72:437-442

197. Piek JM, van Diest PJ, Verheijen RH (2008) Ovarian carcinogenesis: an alternative hypothesis. Adv Exp Med Biol 622:79-87

198. Dubeau L (2008) The cell of origin of ovarian epithelial tumours. Lancet Oncol 9:1191-1197

199. Li GH, Wei H, Lv SQ, Ji H, Wang DL (2010) Knockdown of STAT3 expression by RNAi suppresses growth and induces apoptosis and differentiation in glioblastoma stem cells. Int J Oncol 37:103-110

200. Ward RD, Weigel NL (2009) Steroid receptor phosphorylation: Assigning function to site-specific phosphorylation. Biofactors 35:528-536

201. Bast RC, Jr., Hennessy B, Mills GB (2009) The biology of ovarian cancer: new opportunities for translation. Nat Rev Cancer 9:415-428